Theory of radiation for bounded media systems with highly correlated electron-hole plasmas

Dissertation
zur Erlangung des akademischen Grades
doctor rerum naturalium (Dr. rer. nat.)
der Mathematisch-Naturwissenschaftlichen Fakultät
der Universität Rostock

vorgelegt von

Felix Richter, geb. am 27. November 1978 in Paderborn

Rostock, 31. Juli 2009

urn:nbn:de:gbv:28-diss2010-0044-0

1. Gutachter: Prof. Dr. K. Henneberger, Universität Rostock
2. Gutachter: Prof. Dr. F. Jahnke, Universität Bremen
3. Gutachter: Prof. Dr. H. Stolz, Universität Rostock

Tag der Verteidigung: 17. November 2009

Adresse: Universität Rostock
Institut für Physik
18051 Rostock
Internet: http://www.physik3.uni-rostock.de

Abstract

The theory of light propagation in media needs to consider a vast number of effects arising from the coupling of the many-body system of the medium with the photon field. The breach of translational invariance in bounded media is an additional complication. The problem is described quantum-statistically by nonequilibrium Green's functions. Essential advantages for the further analysis arise from the fact that the contribution of incident light splits off from the photon field propagators. This property provides insight into the interplay of the excitations of light and matter as well as into the mechanisms of emission. A radiation law valid for bounded media in nonequilibrium steady states is derived and discussed in the context of optical properties of excited semiconductors. With the help of this law, predictions for the optical signatures of quantum condensates in the electron-hole plasma of the semiconductor can be made. For this, an analysis of the condensate phase boundary is reviewed and the ionization behavior in the excitonic regime at low temperatures is studied analytically and numerically.

Zusammenfassung

Die Theorie der Lichtausbreitung in Medien hat eine Vielzahl von Effekten aus der Kopplung des Vielteilchen-Systems des Mediums mit dem Photonfeld zu berücksichtigen. In räumlich begrenzten Medien tritt erschwerend zusätzlich ein Bruch der Translationssymmetrie auf. Entscheidende Vorteile bringt in der quantenstatistischen Beschreibung des Problems mit Green'schen Funktionen für das Nichtgleichgewicht die Tatsache, dass sich der Beitrag des einfallenden Lichts von den Photonfeld-Propagatoren abspaltet. Diese Eigenschaft erlaubt Einblicke in das Zusammenspiel der Anregungen von Licht und Materie sowie in die Mechanismen der Emission. Es wird ein Strahlungsgesetz mit erweiterter Gültigkeit für räumlich begrenzte Medien in stationären Nichtgleichgewichtszuständen abgeleitet und im Zusammenhang mit optischen Eigenschaften angeregter Halbleiter diskutiert. Die Theorie ermöglicht ferner Aussagen über die optischen Signaturen von Quantenkondensaten im Elektron-Loch-Plasma des Halbleiters. Dazu werden Untersuchungen zu dessen Phasengrenze referiert und das Ionisations-Verhalten bei niedrigen Temperaturen im exzitonischen Regime analytisch und numerisch untersucht.

Contents

Chapter 1

Introduction and Motivation

"The theory is pretty, but is there some truth to it?"
— A. Einstein, in a letter to P. Ehrenfest (PP05)

Below a certain critical temperature, particles with integer spin may accumulate spontaneously at zero velocity, and their wave packets overlap to develop into a giant (macroscopic) coherent matter wave. This exotic and extreme state of matter was predicted by A. Einstein in 1925 (Ein25) as a consequence of the statistics found by S. N. Bose (Bos24) for integer spin particles, and is called the *Bose–Einstein condensate*.

At the time of its prediction, experimentalists were able to cool matter to a few degrees above absolute zero. Spectacular physical effects were known at this temperature scale, such as superconductivity and superfluidity. The Bose–Einstein condensation (BEC) of atoms in gases, however, occurs at temperatures as low as a few nanokelvin, i.e., up to nine orders of magnitude further towards absolute zero. Now, how spectacular would physics be if one could ever reach these extreme conditions? Thoughts like these let people, including Einstein, express their doubt in the observability of this new state of matter in the decades to follow: "I am betting on nature to hide Bose condensation from us. The last 15 years she's been doing a great job." (Steven Chu in 1994, cited after Ket02)

Seventy years after Einstein's prediction, in 1995, novel experimental methods (e.g., evaporative and laser cooling) were eventually developed far enough, and two independent groups succeeded in realizing the BEC state in gases of alkali atoms (AEM$^+$95; DMA$^+$95). This achievement was awarded with the Nobel prize for physics in 2001. Indeed, it opened fascinating experimental possibilities with coherent matter waves (Ket02; SBR03), and an active scientific community devoted to the study of atomic BEC emerged. Nowadays, these powerful experimental methods have become quite common and the "coldest matter in the universe" is produced routinely in laboratories around the world.

However, a much more promising candidate system for the BEC was proposed as early as in the 1960's (BBB62): In the *electron-hole plasma (EHP)* of an excited

semiconductor, the bosonic bound electron-hole states, the *excitons*, should be able to condense at temperatures of the order of one Kelvin at reasonable density due to their smaller masses. Yet, the excitonic BEC did not win the race, and even today a generally accepted confirmation of excitonic BEC has not been presented, at least not in three-dimensional semiconductor systems (Sno02; KRK$^+$06).

Is Einstein's theory not applicable here? Or is the reason rather to be sought in the short lifetime of excitons and the complex interplay of condensed and non-condensed phases, crystal lattice and radiation, which just hinder the matter to reach the condensation threshold? Einstein considered non-interacting particles, and while atoms can be isolated in a trap, the electron-hole plasma is an integral part of the semiconductor, cannot exist on its own and will thus always be subjected to external perturbations.

For the same reason, evidence for the existence of a condensate can only be deduced from specific signatures in external measurement quantities. These signatures will always be contained in a significant background signal from the surrounding environment, and their precise form is still subject to debate. With ever-improving experimental methods, it appears today that the question of an indisputable signature as the proof of evidence for the condensation has become the predominant problem (Sno03).

Clearly, further efforts from the theoretical side are necessary. Immediately, the following key problems can be pointed out for the theoretical approach:

- The condensate emerges from a *nonequilibrium* excited EHP with a short lifetime under influence of internal Coulomb and exchange interactions. It is a *degeneracy* effect and cannot be explained in a classical theory. Hence, a quantum-mechanical nonequilibrium many-body theory is ultimately needed.
- Under optical probing, the EHP is obviously *coupled to the optical field*, and a joint description of plasma and electromagnetic radiation is needed to develop predictions for the optical signature.
- The semiconductor sample is a *bounded medium*. The loss of translational invariance (as compared to the case of bulk media) is a major complicating fact for the exact theoretical description.

While these problems are driven to an extreme in the context of quantum condensation, they apply in principle to any study of optics in excited semiconductors.

Outline of the Thesis

The present work addresses these problems with *Green's function methods* and reports progress in several closely related aspects:

- development of the theory of light propagation through arbitrary bounded media in nonequilibrium

- correct formulation of the energy conservation condition and material properties with bounded media
- development of the theory of radiative energy flow in steady-state media systems (i.e., emission and absorption), providing insight into the interplay of light and matter
- development of the theory of quantum condensation in electron-hole plasmas as the superordinate physical phenomenon to BEC
- qualitative predictions for the optical signature of quantum condensation[1]
- understanding of the ionization equilibrium in the high density excitonic regime
- quantitative calculations for the conditions for condensation in specific materials

The text is organized as follows: At first, an introduction is given to the coupled description of light and matter, from the axiomatic basis over the Hamiltonian formulation to the Green's function concept (Chapter 2).

Chapter 3 starts with a review of classical wave propagation with emphasis on semiconductors (excitonic systems) and their electromagnetic properties, and correct consideration of medium boundaries.

Then, Section 3.4 reviews own work on the quantum-kinetically exact description of radiation in arbitrary bounded media with the photon Green's function. The universal splitting property is introduced. It opens the possibility for the treatment of quantized light and the discrimination of light by its source, be it externally excited or from ground-state fluctuations.

From consideration of the energy flow balance, the derivation of an energy flow law for nonequilibrium situations in the steady state is possible (Sec. 3.5). It provides insight into the interplay of light and matter as well as mechanisms of emission related to degeneracy, and eventually allows deriving optical signatures based on the specific behavior of the matter.

Chapter 4 starts with an introduction to quantum condensates in general and especially to BEC in electron-hole systems. A paper which gives a universal picture of quantum condensation based on particle Green's functions is reviewed. Finally, own work is presented which deals with the quasi-equilibrium behavior of excitonic systems at low temperatures and high excitation and makes predictions for the occurrence of excitonic BEC with the aim of being quantitatively reliable.

Author's published work, submitted articles, and manuscripts close to publication quality are attached starting from page 73 and referenced in the text using the keys *P-1*, *P-2*, etc.

[1] Although one may think of signatures in other quantities such as the conductivity (JL98), the present work concentrates on optical signatures.

Chapter 2

Theoretical framework

The optical properties of matter are determined by the manifold interactions that arise from the coupling of photons, the quanta of light, to charged particles in the matter. The latter, in turn, constitute a dynamic system of quantum particles interacting on a long range scale via the Coulomb force, and both obviously have to be dealt with self-consistently. In this work, not only the light-matter interaction is of interest but also possible quantum condensation effects in the matter at extreme condictions, and, ultimately, optical properties or signatures of such a condensate.

The complexity of this subject makes high demands on the consistency of the theoretical approach. One approach that can fulfill the requirements for a common and self-consistent description of the coupled system of light and matter on a quantum-statistically exact level is the *nonequilibrium Green's function technique*. It is the main ingredient of the theoretical framework used in this work and whose presentation this chapter is devoted to.

Prior to that, the basic properties of the *semiconductor* will be briefly introduced. It serves as a model system for the derivation of the theory, providing concepts and notions where otherwise the universality of the theoretical approach would lead to a high degree of abstractness, and, equally, as the object under study, e.g., regarding light emission of excited semiconductors.

2.1 Basic theory and properties of the semiconductor

In the periodic lattice of atoms of crystalline materials such as semiconductors, the discrete allowed energy levels for the electrons of the isolated atom widen to electronic *bands*. Electronic transitions in or between different bands (intraband/interband processes) are coupled to the annihilation or creation of light quanta, thus determining the optical properties of the material. This rises the need for an adequate description of the band structure. Various methods exist for its calculation, amongst which are the *tight-binding* method (suitable for wave functions with weak overlap between lattice sites), the $\mathbf{k}\cdot\mathbf{p}$ method (a perturbational method suitable especially for degenerate bands) (HK90; SW02; YC05) or density functional methods (e.g., FSSR09).

Semiconductors are defined by the presence of energetically low fully occupied bands, the *valence bands (v)*, higher empty bands [*conduction bands (c)*], and an energy gap E_g between them. This gap is the reason for their interesting physics and allows for their most important use: The semiconductor can be switched between insulating and conducting (metallic) behavior by an increased temperature, optical excitation or, as in the *transistor*, by an electric potential.

According to the energies involved, electronic transitions in or between different bands usually appear reasonably well separated in spectroscopic experiments, so that for semiconductor materials one may restrict the theoretical description to processes occurring around the band gap energy and to the corresponding valence and conduction bands.

Zinc selenide (ZnSe), for example, is a compound of a group II element with a group IV element crystallizing in the common face-centered cubic (fcc) zinc blende structure, whose reciprocal lattice (Brillouin zone) is body-centered cubic (bcc). The smallest band gap is at the center of the Brillouin zone (Γ point). The valence band here is six-fold degenerate due to cubic symmetry but splits into a four-fold and a two-fold band due to spin-orbit coupling (Mar92; MW05; SW02).

2.1.1 Effective-mass approximation

Compared to the maximal electronic momentum in one Brillouin zone, photonic momenta around the band gap energy are so weak that optically induced interband transitions appear nearly vertical in a band structure graph. These facts make ZnSe a direct-gap semiconductor. Thus, its electronic dispersions will only be needed close around the Γ point ($\mathbf{k} = 0$), and it is reasonable to approximate them with parabolic dispersions. This leads to the intuitive picture of electrons moving freely through the semiconductor and having effective masses[1] which contain the effects of an ideally periodic crystal potential on the electron motion in parabolic approximation.

It is a fruitful concept to consider the missing state in the valence band, where effective masses are negative, a *hole (h)* particle with opposite wave vector, positive effective mass m_h and positive unit charge,

$$\mathbf{k}_h := -\mathbf{k}_v \qquad m_h := -m_v > 0 \qquad m_e := m_c > 0\,, \tag{2.1}$$

while the conduction band state is referred to simply as an *electron (e)*.

In the following, the semiconductor band structure will exclusively be regarded in a two-band effective-mass approximation. Nevertheless, it is possible to consider the full electronic dispersion in numerical calculations if necessary.

[1] In the case of degenerate bands, the $\mathbf{k} \cdot \mathbf{p}$ theory and Luttinger-Kohn models can provide the parabolic approximation or effective masses (SW02; HK90).

2.1.2 Electron-hole plasma and excitons

Electrons and holes attract each other due to the Coulomb force and may combine to a hydrogen-like composite neutral particle, the *exciton (X)*.

A rigorous theoretical introduction of these quasi-particles is possible, e.g., by an evaluation of the interband polarization in second quantization (HK90), which leads to the *Wannier equation* (Wan37), a two-particle Schrödinger equation for the relative motion of an electron and a hole (as Bloch states, which reflect the periodicity of the lattice). It follows immediately that the exciton behaves in many aspects like a hydrogen atom, and many notions known from atomic physics may be applied to excitons, too:

$$\text{reduced mass} \qquad \frac{1}{m_r} = \frac{1}{m_e} + \frac{1}{m_h} \tag{2.2}$$

$$\text{Bohr radius} \qquad a_\mathrm{X} = \frac{\hbar^2 \varepsilon_0 \varepsilon_r}{e^2 m_r} \tag{2.3}$$

$$\text{binding energy} \qquad E_b = -\frac{e^4 m_r}{2(\varepsilon_0 \varepsilon_r)^2 \hbar^2} \tag{2.4}$$

Especially, as the main spectral property of excitons, there is a hydrogen-like series of excited states with main quantum number n and binding energy E_b/n^2. The binding energy is to be understood as relative to the gap energy, and the exciton dispersion is parabolic,

$$E_\mathrm{X}(n, \mathbf{k}_\mathrm{X}) \quad = E_g + \tfrac{1}{n^2} E_b + \tfrac{\hbar^2 k_\mathrm{X}^2}{2 m_\mathrm{X}}, \tag{2.5}$$

where $\mathbf{k}_\mathrm{X} = \mathbf{k}_e + \mathbf{k}_h$ and $m_\mathrm{X} = m_e + m_h$. Furthermore, the Wannier equation also has solutions for energies above the gap, a continuous spectrum of Coulomb *scattering states*.

The ground-state binding energy is often also called the *excitonic Rydberg (Ryd)* and serves as a convenient energy unit. Typical ground-state energies range between $1 \ldots 200\ \mathrm{meV} \ll E_g$ and typical Bohr radii are $50 \ldots 1\ \mathrm{nm}$ (Kli95). Since this is larger than a typical lattice constant, the exciton spreads over many unit cells ("Wannier exciton"), which justifies the effective-mass approximation.

A gas of electrons (and holes as their counterparts) may be generated in the conduction band, e.g., by optical pumping or injection of electric currents. Thermalization occurs within picoseconds, and excitons form. Their lifetime ranges from nanoseconds (in direct-gap semiconductors) up to microseconds (in indirect-gap semiconductors or due to forbidden direct transitions), opening up a window for the coexistence of electrically charged and neutral bound particles. During this time, the electron-hole gas can be assumed to be in the state of a *quasi-equilibrium*, where the electron and hole distributions functions are given by Fermi functions in which the *chemical potential* is a measure for the excitation of the system (i.e., the density of the electron gas).

This system, whether in quasi-equilibrium or not, fulfills the definition of a non-ideal, partially ionized *plasma*, the *electron-hole plasma (EHP)*, such that theoretical methods from plasma physics (KKER86; Mah90; KSK05) may be readily applied to it. In *P-6*, excitons are introduced from this point of view by a statistical analysis of the particle number density in *extended quasiparticle approximation*, which clearly reveals that excitons obey bosonic statistics: Their particle number density is

$$n_{\mathrm{X}}(\mu_{\mathrm{X}}, T) = g_e g_h \int \frac{\mathrm{d}\mathbf{k}}{(2\pi)^3} \frac{1}{\exp\left[\frac{1}{k_b T}\left(\frac{\hbar^2 k^2}{2m_{\mathrm{X}}} - \mu_{\mathrm{X}}\right)\right] - 1}, \tag{2.6}$$

where μ_{X} is their chemical potential, T is the temperature and g_e, g_h are (spin) degeneracy factors of electrons and holes, respectively.

In this context it is to be noted that established (atomic/hydrogen) plasma physics results often have to be re-evaluated before application to electron-hole plasmas. For example, an adiabatic decoupling of ion and electron motion, an assumption on which many simulation techniques are based (e.g., for thermodynamics of planets (warm dense matter) (Des03; KHR$^+$07) or ionization kinetics of clusters in intense laser fields (FBM04)), is not possible here since electron and hole masses are usually of the same order of magnitude. For the same reason, degeneration has to be taken into account for both kinds of particles equally. A further complicating fact is the coupling of the EHP to the radiation field with its continuous mode spectrum, which will be dealt with in the following.

2.2 Particles and electromagnetic fields

2.2.1 Microscopic Maxwell's equations

The axiomatic basis both of classical and quantum electrodynamics are *Maxwell's equations* for the electric and magnetic fields $\mathbf{E}$ and $\mathbf{B}$,

$$\operatorname{div}\mathbf{E}(\mathbf{r},t) = \frac{1}{\varepsilon_0}\rho(\mathbf{r},t) \qquad \operatorname{div}\mathbf{B}(\mathbf{r},t) = 0 \tag{2.7}$$

$$\operatorname{rot}\mathbf{E}(\mathbf{r},t) = -\frac{\partial}{\partial t}\mathbf{B}(\mathbf{r},t) \qquad \operatorname{rot}\mathbf{B}(\mathbf{r},t) = \frac{1}{c^2}\frac{\partial}{\partial t}\mathbf{E}(\mathbf{r},t) - \frac{1}{\varepsilon_0 c^2}\mathbf{j}(\mathbf{r},t) \tag{2.8}$$

together with Newton's second law and the Coulomb and Lorentz force laws, which may be combined into the *Newton–Lorentz equation* (CDG89)

$$m_i \frac{\mathrm{d}^2}{\mathrm{d}t^2}\mathbf{r}_i = e_i \left(\mathbf{E}(\mathbf{r}_i(t),t) + \mathbf{v}_i(t) \times \mathbf{B}(\mathbf{r}_i(t),t)\right) . \tag{2.9}$$

It is to be stressed that any physically present (elementary) particle i (mass m_i, charge e_i, location $\mathbf{r}_i$, non-relativistic velocity v_i) is subjected to these forces. They are exerted

by the electromagnetic fields, and the fields in turn are generated by the presence (density ρ) and movement (current $\mathbf{j}$) of the particles,

$$\rho(\mathbf{r},t) = \sum_i e_i \delta\left(\mathbf{r} - \mathbf{r}_i(t)\right) \qquad \mathbf{j}(\mathbf{r},t) = \sum_i e_i \mathbf{v}_i(t) \delta\left(\mathbf{r} - \mathbf{r}_i(t)\right) . \tag{2.10}$$

In contrast to these universal laws, the *macroscopic* Maxwell equations in terms of the fields $\mathbf{D}, \mathbf{H}$ were introduced to obtain a global, effective description of electrodynamics in the presence of a medium. One can consider their form a well-founded historic convention. It can be reproduced simply by splitting the electric current density into induced and external currents, $\mathbf{j} = \mathbf{j}_{\mathrm{ind}} + \mathbf{j}_{\mathrm{ext}}$, linking the former to polarization and magnetization fields $\mathbf{P}$ and $\mathbf{M}$ inside the medium by the ansatz

$$\mathbf{j}_{\mathrm{ind}} = \dot{\mathbf{P}} + \mathrm{rot}\, \mathbf{M}\,, \tag{2.11}$$

and introducing the constitutive relations

$$\mathbf{D} = \varepsilon_0 \mathbf{E} + \mathbf{P} \qquad \mathbf{H} = \frac{1}{\mu_0}\mathbf{B} - \mathbf{M}\,. \tag{2.12}$$

Another possibility is the ansatz $\mathbf{j}_{\mathrm{ind}} = \dot{\mathbf{P}}$, which will of course combine both polarization and magnetization effects into $\mathbf{P}$, while $\mathbf{M} = 0$ and $\mathbf{H} = \mathbf{B}/\mu_0$ (Hal92). Since magnetization in optical materials is often negligible anyway, this more compact variant will be preferred in this work.[2] In either case, $\mathbf{j}_{\mathrm{ind}}$ contains the full information about the electromagnetic properties of the matter, which will be addressed in Sec. 3.1 et seq.

The clear distinction between the physical fields $\mathbf{E}$ and $\mathbf{B}$ and the derived fields $\mathbf{D}$ and $\mathbf{H}$ however is often not followed, even in established textbooks (see *P-1*). This might be due to historical and experimental reasons, since $\mathbf{D}$ and $\mathbf{H}$ appear to be useful quantities in basic experiments.

Obviously, the quality of $\mathbf{D}$ and $\mathbf{H}$ in theoretical considerations depends on that of the description of the polarization $\mathbf{P}$. Taking the derived fields in basic approximations for real and basing physical conditions on them has lead to innumerous discussions and confusion. Most prominent is the case of the boundary conditions for $\mathbf{D}$ and $\mathbf{H}$ at a medium surface (Nel95) or the debate around the validity of the Poynting vector in one form or the other (see *P-1*).

The definition of $\mathbf{D}$ and $\mathbf{H}$ [Eq. (2.12)] eliminates induced charges and currents and the physical fields generated by them from the macroscopic Maxwell equations. If further external charges and currents are absent, these equations take a form equivalent to the microscopic Maxwell equations for the vacuum [i.e, $\rho \equiv j \equiv 0$ in Eq. (2.7)] and thus "de-renormalize" the physical fields in presence of a medium to freely propagating fields. This idea will become helpful for the discussion of *P-5* in Sec. 3.4.

[2] This concept is also very close to the photon Green's function formalism, where the polarization tensor is the quantity into which effects of the matter on the photon energy are combined.

2.2.2 Energy conservation

Article *P-1* shows the derivation of an energy continuity equation just on the axiomatic basis of the Maxwell and Newton–Lorentz equations:

$$\frac{\partial}{\partial t}\left(U_e + U_m\right) + \operatorname{div}\left(\mathbf{S}_e + \mathbf{S}_m\right) = 0\,, \tag{2.13}$$

where

$$U_e = \frac{1}{2}\left(\varepsilon_0 \mathbf{E}^2 + \frac{1}{\mu_0}\mathbf{B}^2\right) \qquad\qquad \mathbf{S}_e = \frac{1}{\mu_0}\left(\mathbf{E}\times\mathbf{B}\right) \tag{2.14}$$

are the electromagnetic field energy density U_e and the electromagnetic field energy flux vector $\mathbf{S}_e$, and U_m, $\mathbf{S}_m$ their mechanical energy counterparts describing the density and flux of mechanical (kinetic) energy of particles in the medium. The equation clearly distinguishes between the two kinds of energy in the system related to fields and particles, respectively, and associates a change in energy density with a source or drain of an energy flux. Furthermore, it is universal and independent of a particular description or model of a medium possibly present, and thus cannot be affected by the peculiarities of the latter.

Since both types of energy are linked by the dissipation $\mathbf{jE}$, one may regard their conservation separately:

$$\frac{\partial}{\partial t}U_e + \operatorname{div}\mathbf{S}_e = -\mathbf{jE}\,, \tag{2.15}$$

$$\frac{\partial}{\partial t}U_m + \operatorname{div}\mathbf{S}_m = \mathbf{jE}\,. \tag{2.16}$$

Energy conservation is a hard and useful criterion. We will call Eq. (2.13), or, focusing on electromagnetic (radiative) energy only, Eq. (2.15), *Poynting's theorem* and $\mathbf{S} = \mathbf{S}_e$ the *(electromagnetic) Poynting vector* although Poynting originally gave (Poy84)

$$\mathbf{E}\dot{\mathbf{D}} + \mathbf{H}\dot{\mathbf{B}} + \operatorname{div}\mathbf{S}_e = -\mathbf{j}_{\mathrm{ext}}\mathbf{E}\,, \qquad\qquad \mathbf{S}_e = \mathbf{E}\times\mathbf{H}\,. \tag{2.17}$$

This definition is widely followed. However, in *P-1* we point out that it does not fully separate electromagnetic from mechanical energy, as is obvious from the induced currents missing in the dissipation on the r.h.s., and argue that this leads to problems with the definition of an appropriate field energy density U_e and reduces the applicability of the equation in Poynting's original form. Even Landau and Lifshitz relied on this form and conclude after an elaborate discussion of various approximations that they cannot give a universal expression for the energy density (LL60, pp. 298–302).

2.2.3 Vector potential and gauge

The form of Maxwell's equations allows to represent the electric and magnetic fields by two potentials, the *scalar potential* Φ and the *vector potential* $\mathbf{A}$. This step introduces a redundancy which opens the choice for a *gauge* with convenient properties. For the present work, the Coulomb gauge ($\operatorname{div}\mathbf{A} = 0$) is chosen. It separates longitudinal interactions associated with charge distributions and electrostatic interactions from transverse interactions associated with the fast-oscillating, transverse optical fields. Then fields and potentials are related as follows (CDG89)

$$\mathbf{E}_\perp = -\dot{\mathbf{A}}_\perp \qquad \mathbf{E}_\parallel = -\operatorname{grad}\Phi \qquad \mathbf{B} = \operatorname{rot}\mathbf{A}_\perp \tag{2.18}$$

and the scalar potential turns out to be the Coulomb potential of the charge distribution,

$$\Phi(\mathbf{r},t) = \frac{1}{4\pi\varepsilon_0}\int \mathrm{d}\mathbf{r}'\,\frac{\rho(\mathbf{r}',t)}{|\mathbf{r}-\mathbf{r}'|} \tag{2.19}$$

While the longitudinal interaction gives rise to phonon and plasmon effects, we shall concentrate on the transverse interaction in this work and omit the corresponding vector potential and field index ($\perp$) in the following.

2.2.4 Many-particle Hamiltonian

From the standard Lagrangian of classical electrodynamics, which reproduces the Maxwell–Lorentz equations [Eqs. (2.7),(2.9)], the following standard Hamiltonian for a system of charged particles in an electric field may be obtained (CDG89):

$$\mathcal{H}_1 = \sum_i \frac{\left[\mathbf{p}_i - e_i\mathbf{A}(\mathbf{r}_i)\right]^2}{2m_i} + \sum_i e_i\Phi(\mathbf{r}_i) \tag{2.20}$$

The Hamiltonian of the free transverse field is

$$\mathcal{H}_2 = \frac{\varepsilon_0}{2}\int \mathrm{d}\mathbf{r}\left[\mathbf{E}(\mathbf{r})^2 + c^2\mathbf{B}(\mathbf{r})^2\right]. \tag{2.21}$$

After expansion and second quantization, one obtains (CDG89; HK95; SW02) for the complete Hamiltonian

$$\mathcal{H} = \mathcal{H}_{\text{particle}} + \mathcal{H}_{\text{field}} + \mathcal{H}_{\text{Coul}} + \mathcal{H}_{\text{int},1} + \mathcal{H}_{\text{int},2}\,. \tag{2.22}$$

Its contributions are:

$$\mathcal{H}_{\text{particle}} = \sum_i \int \mathrm{d}\mathbf{r}\,\hat{\Psi}_i^+(\mathbf{r})\left(-\frac{\hbar^2}{2m_i}\Delta\right)\hat{\Psi}_i(\mathbf{r})\,, \tag{2.23}$$

the kinetic energy of the particles, where $\hat{\Psi}_i$ ($\hat{\Psi}_i^+$) are fermionic annihilation (creation) operators for particle species i,

$$\mathcal{H}_{\text{field}} = \sum_{\lambda,\mathbf{q}} \hbar\omega_{\mathbf{q}} \left[\hat{a}^+_{\lambda,\mathbf{q}}\hat{a}_{\lambda,\mathbf{q}} + \frac{1}{2}\right] , \tag{2.24}$$

the field energy, where $\hat{a}_{\lambda,\mathbf{q}}$ ($\hat{a}^+_{\lambda,\mathbf{q}}$) are photonic annihilation (creation) operators for wave vector $\mathbf{q}$ and polarization λ,

$$\mathcal{H}_{\text{Coul}} = \frac{1}{2}\sum_{i,j} e_i e_j \int \mathrm{d}\mathbf{r}\mathrm{d}\mathbf{r}'\, \hat{\Psi}_i^+(\mathbf{r})\hat{\Psi}_j^+(\mathbf{r}')v(\mathbf{r}-\mathbf{r}')\hat{\Psi}_j(\mathbf{r}')\hat{\Psi}_i(\mathbf{r}) , \tag{2.25}$$

the Coulomb interaction energies of the particles with the Coulomb potential $v(r) = 1/(4\pi\varepsilon_0 r)$,

$$\mathcal{H}_{\text{int},1} = -\int \mathrm{d}\mathbf{r}\, \mathbf{j}_0(\mathbf{r})\mathbf{A}(\mathbf{r}) , \tag{2.26}$$

and

$$\mathcal{H}_{\text{int},2} = \sum_i \frac{e_i}{2m_i}\int \mathrm{d}\mathbf{r}\, \rho_i(\mathbf{r})\mathbf{A}^2(\mathbf{r}) , \tag{2.27}$$

the field-particle interactions. Here, $\mathbf{j}_0$ denotes the contribution to the current field operator that is given by the fermion field operators alone and thus yields a linear charge-field interaction $\mathcal{H}_{\text{int},1}$, while currents driven by the electromagnetic field are separated into the nonlinear $\mathcal{H}_{\text{int},2}$.

Up to this point, only internal (induced) charges and currents are considered (i.e., $\rho \equiv \rho_{\text{ind}}$, $\mathbf{j} \equiv \mathbf{j}_{\text{ind}}$ in the above Hamiltonian). For the coupling to an externally controlled perturbation, one may introduce the explicitly time-dependent

$$\mathcal{H}_{\text{ext}}(t) = \int \mathrm{d}\mathbf{r}\, \left(\hat{\rho}_{\text{ext}}(\mathbf{r})\Phi(\mathbf{r},t) - \hat{\mathbf{j}}_{\text{ext}}(\mathbf{r})\mathbf{A}(\mathbf{r},t)\right) . \tag{2.28}$$

Under the condition that the external perturbations behave classically and are not influenced by the internal quantities, i.e., that they obey the classical field equations

$$\Delta\Phi_{\text{ext}}(\mathbf{r},t) = -\frac{1}{\varepsilon_0}\rho_{\text{ext}}(\mathbf{r},t) , \qquad \Box\mathbf{A}_{\text{ext}}(\mathbf{r},t) = -\mu_0\mathbf{j}_{\text{ext}}(\mathbf{r},t) , \tag{2.29}$$

one may equivalently write (HK95; SW02)

$$\mathcal{H}_{\text{ext}}(t) = \int \mathrm{d}\mathbf{r}\, \left(\hat{\rho}(\mathbf{r})\Phi_{\text{ext}}(\mathbf{r},t) - \hat{\mathbf{j}}(\mathbf{r})\mathbf{A}_{\text{ext}}(\mathbf{r},t)\right) . \tag{2.30}$$

2.3 Green's functions for particles and fields

2.3.1 Expectation values and time evolution

The electron-hole plasma is an intrinsic component of the semiconductor and cannot exist on its own. Its properties can only be measured as responses to controlled external perturbations, e.g., in spectroscopic experiments. This fact as well as the structure of the Hamiltonian governing such a system, $\mathcal{H}_{\mathrm{tot}} = \mathcal{H} + \mathcal{H}_{\mathrm{ext}}(t)$, strongly suggest to perform the quantum-statistical analysis within the *Dirac* (or *interaction*) *picture* (CDL77).

At first, one finds from Heisenberg's equation of motion that consideration of the external sources by addition of $\mathcal{H}_{\mathrm{ext}}$ leaves unchanged the equations of motion of the particle operators, while Maxwell's equations for the potential operators are changed in a physically obvious way (DuB67; HK95):

$$\Delta\hat{\Phi}(\mathbf{r},t) = -\frac{1}{\varepsilon_0}\left(\hat{\rho}_{\mathrm{ind}}(\mathbf{r},t) + \rho_{\mathrm{ext}}(\mathbf{r},t)\right) , \qquad \Box\hat{\mathbf{A}}(\mathbf{r},t) = -\mu_0\left(\hat{\mathbf{j}}_{\mathrm{ind}}(\mathbf{r},t) + \mathbf{j}_{\mathrm{ext}}(\mathbf{r},t)\right) . \tag{2.31}$$

In the interaction picture, the free time evolution (i.e., due to $\mathcal{H}$) is considered in the Heisenberg-like evolution of the operators,

$$\bar{O}(t) = \mathrm{e}^{\frac{\mathrm{i}}{\hbar}\mathcal{H}(t-t_0)}\hat{O}(t_0)\mathrm{e}^{-\frac{\mathrm{i}}{\hbar}\mathcal{H}(t-t_0)} , \tag{2.32}$$

while the state is propagated by

$$\hat{S}(t_2,t_1) = \begin{cases} \mathbf{T}_+ \exp\left[-\frac{\mathrm{i}}{\hbar}\int_{t_1}^{t_2}\mathrm{d}\tau\,\bar{\mathcal{H}}_{\mathrm{ext}}(\tau)\right] & t_2 > t_1 \\ \mathbf{T}_- \exp\left[\frac{\mathrm{i}}{\hbar}\int_{t_2}^{t_1}\mathrm{d}\tau\,\bar{\mathcal{H}}_{\mathrm{ext}}(\tau)\right] & t_2 < t_1 \end{cases} , \tag{2.33}$$

where $\mathbf{T}_\pm$ denotes ordering the $\bar{\mathcal{H}}_{\mathrm{ext}}$ factors in the exponential function power series with increasing (decreasing) time arguments, such that the expectation value of $\hat{O}$ is written as

$$\left\langle\hat{O}(t)\right\rangle = \mathrm{Tr}\left\{\hat{\varrho}(t_0)\,\hat{S}(t_0,t)\bar{O}(t)\hat{S}(t,t_0)\right\} . \tag{2.34}$$

In this trace operation, $\hat{\varrho}$ denotes the statistical operator of the (mixed) system and should not be confused with the charge density operator $\hat{\rho}$.

The initial time t_0 should be chosen as $t_0 \to -\infty$, since the vector of state Ψ_0 or the corresponding density operator $\hat{\varrho}$ need to be known for this point in time, but even a stabilizing heat bath at $t_0 > -\infty$ is essentially a perturbation and the resulting state unknown. At $t_0 \to -\infty$, however, perfect thermodynamic equilibrium may be assumed, and the Hamiltonian of the heat bath can be easily considered additionally (Kel03).

The expectation value or *ensemble average* of the operator Maxwell equations (2.31) yields the propagation equation for the *effective fields* (DuB67),

$$\Delta\Phi_{\rm eff}(\mathbf{r},t) = \Delta\left\langle\hat{\Phi}(\mathbf{r},t)\right\rangle = -\frac{1}{\varepsilon_0}\left(\langle\hat{\rho}_{\rm ind}(\mathbf{r},t)\rangle + \rho_{\rm ext}(\mathbf{r},t)\right) \tag{2.35}$$

$$\Box\mathbf{A}_{\rm eff}(\mathbf{r},t) = \Box\left\langle\hat{\mathbf{A}}(\mathbf{r},t)\right\rangle = -\mu_0\left(\left\langle\hat{\mathbf{j}}_{\rm ind}(\mathbf{r},t)\right\rangle + \mathbf{j}_{\rm ext}(\mathbf{r},t)\right) . \tag{2.36}$$

2.3.2 Nonequilibrium Green's function on the double time contour

Both increasing and decreasing time orders appear in the definition of the expectation value, Eq. (2.34). This can be reduced by factorization to positive time order exclusively for the ground state and for vacuum ("vacuum stability condition", $T = 0$). For equilibrium conditions at finite temperatures, the problem can be tackled with the *Matsubara (imaginary time) formalism* (Mah90), but for nonequilibrium systems both types are inevitably needed.

An elegant mathematical trick was proposed by Keldysh (Kel64; Kel03), which allows to keep a close analogy to the usually much simpler equilibrium case: By rewriting Eq. (2.34) as, e.g.,

$$\left\langle\hat{O}(t)\right\rangle = \mathrm{Tr}\left\{\hat{\varrho}\,\hat{S}(-\infty,t)\hat{S}(t,\infty)\hat{S}(\infty,t)\bar{O}(t)\hat{S}(t,-\infty)\right\} , \tag{2.37}$$

the time evolution is distorted to occur on a double time contour $\mathcal{C}$ which runs along the real axis on a chronological and an antichronological branch from $t = -\infty \to +\infty \to -\infty$ (Fig. 2.1). A modified time ordering operator $\mathbf{T}_\mathcal{C}$ is introduced, which also places the operators on the appropriate branch. Physical quantities in $\mathcal{H}_{\rm ext}$ are imagined to be different on both branches at first. After the desired calculations are performed, the *physical limit* ($\langle\hat{O}\rangle_\mathcal{C} \to \langle\hat{O}\rangle$) is taken by identifying these quantities again with the physical $\mathcal{H}_{\rm ext}$ (DuB67).

The averaging recipe on the double time contour also holds for operator products. Then, due to the convention that times on the antichronological branch are always to be considered "later" than those on the chronological branch, four different time orders of an operator pair are possible, giving rise to a 2×2 matrix of possible physical functions, the *Keldysh components*, with different physical contents. These expectation values of operator correlations on the double time contour are the *nonequilibrium* (or *Keldysh*) Green's functions. The name "Green's function" (GF) was obviously chosen *pars pro toto* — we shall see later why it applies for such a general concept.

Let us consider in the remainder of this section as an example the product of two fermion field operators (in the interaction picture), i.e., the *particle Green's function*. The following combinations of operators are possible (the argument $1+$ is an abbreviation for $\{\mathbf{r}_1, t_1+\}$, where $t+$ denotes a time on the upper branch, and $t-$ stands for

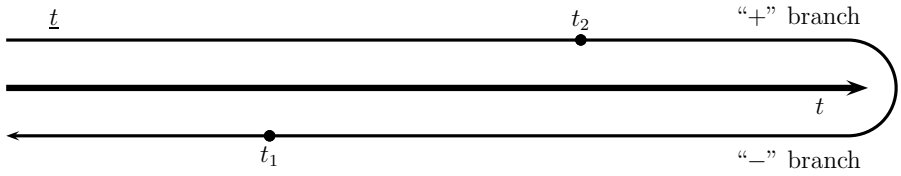

Figure 2.1: The *double time contour* or *Keldysh time contour*. A time on the lower branch is always "later" than one on the upper branch: Even though $t_2 > t_1$ on the real time axis, $\underline{t}_2 < \underline{t}_1$ on the time contour. This case describes $G^{-+}(1,2)$, i.e., the "greater" function, in which the operator order is fixed by the branches and independent of the actual value of the times.

the lower branch, cf. Fig. 2.1):

$$G^{++}(1,2) = G(1+,2+) = -\frac{\mathrm{i}}{\hbar}\left\langle \mathbf{T}_+ \left[\hat{\Psi}(1)\hat{\Psi}^+(2)\right]\right\rangle , \tag{2.38}$$

$$G^{--}(1,2) = G(1-,2-) = -\frac{\mathrm{i}}{\hbar}\left\langle \mathbf{T}_- \left[\hat{\Psi}(1)\hat{\Psi}^+(2)\right]\right\rangle , \tag{2.39}$$

$$G^{+-}(1,2) = G(1+,2-) = +\frac{\mathrm{i}}{\hbar}\left\langle \hat{\Psi}^+(2)\hat{\Psi}(1)\right\rangle , \tag{2.40}$$

$$G^{-+}(1,2) = G(1-,2+) = -\frac{\mathrm{i}}{\hbar}\left\langle \hat{\Psi}(1)\hat{\Psi}^+(2)\right\rangle \tag{2.41}$$

In the former two functions, time ordering can be considered by step functions, while in the latter two functions, time ordering is fixed by the branches, independent of the actual value of t_1, t_2. All four can be combined compactly into the *contour-ordered Green's function*

$$G(\underline{1},\underline{2}) = -\frac{\mathrm{i}}{\hbar}\left\langle \hat{\Psi}(\underline{1})\hat{\Psi}^+(\underline{2})\right\rangle_{\mathcal{C}} = -\frac{\mathrm{i}}{\hbar}\left\langle \mathbf{T}_{\mathcal{C}}\, \hat{\Psi}(\underline{1})\hat{\Psi}^+(\underline{2})\right\rangle , \tag{2.42}$$

where $\underline{1} = \{\mathbf{r}_1, \underline{t}_1\}$ denotes a time on the contour. A convenient matrix-like calculus (Lan76; HJ96) applies for these, which will be addressed later.

Only two of the Keldysh components are independent, so that several identities exist between them. The "greater" ($G^{-+} = G^{>}$) and "less" ($G^{+-} = G^{<}$) functions are often called "correlators" and are directly linked to particle densities, currents and fluctuations. Additionally, one usually defines the *retarded* and *advanced functions* G^{ret} and G^{adv},

$$G^{\mathrm{ret}}(1,2) = \Theta(t_1 - t_2)\left(G^{>}(1,2) - G^{<}(1,2)\right) , \tag{2.43}$$

$$G^{\mathrm{adv}}(1,2) = -\Theta(t_2 - t_1)\left(G^{>}(1,2) - G^{<}(1,2)\right) , \tag{2.44}$$

which are useful to describe responses to perturbations of the system[3], and the *spectral function* $\hat{G}$,

$$\hat{G}(1,2) = G^{>}(1,2) - G^{<}(1,2) = G^{\mathrm{ret}}(1,2) - G^{\mathrm{adv}}(1,2) \tag{2.45}$$

which describes spectral properties (HJ96).

The Green's function technique is considered to be initiated chiefly by Martin and Schwinger (MS59) and put forward by Kadanoff and Baym (KB62), who derived and discussed equations of motion for $G^{\gtrless}$, as well as by Keldysh (Kel64), who developed the nonequilibrium approach presented here, and DuBois (DuB67), who worked out its application to the coupled system of plasma and radiation. An early review which jointly discusses these approaches was given by Danielewicz (Dan84).

2.3.3 The photon Green's function

The nonequilibrium Green's function of the vector potential operator $\hat{\mathbf{A}}$ is called the *photon Green's function (PGF)*. Instead of its definition via operator correlators, it may be introduced equivalently by functional derivation of $\mathbf{A}_{\mathrm{eff}}$ on the double time contour $\mathcal{C}$ (i, j denote vector component indices) (DuB67; HK95):

$$D_{ij}(\underline{1},\underline{2}) = -\frac{1}{\mu_0}\frac{\delta A_{\mathrm{eff},i}(\underline{1})}{\delta j_{\mathrm{ext},j}(\underline{2})} = -\frac{1}{\mu_0}\frac{\mathrm{i}}{\hbar}\left(\left\langle \hat{A}_i(\underline{1})\hat{A}_j(\underline{2})\right\rangle_{\mathcal{C}} - \left\langle \hat{A}_i(\underline{1})\right\rangle_{\mathcal{C}}\left\langle \hat{A}_j(\underline{2})\right\rangle_{\mathcal{C}}\right) \tag{2.46}$$

Note that uncorrelated expectation values $\left\langle \hat{A}_i(\underline{1})\right\rangle_{\mathcal{C}} = A_{\mathrm{eff},i}(\underline{1})$ are explicitly subtracted here. In the particle Green's function G, these terms do not appear, since $\langle\Psi\rangle \equiv 0$.

The photon Green's function appears here as the response of the system to a variation of the perturbation due to external currents.

The functional derivation technique (MS59; DuB67) allows to obtain directly a closed set of equations. In contrast, establishing equations of motion following the Kadanoff–Baym approach (KB62) results in an infinite *(Martin–Schwinger) hierarchy* (MS59) of equations of motion coupled to higher order correlations, requiring a truncation scheme for its further treatment. In either case, the decoupling to a closed set of equations is accomplished by introduction of the *self-energy*, a single quantity into which the higher order correlations, which cannot be determined exactly, are formally combined. For practical purposes, it has to be approximated. The consistency of such approximations is automatically ensured because they enter at a single point in the formalism, and unbalanced approximations are avoided consequently.

The self-energy of the photon Green's function appears in the functional derivation of Eq. (2.36) on $\mathcal{C}$ in the term $\frac{\delta \mathbf{j}_{\mathrm{ind}}}{\delta \mathbf{j}_{\mathrm{ext}}}$, which can be expanded with the help of the chain

[3] For the photon Green's function, we will see that the retarded function *represents* directly the response. For the particle Green's function, this relation is less obvious (HJ96).

rule to

$$\frac{\delta j_{\mathrm{ind},i}(\underline{1})}{\delta j_{\mathrm{ext},j}(\underline{2})} = \sum_k \int \mathrm{d}\underline{3}\, \frac{\delta j_{\mathrm{ind},i}(\underline{1})}{\delta A_{\mathrm{eff},k}(\underline{3})} \frac{\delta A_{\mathrm{eff},k}(\underline{3})}{\delta j_{\mathrm{ext},j}(\underline{2})} = \sum_k \int \mathrm{d}\underline{3}\, P_{ik}(\underline{1},\underline{3}) D_{kj}(\underline{3},\underline{2})\,, \tag{2.47}$$

where the *polarization function*

$$P_{ik}(\underline{1},\underline{3}) = -\mu_0 \frac{\delta j_{\mathrm{ind},i}(\underline{1})}{\delta A_{\mathrm{eff},k}(\underline{3})} \tag{2.48}$$

has been introduced in the role of the self-energy. It can obviously be interpreted as the response of the induced currents in the medium to changes in the effective electromagnetic field. Together with the *inverse, free photon Green's function*

$$D^{-1}_{0,ij}(\underline{1},\underline{2}) = \left(\Delta_{r_1} - \frac{1}{c^2}\frac{\partial^2}{\partial \underline{t}_1^2}\right) \delta(\underline{1}-\underline{2})\,, \tag{2.49}$$

the derivative of Eq. (2.36) can now be written as a closed equation for the Keldysh photon GF:

$$D^{-1}_{0,ij}(\underline{1},\underline{2}) D_{jk}(\underline{2},\underline{3}) = \delta^{\mathrm{T}}(\mathbf{r}_1 - \mathbf{r}_3)\delta(\underline{t}_1 - \underline{t}_3) + P_{ij}(\underline{1},\underline{2}) D_{jk}(\underline{2},\underline{3}) \tag{2.50}$$

Here, the *sum convention* was applied, i.e., summations or integrations over indices and arguments appearing twice on one side of the equation are not written out. The *transverse delta function* δ^{T} (CDG89) results from the derivation of the transverse $\mathbf{j}_{\mathrm{ext}}$. In the following, $\delta^{\mathrm{T}}(\mathbf{r}_1 - \mathbf{r}_3)\delta(\underline{t}_1 - \underline{t}_3)$ will be abbreviated by $\delta(\underline{1}-\underline{3})$.

After rearrangement of Eq. (2.50), one obtains the *Dyson equation* (Dys49)

$$\left(D^{-1}_{0,ij}(\underline{1},\underline{2}) - P_{ij}(\underline{1},\underline{2})\right) D_{jk}(\underline{2},\underline{3}) = \delta(\underline{1}-\underline{3})\,, \tag{2.51}$$

which corresponds to an equation of motion, or, equivalently, in the integral form

$$D_{ij}(\underline{1},\underline{2}) = D_{0,ij}(\underline{1},\underline{2}) + D_{0,ik}(\underline{1},\underline{3}) P_{kl}(\underline{3},\underline{4}) D_{lj}(\underline{4},\underline{2})\,. \tag{2.52}$$

The introduction of $D^{-1} = D_0^{-1} - P$ reveals the matrix identity form of Eq. (2.51) and suggests to identify P with the influence of the matter subsystem on the photons, whose free evolution is determined by D_0^{-1}. Accordingly, D_0 describes the free (non-interacting) system ($P \to 0$). For a further discussion of the physical contents of the quantities introduced here, it is insightful to compare the highly abstract Keldysh formalism case to that of the classical case (DuB67; HK95, *P-2*), which are found to be linked through the retarded component of the contour-ordered Dyson equation. For example, the classical wave propagation equation can be written (in linear approximation, i.e., assuming P does not depend on $\mathbf{j}_{\mathrm{ext}}$) as

$$\mathbf{A}_{\mathrm{eff}}(1) = -\mu_0 D^{\mathrm{ret}}(1,2)\mathbf{j}_{\mathrm{ext}}(2)\,, \tag{2.53}$$

which justifies denoting D as a "Green's function". Then, the relations

$$\mathbf{j}_{\mathrm{ind}}(1) = \frac{\partial}{\partial t_1}\mathbf{P}(1) = -\frac{1}{\mu_0}P^{\mathrm{ret}}(1,2)\mathbf{A}_{\mathrm{eff}}(2)\,, \tag{2.54}$$

$$P^{\mathrm{ret}}_{ij}(1,2) = -\frac{1}{c^2}\frac{\partial^2\chi_{ij}(1,2)}{\partial t_1 \partial t_2}\,, \tag{2.55}$$

where χ is the *susceptibility* (Hal92, Sec. 3.1), show the close relation between the polarization field $\mathbf{P}$ and the GF P, and thus may explain why the latter is called the "polarization function".

Note that through the Dyson equation, identities and symmetries between the Keldysh components of D are directly promoted to D_0, P, and the inverse functions.

A surprisingly similar set of equations with widely similar notions may be obtained for the *longitudinal (plasmon) Green's function* defined in terms of the scalar potential operator $\hat{\Phi}$ (DuB67).

2.3.4 The particle Green's function

The equation of motion of the particle Green's function G [as defined in Eq. (2.42)] in presence of the Hamiltonian [Eq. (2.22)] exhibits second-order correlation terms, giving rise to the hierarchy problem (KB62; KSK05). Similarly to the approach described above for the photon Green's function, these terms may be identified and eliminated with the functional derivatives $\delta G/\delta\rho_{\mathrm{ext}}$ and $\delta G/\delta j_{\mathrm{ext}}$ (DuB67).

In the following, we will ignore the coupling of the particles to the transverse electromagnetic field $\mathbf{A}$ (and thus $\delta G/\delta j_{\mathrm{ext}}$) in the equation of motion (see Jah96), since the transverse interactions in a plasma can be assumed to be usually much weaker than the longitudinal ones in non-relativistic plasmas anyway (DuB67). This step leads to a much simpler set of equations below, but care must be taken to ensure the validity of this assumption. It should be reconsidered especially in the case of lasing or quantum condensation effects. However, even though this work touches these topics, the restriction to longitudinal coupling will be maintained. First essential formal considerations for the inclusion of transverse interactions are given in Appendix A of DuB67.

By rewriting

$$\frac{\delta G(\underline{1},\underline{1}')}{\delta\rho_{\mathrm{ext}}(\underline{1})} = -G(\underline{1},\underline{2})\frac{\delta G^{-1}(\underline{2},\underline{3})}{\delta\rho_{\mathrm{ext}}(\underline{1})}G(\underline{3},\underline{1}') \tag{2.56}$$

one may introduce the *longitudinal self-energy*

$$\Sigma(\underline{1},\underline{1}') = -\mathrm{i}\hbar e G(\underline{1},\underline{2})\frac{\delta G^{-1}(\underline{2},\underline{1}')}{\delta\rho_{\mathrm{ext}}(\underline{1})} \tag{2.57}$$

to obtain from the equation of motion the closed Dyson equation

$$\left(G_0^{-1}(\underline{1},\underline{2}) - \Sigma(\underline{1},\underline{2})\right) G(\underline{2},\underline{1}') = \delta(\underline{1}-\underline{2})\,. \tag{2.58}$$

(Considering $\delta G/\delta \mathbf{j}_{\mathrm{ext}}$ accordingly leads to a *transverse self-energy* contribution.)

In contrast to D_0 in the PGF case, G_0 is not the GF of a completely free particle. Rather, the one-particle energies are contained in it, and it describes the motion of a non-interacting particle in an effective potential (Hartree approximation):

$$G_0^{-1}(\underline{1},\underline{2}) = \left(\mathrm{i}\hbar\frac{\partial}{\partial t_{\underline{1}}} + \frac{\hbar^2}{2m}\Delta_{\mathbf{r}_1} - e\Phi_{\mathrm{eff}}\right)\delta(\underline{1}-\underline{2}) \tag{2.59}$$

Again, the self-energy is a useful quantity for formal considerations but has to be approximated for any further calculation. A path for systematic approximations is opened by the introduction of the *vertex functions*. They emerge from application of the chain rule with respect to Φ_{eff} in the self-energies. In the longitudinal case, we have in Eq. (2.57)

$$\frac{\delta G^{-1}(\underline{1},\underline{1}')}{\delta\rho_{\mathrm{ext}}(\underline{2})} = \frac{\delta G^{-1}(\underline{1},\underline{1}')}{\delta\Phi_{\mathrm{eff}}(\underline{3})}\frac{\delta\Phi_{\mathrm{eff}}(\underline{3})}{\delta\rho_{\mathrm{ext}}(\underline{2})} = -\gamma(\underline{1},\underline{1}',\underline{3})v_s(\underline{3},\underline{2}) \tag{2.60}$$

where the longitudinal vertex function γ and the *screened potential* v_s were introduced. Accordingly, one obtains the transverse vertex function $\mathbf{\Gamma}$ together with the photon GF D in the transverse self-energy. Now, the full self-energy can be obtained by iteration from the zeroth-order ("collisionless") vertex function $\gamma^{(0)}(1,1',3) = e\delta(\underline{1}-\underline{3})\delta(\underline{1}-\underline{1}')$, which arises for $\Sigma = 0$ in Eq. (2.58) (DuB67).

The particle Green's function G as the solution of the Dyson equation contains the full statistical and spectral information about the many-particle system, so that, of course, physical quantities can be extracted from it. One example is the particle or charge density, which with regard to the definition of G is obviously given by $G^<$ for equal arguments,

$$\rho(1) = -\mathrm{i}\hbar e G^<(1,1)\,. \tag{2.61}$$

(See also *P-6*, where this fact serves as the starting point.)

2.3.5 Self-energy approximations for the particle Green's function

Let us briefly classify some frequently applied approximation schemes for the self-energy of the particle GF. Complete neglection of higher-order correlations leads to the *Hartree-Fock approximation*,

$$\Sigma^{\mathrm{HF}} = \Sigma^{\mathrm{H}} + \Sigma^{\mathrm{F}}\,, \tag{2.62}$$

which accounts for a mean field (Hartree) and the exchange interaction (Fock) only. In the GF definition used here, the Hartree component is contained in G_0^{-1} [Eq. 2.59], and the exchange term remains to be specified,

$$\Sigma^{\mathrm{F}}(\underline{1},\underline{2}) = \mathrm{i}v(\underline{1},\underline{2})G(\underline{1},\underline{2})\,, \tag{2.63}$$

where v is the bare Coulomb potential, which is local in time: $v(\underline{1},\underline{2}) = v(\mathbf{r}_1-\mathbf{r}_2)\delta(\underline{t}_1-\underline{t}_2)$. Indeed, the integral form of the Dyson equation shows that the Hartree-Fock approximation gives a simple product of one-particle GFs instead of two-particle correlations:

$$G(\underline{1},\underline{2}) = G_0(\underline{1},\underline{2}) + \mathrm{i}v(\underline{1},\underline{3})G(\underline{1},\underline{3})G(\underline{3},\underline{2})\,.$$

Second, the *random phase approximation (RPA)* for the self-energy is defined as the self-energy resulting from the collisionless vertex function $\gamma^{(0)}$,

$$\Sigma^{\mathrm{RPA}}(\underline{1},\underline{2}) = \mathrm{i}\hbar e^2 G(\underline{1},\underline{2})v_s(\underline{2},\underline{1})\,. \tag{2.64}$$

Other, equivalent names are *linear v_s approximation* or *GW approximation*. It is usually attributed to Hedin (Hed65), who presented it in the context of the one-component electron gas. A fully self-consistent calculation has first been performed by Holm and von Barth (Hv98); a review can be found, e.g., in ORR02. A notable numerical investigation is Sch01, a more recent one For09.

While the RPA through the screened potential v_s is well suited for systems with dominance of collective effects, the *T-matrix approach* is useful to account for binary particle collisions (KB62; KSK05). Both are combined in the *screened ladder approximation*. The *Born approximation* appears as common terms in the iteration of the integral equations for the self-energy in RPA and T matrix approaches (KSK05). For application of the RPA and T-matrix to semiconductors and comparison, see also Sch01.

2.3.6 Summary of the Green's function concept

The Green's function concept as presented here allows to tackle the nonequilibrium description of coupled light-matter systems governed by the highly complicated Hamiltonian (2.22) with a manageable set of equations.

The approach is non-perturbative, and closed equations are obtained not by truncation of the hierarchy of equations coupled to higher order correlations, but rather the self-energies are introduced by functional derivation. The fact that inevitable approximations are performed for a single quantity, the self-energy, ensures the all-important consistency. A recipe for systematic approximations based on the vertex functions exists.

While the transverse self-energy can be traced back to the photon GF, the polarization function as the photon self-energy can be expressed in terms of particle GFs (DuB67; HK95). In this way, the matter and photon subsystems are coupled to each other by the respective self-energies. As is obvious from the consideration of the Hamiltonian in this technique, the contour-ordered GFs D and G together contain in principle the full information about the complete system. However, in practice, the coupling will have to be broken at least partially to provide a starting point for approximations.

Experiments confirm that nonequilibrium Green's functions appropriately describe the quantum kinetics in a charged particle system even on a femtosecond timescale, where semiclassical Boltzmann kinetics can no longer be applied due to coherence and memory effects (HJ96; Hau01).

Chapter 3

Radiation in bounded media systems

3.1 Spatial inhomogeneity and spatial dispersion

The polarization field $\mathbf{P}$ introduced as the time derivative of the induced current $\mathbf{j}_{\mathrm{ind}}$ is generated by the electric field. In a very general picture, this can be described by establishing the relation

$$\mathbf{P}(\mathbf{r},t) = \varepsilon_0 \int \mathrm{d}\mathbf{r}'\mathrm{d}t' \chi(\mathbf{r},\mathbf{r}',t,t';\not{\mathbf{E}})\, \mathbf{E}(\mathbf{r}',t')\,, \tag{3.1}$$

in which the tensor-valued susceptibility function χ determines the strength of the polarization field as the response to the electric field. Then, it represents exactly and fully the microscopic nature of the medium with respect to its response to radiation. Non-linear effects, arising from dependence of χ on $\mathbf{E}$, are an interesting field of research and technology but will be neglected in this work, i.e., the theory is restricted to the *linear response* and, hence, weak fields.

However, it is important to keep the dependence of χ on two times and two positions, so that a delay between the action of $\mathbf{E}$ and the build-up of $\mathbf{P}$ as well as an analogous spatial offset, as for example mediated by finite-size dipoles in the medium, can be modeled (Hal92).

In a *temporally homogeneous* or steady-state system, the delay will not depend on the absolute time of the action. Then, the double time dependence can be entirely replaced by one on $t - t'$, and the Fourier transform $t - t' \to \omega$ of Eq. (3.1) can be taken. One obtains a susceptibility function $\chi(\mathbf{r},\mathbf{r}',\omega)$ describing *temporal* or *frequency dispersion*.

Analogously, the *non-locality* or *spatial inhomogeneity* in χ, i.e., its dependence on two positions, reduces in an infinite (bulk) medium to *spatially homogeneous* dependence on $\mathbf{r} - \mathbf{r}'$. Fourier transformation $\mathbf{r} - \mathbf{r}' \to \mathbf{q}$ yields a susceptibility function $\chi(\mathbf{q},t,t')$ describing *spatial dispersion*. One may explicitly neglect spatial dispersion by setting $\mathbf{q} = 0$ in χ, which is equivalent to a long-wavelength limit. This may be suitable in many cases, where the wave length of $\mathbf{E}$ is much greater than the polarizable units (dipoles). In the vicinity of a surface, however, $\mathbf{E}$ may vary rapidly in space and

thus exhibit short wavelength components. A number of physical effects and problems requiring to consider spatial dispersion, e.g. surface waves, thin films and small particles, are discussed in AG84; Hal92, including the case of excitonic systems, which will be addressed in detail in the following. Two major effects of spatial dispersion in excitonic systems shall be briefly mentioned here beforehand (see Sec. 3.3.3 for details): (i) appearance of additional Fabry–Perot resonances in the absorption spectrum (*P-2*; SKS$^+$08), (ii) appearance of periodic *polariton beats* in the temporal behavior of transmitted light (FKU$^+$91).

Putting away these physical considerations, it is important from the conceptual point of view that χ is taken as spatially inhomogeneous in any global description of a system containing a bounded medium, because of the breach of the translational invariance, or, as a more intuitive argument, since the spatial offset must be allowed to change when approaching (or moving away from) the medium surface, thus requiring a dependence on the absolute position of the action. This will avoid the *a priori* exclusion of possible physical effects from the theory; neglecting the medium boundary in χ also has proven to be error-prone in the discussion of the energy conservation, see the discussion in *P-1*.

3.2 Susceptibility in the excitonic spectral range

Writing the polarization as a superposition of microscopic dipole moments, either classically or as expectation values of the dipole operator, opens several ways for a microscopical description of the susceptibility χ within the two-band model of the semiconductor and in the excitonic spectral range which are of interest here.

Four relevant approaches shall be presented in the following, starting with the simplest, classical one. Trailer effects from processes not contained in the (two-band) model can be subsumed into an effective background contribution χ_{bg}.

3.2.1 Oscillator model

The classical equation of motion for a harmonic dipole oscillator in a driving monochromatic field yields after straightforward calculation (HK90)

$$\chi(\omega) = -\frac{n_{\mathrm{X}} e^2}{2m} \frac{1}{\omega^2 - \omega_0^2 + 2\mathrm{i}\gamma\omega}\,, \tag{3.2}$$

which after employment of the exciton parameters for exciton energy $E_g - E_b = \hbar\omega_0$, reduced mass $m = m_r$, mean exciton density n_{X} and of a phenomenological damping γ already provides a reasonable description of the bulk susceptibility close to the resonance energy. Different exciton number states can be readily considered by super-

position of multiple oscillators (3.2) with appropriate parameters. This result can be confirmed in a quantum-mechanical treatment.

If the kinetic energy of the exciton center-of-mass motion is taken into account [Eq. (2.5)], the susceptibility function (3.2) becomes spatially dispersive, i.e., dependent on the wave vector (FKU$^+$91; Hal92):

$$\chi(\mathbf{q},\omega) = -\frac{n_\mathrm{X} e^2}{2m_r} \frac{1}{\omega^2 - \omega_0^2 - \omega_0 D q^2 + 2\mathrm{i}\gamma\omega}\,, \qquad D = \frac{\hbar}{2m_\mathrm{X}}\,. \tag{3.3}$$

3.2.2 Elliott and Tanguy formulas

For the quantum-mechanical treatment of interband transitions in the two-band model in the context of optical wavelengths, it is reasonable to approximate the general field-charge interaction Hamiltonians $\mathcal{H}_{\mathrm{int},1}$, $\mathcal{H}_{\mathrm{int},2}$ [cf. Eq. (2.22)] as a dipole Hamiltonian

$$\mathcal{H}_\mathrm{int} = \int \mathrm{d}\mathbf{r}\, \hat{\Psi}^+(\mathbf{r})[-e\mathbf{r}]\mathbf{E}(\mathbf{r},t)\hat{\Psi}(\mathbf{r})\,, \tag{3.4}$$

which in the bulk two-band model for monochromatic fields yields (interband dipole moment d_{cv})

$$\mathcal{H}_\mathrm{int} \approx -\sum_\mathbf{q} E(t)\left(a^+_{c,\mathbf{q}} a_{v,\mathbf{q}} d_{cv} + \mathrm{h.c.}\right)\,. \tag{3.5}$$

While this term represents explicitly electronic transitions between bands due to the field, Coulomb scattering of carriers giving rise to interband transitions is neglected in $\mathcal{H}_\mathrm{Coul}$. Then, an equation of motion for the microscopic *interband polarization* $p_{v,c} = \langle a^+_v a_c\rangle$ can be derived from the full Hamiltonian in this representation (HK90; KK06) by splitting up four-operator terms in the sense of a Hartree-Fock approximation into $p_{v,c}$ and the carrier number densities $n_a = \langle a^+_a a_a\rangle$ in the two bands $a = c, v$.

In the limit of an nonexcited semiconductor, i.e., with empty conduction and full valence band, using this equation together with the Wannier equation for the relative motion of electron-hole pairs, a susceptibility function similar to that of the oscillator model is found. The oscillator strength now is given by the absolute squares of the interband dipole moment and of the electron wave function at the origin of the Brillouin cell.

Now, for vanishing damping, a relation for the imaginary part of the susceptibility follows, the so-called *Elliott formula* (Ell57; HK90):

$$\mathrm{Im}\,\chi(E) \propto \frac{1}{E^2}\left[\sum_{n=1}^{\infty} \frac{4\pi E_b^{3/2}}{n^3}\delta\left(E - E_g + \frac{E_b}{n^2}\right) + \frac{2\pi\sqrt{E}\Theta(E-E_g)}{1-\exp\left[-2\pi\sqrt{E_b/(E-E_g)}\right]}\right] \tag{3.6}$$

Its advantage is that not only all exciton number states n are included (first term), but also the contribution of the continuum of unbound scattering states above the band edge E_g is described (second term). The real part of the susceptibility can be obtained by a Kramers-Kronig transform of Eq. (3.6).

Tanguy (Tan95) proposed a way to include a phenomenological damping γ while keeping the formula analytical and leaving the Kramers-Kronig transform possible. The resulting complex function is known as the *broadened Elliott* or *Tanguy formula*. In a later work, Tanguy describes a generalization of this formula to excited media, in which the screening is considered via the Hulthén potential (Tan99).

As in the oscillator model, spatial dispersion follows from taking into account the center-of-mass motion in the exciton energy.

3.2.3 Semiconductor Bloch Equations

While the approaches presented above are valid for the nonexcited semiconductor and can only take into account weak excitation described artificially by damping, the *semiconductor Bloch equations (SBE)* allow calculating the susceptibility with microscopical consideration of the excitation, i.e., the carrier density in the conduction band. The SBEs are the coupled equations of motion for the interband polarization and the carrier densities, in which interaction terms above the Hartree-Fock level are separated out into a collision term (HK90; KK06).

The restriction to the linear response [Eq. (3.1)] allows only negligible changes $\partial n/\partial t$. In a pump-probe experiment, this corresponds to a strong pump pulse generating the excitation and a weak probe pulse for the measurement of the linear response. Thus, we are only interested in the case of quasi-equilibrium with constant carrier densities, and just the kinetic equation for the polarization needs to be solved. It contains now a phase-space filling (Pauli blocking) factor and Fermi functions for the carrier distributions, which link the polarization to the excitation of the system given by its chemical potentials.

The collision term can be expressed by carrier Green's functions, which allows for a further treatment of the many-body effects influencing the polarization, systematic approximations, and, eventually, self-consistent calculations. This is demonstrated and developed further for excitonic systems, e.g., in a series of articles by G. Manzke et al. (MPH$^+$98; NSB$^+$01; MH02; SKS$^+$05), and summarized in *P-6*. Resulting susceptibility functions are shown in Fig. 3.1. Spatial dispersion is considered in the usual way in SKS$^+$05.

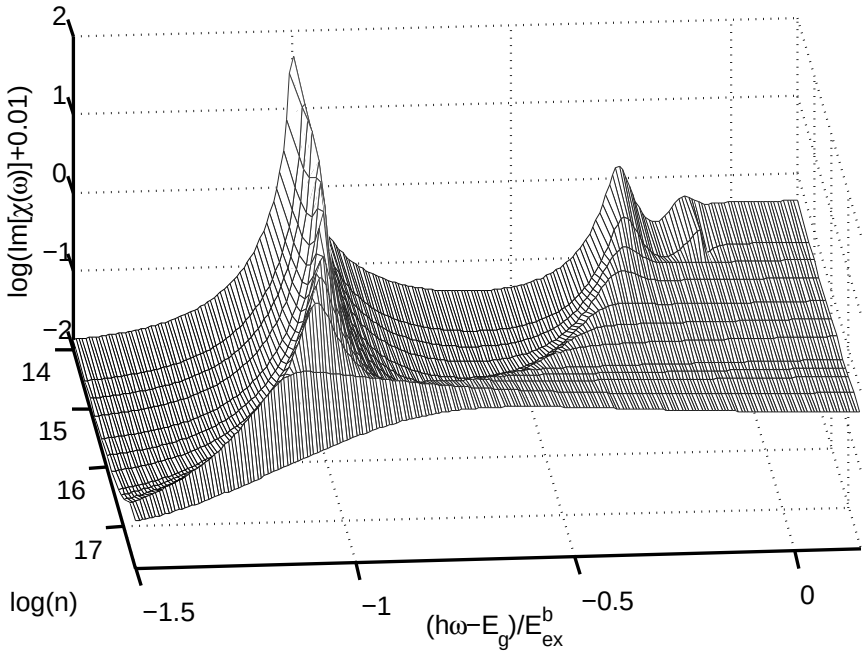

Figure 3.1: Imaginary part of the susceptibility $\chi(\omega)$ calculated with the SBE for different carrier densities n on a logarithmic scale showing distinct excitonic properties (from *P-6*). Energy scale given in excitonic units ($E^b_{ex} = |E_b|$). At low densities, an intense $1s$ exciton resonance can be seen together with weaker higher resonances and a continuum above the band edge. The higher resonances are quickly damped out, and the continuum onset moves down to lower energies. The spectral position and width of the $1s$ resonance changes only at highest carrier densities. There, the spectrum also exhibits negative values at the low frequency end, which give rise to light amplification [cf. Sec. 3.5.4]. – The Tanguy susceptibility (not shown), in comparison, reproduces well the SBE spectrum for vanishing excitation, but overstates the strength of the higher resonances. This can be compensated by consideration of a phenomenological frequency-dependent damping function (Fra03).

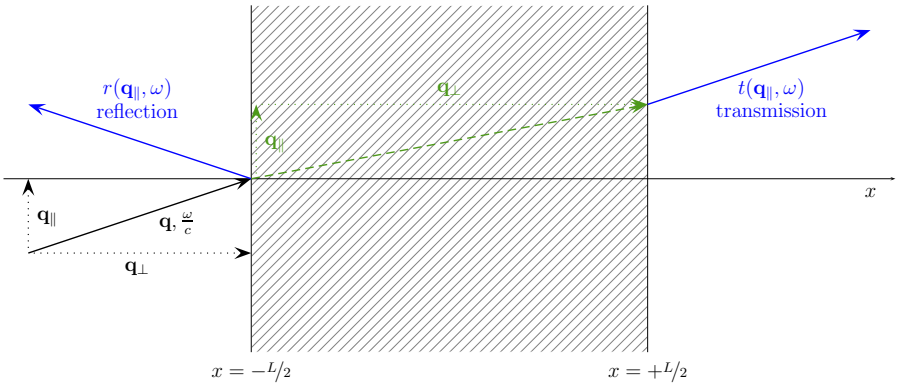

Figure 3.2: Slab geometry and wave vector components of incident, reflected and transmitted light (solid) as well as of a light mode propagating in the medium (dashed) at fixed frequency ω and angle of incidence given by $\mathbf{q}_\parallel$. Not shown are inner reflections, which are nevertheless automatically contained in the theory.

3.2.4 Microscopic bounded media calculation

If surface effects are to be taken into account, one has to resort to a full microscopical calculation of the coupled equation system of the interband polarization together with Maxwell's equations and appropriate microscopic boundary conditions at the surfaces, yielding a spatially inhomogeneous susceptibility (THC$^+$00; SJK$^+$01; MZ02) as depicted, e.g., in SCJ02.

3.3 Classical wave propagation in bounded media systems

In spectroscopic experiments, amplitudes and phases of light emitted or reflected by a medium surface are the key quantities of the measurement. Their quantitative description is, hence, of general interest, but an inherently spatially inhomogeneous problem. In this section, classical approximative solutions shall be briefly presented. Let us at first introduce a convenient quasi-onedimensional geometry adapted to the problem, the *slab geometry*, and the according solution structure for the vector potential (HK95; Hen08b, *P-2*).

3.3.1 Slab geometry

We regard an isotropic medium at $\mathbf{r} = 0$ which is infinitely extended in the y-z direction, has a finite thickness in the x direction and is surrounded by free space. TE-polarized light propagates freely in the transverse direction (Fig. 3.2).

Due to the cylindrical symmetry, we may choose the vector potential in the z direction: $\mathbf{A}_{\text{eff}} = (0, 0, A_{\text{eff}})$, $A_{\text{eff}} =: A$. Maxwell's potential equation (2.53) as well as the Dyson equation for the photon Green's function, Eq. (2.51), become invariant to transverse translations and can be Fourier transformed with respect to $(y, z) \to \mathbf{q}_\parallel$. The medium is assumed to be steadily excited, such that the Fourier transform $t - t' \to \omega$ is possible, too.

The mode decomposition of the vector potential will yield the general form

$$A_{\mathbf{q}}(\mathbf{r}, t) = \exp\left[\mathrm{i}\mathbf{q}_\parallel\mathbf{r}_\parallel - \mathrm{i}cqt\right] A_{\mathbf{q}}(x) \tag{3.7}$$

for the modes. The homogeneous wave equation can now be written as

$$\int \mathrm{d}x' \left[\left(\frac{\partial^2}{\partial x^2} + q_\perp^2(x)\right)\delta(x - x') + \frac{\omega^2}{c^2}\chi(x, x', \mathbf{q}_\parallel, \omega)\right] A(x', \mathbf{q}_\parallel, \omega) = 0\,, \tag{3.8}$$

where $A_{\mathbf{q}}(x)$ and $A(x, \mathbf{q}_\parallel, \omega)$ are related via $\mathbf{q} = q_\perp\mathbf{e}_x + \mathbf{q}_\parallel$, such that $\mathbf{q}_\parallel = 0$ for normal incidence. The in-plane wave vector $\mathbf{q}_\parallel$ and the frequency ω are considered as outer parameters, and may be suppressed in the following for brevity. The $\mathbf{q}$ component in x direction, $q_\perp$, adapts to $\mathbf{q}_\parallel$ and ω according to the wave vector *dispersion relation* $\mathbf{q} = \mathbf{q}(\omega, x)$.

Furthermore, the global susceptibility function takes the form

$$\chi(x, x', \mathbf{q}_\parallel, \omega) \to \Theta(L/2 - |x|)\chi(x, x', \mathbf{q}_\parallel, \omega)\Theta(L/2 - |x'|)\,, \tag{3.9}$$

where L is the thickness of the slab defined such that any polarization (or Keldysh component of the polarization function) vanishes outside.

3.3.2 Solution structure for the vector potential

As a consequence of Eq. (3.9), Eq. (3.8) can be regarded separately for $|x| < L/2$ (inside the medium) and $|x| > L/2$ (outside). In the free space, where simply $q = \omega/c$, the solution for light incident from the left ($x < 0$) is (Fig. 3.2)

$$A(x, \mathbf{q}_\parallel, \omega) = \begin{cases} \exp(\mathrm{i}q_\perp x) - r(\mathbf{q}_\parallel, \omega)\exp(-\mathrm{i}q_\perp x) & x \le -L/2 \\ t(\mathbf{q}_\parallel, \omega)\exp(\mathrm{i}q_\perp x) & x \ge L/2\,. \end{cases} \tag{3.10}$$

It can be regarded as coming from a source $\mathbf{j}_{\text{ext}}$ at $x = -\infty$. The amplitude is chosen as unity, so that r, t are the reflection and transmission coefficients. They represent the full reflection and transmission, i.e., contributions from inner reflections are contained. The (straightforward) solution structure for multiple incident light waves is described in *P-7*. In *P-2* we have explicitly proven by evaluation of the energy conservation condition that the coefficients r, t are linked to the classical absorptivity $a(\mathbf{q}_\parallel, \omega)$

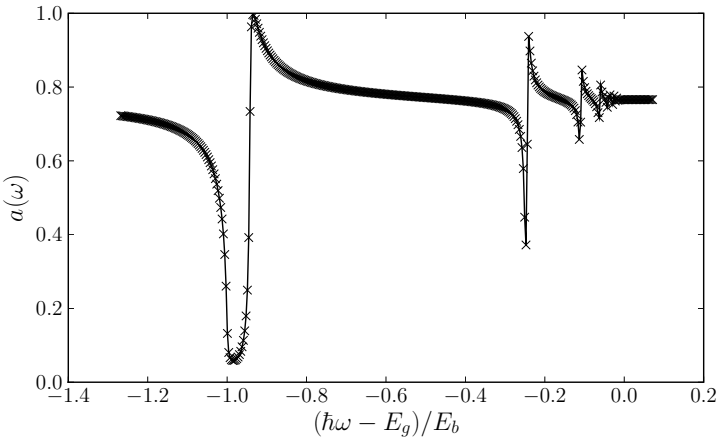

Figure 3.3: *Demonstrational calculation* of the absorptivity $a(\mathbf{q} = 0, \omega)$ in a $50\ \mathrm{cm}$ ZnSe block comparing both sides of Eq. (3.11) to verify the energy conservation in the underlying model (here: bulk approximation with Pekar's ABC's [see Sec. 3.3.3]). In such a thick slab, electrical field strengths are extremely weak, such that arbitrary precision methods need to be used. The calculation yields field strengths on the order of $10^{-10^6} \ldots 10^{-10^3}$ of the incoming field.

of the medium as

$$1 - |r(\mathbf{q}_\parallel, \omega)|^2 - |t(\mathbf{q}_\parallel, \omega)|^2 = a(\mathbf{q}_\parallel, \omega) \\ = \frac{\omega^2}{q_\perp c^2} \mathrm{Im} \int_{-L/2}^{L/2} \mathrm{d}x \mathrm{d}x' A^*(x, \mathbf{q}_\parallel, \omega) \chi(x, x', \mathbf{q}_\parallel, \omega) A(x', \mathbf{q}_\parallel, \omega)\,. \quad (3.11)$$

While the first identity is intuitive, the second is a microscopic foundation for the classical and effective quantity a. As an energy conservation equation, it can serve as a hard criterion for theoretical models and numerical calculations (see Fig. 3.3), and it was used successfully in the check of a model for the polarization in *P-1*.

In contrast, inside the medium, the dispersion relation $\mathbf{q}(\omega, x)$ and, hence, $A_\mathbf{q}$ will depend on the position in a non-trivial way and must be considered unknown unless further assumptions on the susceptibility are made.

A first pragmatic step is the assumption of spatially homogeneous (bulk) properties for the medium. If spatial dispersion is neglected ($\chi \to \chi(\mathbf{q} = 0, \omega)$), the solution of Eq. (3.8) inside the slab is a forward and a backward propagating mode,

$$A(x, \mathbf{q}_\parallel, \omega) = A^+(\mathbf{q}_\parallel, \omega) \exp(\mathrm{i}q_\perp x) + A^-(\mathbf{q}_\parallel, \omega) \exp(-\mathrm{i}q_\perp x)\,, \quad (3.12)$$

with the dispersion relation

$$q^2(\omega) = \frac{\omega^2}{c^2} \left[1 + \chi(\mathbf{q} = 0, \omega)\right]\,; \quad (3.13)$$

if further homogeneous spatial dispersion is allowed ($\chi \rightarrow \chi(\mathbf{q},\omega)$), the dispersion relation becomes transcendent and permits multiple solutions, such that the vector potential is a superposition of multiple modes $\mathbf{q}_i$ propagating in both directions,

$$A(x,\mathbf{q}_\parallel,\omega) = \sum_i \left(A_i^+(\mathbf{q}_\parallel,\omega)\exp(\mathrm{i}q_{\perp,i}x) + A_i^-(\mathbf{q}_\parallel,\omega)\exp(-\mathrm{i}q_{\perp,i}x)\right) . \tag{3.14}$$

The splitting into multiple modes, however, should be considered an artifact of the assumption of spatial homogeneity, since the general solution, Eq. (3.7), exhibits only one mode (with a locally varying wave vector).

In model susceptibilities for the excitonic spectral range, the dispersion branches $q_i(\omega)$ differ significantly from each other as well as from free photonic or free excitonic dispersions. This behavior, due to the coupling of the mechanical exciton motion to light, cannot be described by perturbational approaches and lead to the introduction of the *polariton* as a quasiparticle of the polarization (Hop58). This topic has been studied in depth and shall not be followed further here. See also, e.g., Hal92 for a discussion of the *polariton dispersion* with respect to spatial dispersion.

3.3.3 Spatial dispersion and the boundary condition problem

If the dispersion relation is known, four complex variables remain in the single mode case: the amplitudes of the internal field A^+ and A^-, and the reflectivity and transmittivity coefficients r and t. They are determined by the condition of continuity for the transverse parts of the electromagnetic fields at the medium boundaries $x = \pm L/2$, also known as *Maxwell's boundary conditions*. In the case of TE polarization, this means simply continuity of $A(x)$ and $\partial_x A(x)$. The solution is thus straightforward.

However, in the case of homogeneous spatial dispersion, the system becomes underdetermined by the introduction of additional polariton modes and their corresponding complex amplitudes, and *additional boundary conditions (ABCs)* are needed. The correct choice of the ABCs was subject to debate for several decades since the first proposition of concrete ABCs by Pekar (Pek57), which are derived from the pragmatic assumption of a vanishing polarization at the medium boundaries. Overviews over different ABC schemes discussed over the years are given, e.g., in Hal92 and VP04. Comparisons to numerically expensive microscopical calculations (THC$^+$00; SJK$^+$01; MZ02) indicate that Pekar's ABCs, possibly supplemented by a *dead (polarization free) layer* (SCJ02), give good agreement in several interesting cases.

Yet, due to their artificial nature, there is no microscopic foundation for the ABCs. We were able to show that energy conservation is ensured independently of particular ABCs by Maxwell's boundary conditions alone (*P-1*), as was questioned for the *dielectric approximation (DA)* ABCs (MM73; BM76; VP04). So the choice is, in principle, free, but introduces some arbitraryness into the problem. It is thus desirable to employ ABCs that are free of (phenomenological) assumptions but arise solely from the prop-

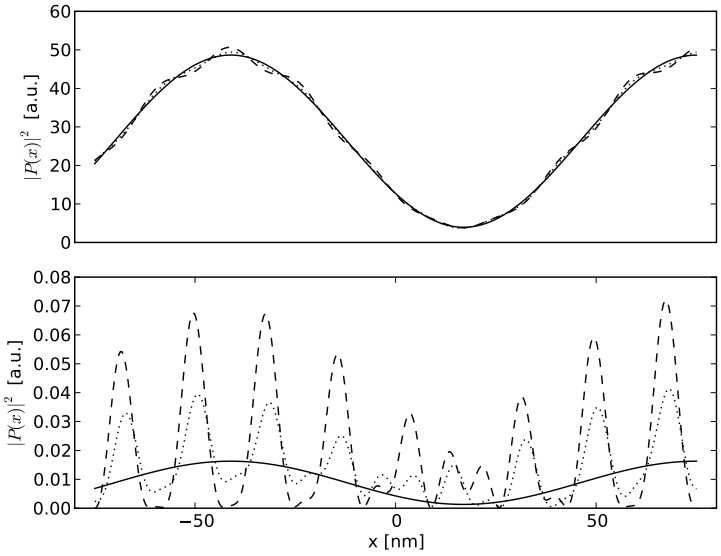

Figure 3.4: Spatial dependence of the polarization field strength in a GaAs slab of length $L = 150\,\mathrm{nm}$ at $\hbar\omega = 1520\,\mathrm{meV}$ slightly above the $1s$ exciton resonance at $1515\,\mathrm{meV}$. Upper panel: including background contribution, lower panel: excitonic oscillator contribution only. – Solid line: without spatial dispersion, dotted: DA ABCs, dashed: Pekar's ABCs. The decay of the Pekar polarization at the boundaries is visible; the DA polarization has less pronounced peaks and does not fully decay at the boundaries.

erties of the susceptibility. Two examples for such ABCs are the delta-source approach (Hen98) and the dielectric approximation (MM73; Flo08), but, in the mentioned comparisons, these yield results inferior to Pekar's.

With regard to excitonic susceptibilities, the consideration of homogeneous spatial dispersion leads to additional peaks in the absorptivity spectrum $a(\mathbf{q}_\parallel, \omega)$, which can be explained as Fabry–Perot resonances of the additional polariton branches or by quantization of the exciton motion due to the confining polarization decay at the surfaces. Example absorption spectra are shown in *P-2* and *P-3*; Fig. 3.4 shows the polarization in a slab for different ABCs and compares them to the behavior without spatial dispersion. The spatial dispersion peaks wash out for longer slabs (broader confinement); for shorter slabs, where the length reaches a low multiple of the exciton Bohr radius, the basis for the homogeneous approximation is certainly not given. As already mentioned, a second manifestation of spatial dispersion is found in the temporal behavior of light pulses transmitted through excitonic media, where interference of polaritons of different branches lead to *polariton beats* (FKU$^+$91).

3.3.4 Polarization in a semiconductor heterostructure

The approach described above can be extended straightforwardly to layers of different slabs, e.g., semiconductor heterostructures. The exciton confinement at the material

interfaces is not as strong as at the surfaces (interface to vacuum), and microscopical calculations show that the dead layer concept is no longer appropriate. To the contrary, the polarization then spills out weakly into the cladding layers (SCJ$^+$04). Nevertheless, macroscopic calculations with Pekar's ABCs and appropriate effective layer thicknesses yield good agreement of field amplitudes and phases with experimental observations (SKS$^+$05; SKS$^+$06; SKS$^+$08).

Often, experimental data leave room for an adjustment or *fit* of parameters like (effective) layer thickness or exciton energies and masses. M. Florian and the author have written a program that is able to dynamically build up the representation of an arbitrary layer system together with different susceptibilities and ABCs, automatically establishes the corresponding boundary condition equation system and solves it, and thus allows to perform, e.g., automated fits.

3.4 Splitting of the photon Green's function

3.4.1 Introduction — the "vacuum polarization"

Classical wave propagation problems, as presented in the preceding section, can be equivalently described by the retarded photon Green's function D^{ret} [see Eq. (2.53)]. The Dyson equation for D^{ret} follows equally as its matrix identity equation or from extraction of the retarded component of the PGF Dyson equation on the Keldysh contour:

$$\left(D_{0,ij}^{-1,\mathrm{ret}}(1,2) - P_{ij}^{\mathrm{ret}}(1,2)\right) D_{jk}^{\mathrm{ret}}(2,3) = \delta_{ik}^{\mathrm{T}}(1-3) \tag{3.15}$$

The quantum-statistically founded Keldysh PGF, however, is much more powerful. Its "greater" and "less" components, given by the PGF (2.46) as

$$\mathrm{i}\hbar\mu_0 D_{ij}^{>}(1,2) = \mathrm{i}\hbar\mu_0 D_{ji}^{<}(2,1) = \langle \hat{A}_i(1)\hat{A}_j(2)\rangle - \langle \hat{A}_i(1)\rangle \langle \hat{A}_j(2)\rangle \ , \tag{3.16}$$

are just the *fluctuations* of the electromagnetic field as the difference of its correlated and uncorrelated expectation values. Thus, $D^{\gtrless}$ can also describe quantum-mechanical phenomena like ground-state fluctuations and spontaneous emission. The fluctuations obey the *kinetic Dyson equation*

$$D_{ik}^{-1,\mathrm{ret}}(1,2) D_{kj}^{\gtrless}(2,3) - P_{ik}^{\gtrless}(1,2) D_{kj}^{\mathrm{adv}}(2,3) = 0 \, , \tag{3.17}$$

which follows from the Keldysh–Dyson equation. Multiplication with D^{ret} yields the *optical theorem* as its formal solution (or *dissipation-fluctuation theorem*, since it links fluctuations $D^{\gtrless}$ to dissipation processes $P^{\gtrless}$ in the medium), which we will temporarily

write as

$$D_{ij}^{\gtrless}(1,2) = D_{ik}^{\mathrm{ret}}(1,3)P_{kl}^{\gtrless}(3,4)D_{lj}^{\mathrm{adv}}(4,2) + D_{h,ij}^{\gtrless}(1,2)\,, \tag{3.18}$$

with the homogeneous ($P \to 0$) solution to the kinetic Dyson equation, $D_h^{\gtrless}$.

In the case of vacuum (absence of media), the PGF reduces essentially to a scalar function in the Fourier domain $(\mathbf{q},\omega)$ due to temporal and spatial homogeneity, and isotropy. Then, the form of D^{ret} can be readily derived as

$$D_0^{\mathrm{ret}}(\mathbf{q},\omega) = \frac{c^2}{(\omega+\mathrm{i}\epsilon)^2 - c^2q^2} = D_0^{\mathrm{adv},*}(\mathbf{q},\omega)\,, \tag{3.19}$$

in which the infinitesimal imaginary displacement $\propto \epsilon \to +0$ is added to ensure causality (Tol56). Equation (3.17) now suggests to add an additional, infinitesimal contribution to P in order to assure its validity in the vacuum limit $P \to 0, D^{\mathrm{ret}} \to D_0^{\mathrm{ret}}$ (HK95; HK96a; Hen08b):

$$P^{\gtrless}(\omega) \to P^{\gtrless}(\omega) \mp \mathrm{i}\epsilon\Theta(\pm\omega)\frac{2\omega}{c^2} \tag{3.20}$$

This contribution was called "vacuum polarization" or "infinitely weak absorber". Its addition can be justified as being a representation of the homogeneous solution $D_h^{\gtrless}$.

In HK95; HK96a, it was found that this contribution determines the entire electromagnetic emission of the bounded steady-state medium while the remainder cancels out completely, and a theory of the semiconductor emission was build up on this finding. In *P-2*, this theory including its PGF foundations was developed further and extended to exactly consider spatial inhomogeneity in the slab geometry, continuing ideas from Hen08b. The infinitely weak absorber was associated with the photon distribution in the free space, and a nonequilibrium energy flow law was derived.

However, the physical interpretation of the infinitely weak absorber as well as its derivation and mathematical representation by infinitesimally vanishing factors still appeared unsatisfying in view of its important physical role. This situation has changed with the recent finding of a universal property of the photon Green's function in *P-5* and Hen08a, namely its splitting into two contributions connected with sources inside and outside of the medium. The splitting property, its implications and examples for applications are analyzed in depth in *P-5* and *P-7*. In the following, the results will be summarized, and the theory of the emission and the energy flow law described in *P-2* will be presented in the light of the new findings in Sec. 3.5.

A note on terminology: The term "energy flow" will be used for the global picture of energy transport and conversion ruled by Poynting's theorem [Eq. (2.13)], while "energy flux" denotes the physical quantity $\mathbf{S}$.

3.4.2 The splitting property

The splitting property is found to be a universal property of the fluctuations of the light field represented by the greater/less components of the nonequilibrium photon Green's function as defined in Sec. 2.3.3, independent of further assumptions like, e.g., a specific geometry or the state of the medium (*P-5*). To see this, let us start with the Dyson equation in its integral form on the Keldysh contour [Eq. (2.52)],

$$D_{ik}(\underline{1},\underline{2}) = D_{0,ik}(\underline{1},\underline{2}) + D_{0,ij}(\underline{1},\underline{3})P_{jl}(\underline{3},\underline{4})D_{lk}(\underline{4},\underline{2})\,. \tag{3.21}$$

The field-field fluctuations $D^{\gtrless}$ can be extracted from this equation with the help of the *Langreth rules* (Lan76; HJ96) and, after a few rearrangements, already exhibit the split structure:

$$D^{\gtrless} = D^{\gtrless}_{\mathrm{med}} + D^{\gtrless}_{\mathrm{vac}}\,, \tag{3.22a}$$

$$D^{\gtrless}_{\mathrm{med}} = D^{\mathrm{ret}} P^{\gtrless} D^{\mathrm{adv}}\,, \tag{3.22b}$$

$$D^{\gtrless}_{\mathrm{vac}} = \varepsilon_T^{-1,\mathrm{ret}} D_0^{\gtrless} \varepsilon_T^{-1,\mathrm{adv}}\,. \tag{3.22c}$$

These equations are a generalization of the optical theorem [Eq. (3.18)]. The field-field fluctuations appear as composed by two contributions with different sources: The first is the *medium-induced contribution* $D^{\gtrless}_{\mathrm{med}}$ known from Eq. (3.18), which is caused by the medium kinetics, i.e., recombination and generation processes $P^{\gtrless}$ related to charge displacement in the medium.

The second contribution is the *vacuum-induced contribution* $D^{\gtrless}_{\mathrm{vac}}$. Its sources are $D_0^{\gtrless}$, i.e., fluctuations following from the free PGF $D_0(\underline{1},\underline{2})$ and defined in terms of the freely evolving vector potential $\hat{\mathbf{A}}_0$ according to Eq. (3.16). Since they are not induced by medium processes ($P, \mathbf{j}_{\mathrm{ind}}$), they must result from external stimulation ($\mathbf{j}_{\mathrm{ext}}$) and can be considered as light incident on the medium. These free fluctuations are renormalized due to the presence of the medium by the inverse of the *transverse dielectric tensor* $\varepsilon_T^{\mathrm{ret}}$,

$$\varepsilon_T^{\mathrm{ret}} = \delta - D_0^{\mathrm{ret}} P^{\mathrm{ret}}\,, \tag{3.23}$$

which solves the classical wave propagation problem, Eq. (2.36), for an incident classical free wave

$$\Box \mathbf{A}_{\mathrm{ext}}(1) = -\mu_0 \mathbf{j}_{\mathrm{ext}}(1) \tag{3.24}$$

in linear approximation (cf. Sec. 3.1) as

$$\mathbf{A}_{\mathrm{eff}}(1) = \varepsilon_T^{-1,\mathrm{ret}}(1,2)\mathbf{A}_{\mathrm{ext}}(2)\,. \tag{3.25}$$

(See Appendix A of *P-5* for details.)

At this point, we note the following observations and conclusions:

- In this approach, P is left being the pure photon self-energy of the medium without any vacuum contribution whatsoever, as is desirable from a formal point of view, and represents fully and exclusively the electronic processes in the medium.
- The simple structure of Eq. (3.22a) allows to discriminate light by its source, either generated by the medium or by external stimulation, and discuss the different contributions separately.
- Incident light is described as freely evolving fluctuations $D_0^{\gtrless}$ with a global domain. This will provide a valuable starting point for the description of the propagation of quantized light, as demonstrated in the following.
- The renormalization of the incident light to effective waves propagating in the system appears *globally* by the inverse dielectric tensor $\varepsilon_T^{-1,\mathrm{ret}}$ [Eq. (3.25)] appearing in $D_{\mathrm{vac}}^{\gtrless}$, i.e., information about medium boundaries is contained in $\varepsilon_T^{-1,\mathrm{ret}}$.
- Since the dielectric tensor solves the classical wave propagation problem, the propagation of incident fluctuations can always be traced back to classical waves. This includes reflection, absorption and transmission. It will not be affected directly by microscopic generation or recombination processes $P^{\gtrless}$ in the medium but only by the effective (optical) properties of the latter [cf. Eq. (3.23)].
- No assumption is made about the geometry of the system, its temporal behavior, the properties of the matter, or the properties of the light, except for the condition of linearity.
- Since recombination and generation processes in the medium are associated with the creation and annihilation of light quanta, one would intuitively assume that the balance of the medium-induced fluctuations $D_{\mathrm{med}}^{\gtrless}$ is chiefly responsible for the optical behavior. However, its contribution to energy transport is known to cancel out in the steady-state slab geometry, such that $D_{\mathrm{vac}}^{\gtrless}$ alone determines the emission and absorption in this case (see Sec. 3.5, *P-2*).

3.4.3 Propagation of incident quantized light

In *P-5* and *P-7*, the propagation of different types of incident light is studied. For this, a normal mode expansion for the freely evolving vector potential operator (VW06) is applied in $D_0^{\gtrless}(1,2)$,

$$\hat{\mathbf{A}}_0(\mathbf{r}) = \sum_{\lambda\mathbf{q}} \sqrt{\frac{\hbar}{2\varepsilon_0 cqV}}\mathbf{e}_{\lambda\mathbf{q}} \left(\hat{a}_{\lambda\mathbf{q}}\mathrm{e}^{\mathrm{i}\mathbf{qr}} + \hat{a}^{+}_{\lambda\mathbf{q}}\mathrm{e}^{-\mathrm{i}\mathbf{qr}}\right) , \tag{3.26}$$

where $\mathbf{e}_{\lambda\mathbf{q}}$ denote the transverse polarization vectors. The expansion with respect to wave vectors instead of frequencies is chosen since it avoids the inclusion of the dispersion relation problem [cf. Sec. 3.3.2] into the definition of $\hat{\mathbf{A}}_0$ and subsequent considerations.

Using Eq. (3.16), one obtains for $D_0^{\gtrless}(1,2)$:

$$\begin{aligned} D_{0,ij}^{<}(1,2) &= \frac{c}{2\mathrm{i}V}\sum_{\lambda\mathbf{q}}\sum_{\lambda'\mathbf{q}'}\frac{1}{\sqrt{qq'}}\Big\{C_{n,\lambda\mathbf{q}\lambda'\mathbf{q}'}^{<}\,F_{\lambda\mathbf{q},i}(1)F_{\lambda'\mathbf{q}',j}^{*}(2)+C_{n,\lambda\mathbf{q}\lambda'\mathbf{q}'}^{>}\,F_{\lambda\mathbf{q},i}(1)F_{\lambda'\mathbf{q}',j}^{*}(2) \\ &\quad +(C_{a,\lambda\mathbf{q}\lambda'\mathbf{q}'}\,F_{\lambda\mathbf{q},i}(1)F_{\lambda'\mathbf{q}',j}(2)+\ldots\text{ c.c. }\ldots)\Big\} \qquad (3.27a) \\ D_{0,ij}^{>}(1,2) &= \frac{c}{2\mathrm{i}V}\sum_{\lambda\mathbf{q}}\sum_{\lambda'\mathbf{q}'}\frac{1}{\sqrt{qq'}}\Big\{C_{n,\lambda'\mathbf{q}'\lambda\mathbf{q}}^{>}\,F_{\lambda\mathbf{q},i}(1)F_{\lambda'\mathbf{q}',j}^{*}(2)+C_{n,\lambda'\mathbf{q}'\lambda\mathbf{q}}^{<}\,F_{\lambda\mathbf{q},i}(1)F_{\lambda'\mathbf{q}',j}^{*}(2) \\ &\quad +(C_{a,\lambda\mathbf{q}\lambda'\mathbf{q}'}\,F_{\lambda\mathbf{q},i}(1)F_{\lambda'\mathbf{q}',j}(2)+\ldots\text{ c.c. }\ldots)\Big\} \qquad (3.27b) \end{aligned}$$

where

$$\mathbf{F}_{\lambda\mathbf{q}}(1)=\mathbf{e}_{\lambda\mathbf{q}}\,\exp\left[\mathrm{i}(\mathbf{q}\mathbf{r}_1-c|\mathbf{q}|t_1)\right] \qquad (3.28)$$

describe classical plane waves with polarization $\mathbf{e}_{\lambda\mathbf{q}}$ and wave vector $\mathbf{q}$.

The prefactors C are expectation value differences of correlated and uncorrelated creation and annihilation operators in an arbitrary base and thus describe the state of the system:

$$\begin{aligned} C_{n,\lambda\mathbf{q},\lambda'\mathbf{q}'}^{>} &= \langle\hat{a}_{\lambda\mathbf{q}}\hat{a}_{\lambda'\mathbf{q}'}^{+}\rangle-\langle\hat{a}_{\lambda\mathbf{q}}\rangle\langle\hat{a}_{\lambda'\mathbf{q}'}^{+}\rangle\,, \qquad (3.29a) \\ C_{n,\lambda\mathbf{q},\lambda'\mathbf{q}'}^{<} &= \langle\hat{a}_{\lambda\mathbf{q}}^{+}\hat{a}_{\lambda'\mathbf{q}'}\rangle-\langle\hat{a}_{\lambda\mathbf{q}}^{+}\rangle\langle\hat{a}_{\lambda'\mathbf{q}'}\rangle\,, \qquad (3.29b) \\ C_{a,\lambda\mathbf{q},\lambda'\mathbf{q}'} &= \langle\hat{a}_{\lambda\mathbf{q}}\hat{a}_{\lambda'\mathbf{q}'}\rangle-\langle\hat{a}_{\lambda\mathbf{q}}\rangle\langle\hat{a}_{\lambda'\mathbf{q}'}\rangle \qquad (3.29c) \end{aligned}$$

The terms $\propto C_n^{\gtrless}$ are *normal* terms, which depend on the difference variables $(1-2)$ only and are thus spatially and temporally homogeneous. In contrast, the *anomalous* terms $\propto C_a$ depend on $(1+2)$ and thus pertain to inhomogeneous systems.

Application of the commutation relation $[\hat{a}_{\lambda\mathbf{q}},\hat{a}_{\lambda'\mathbf{q}'}^{+}]=\delta_{\lambda\mathbf{q}\lambda'\mathbf{q}'}$ in the expectation values above, which is necessary to obtain normal order in $C_n^{>}$, reveals the contribution of the *spontaneous (ground-state) vacuum fluctuations* to $D_0^{\gtrless}$,

$$D_{0,\mathrm{sp},ij}^{>}(1-2)=D_{0,\mathrm{sp},ij}^{<}(2-1)=\sum_{\lambda\mathbf{q}}\frac{c}{2\mathrm{i}Vq}F_{\lambda\mathbf{q},i}(1)F_{\lambda\mathbf{q},j}^{*}(2)\,, \qquad (3.30)$$

since, in any (mixed) quantum state described by a statistical operator $\hat{\varrho}$,

$$\langle\hat{a}_{\lambda\mathbf{q}}\hat{a}_{\lambda'\mathbf{q}'}^{+}\rangle=\mathrm{Tr}\left\{\hat{\varrho}\,\hat{a}_{\lambda\mathbf{q}}\hat{a}_{\lambda'\mathbf{q}'}^{+}\right\}=\delta_{\lambda\mathbf{q}\lambda'\mathbf{q}'}+\mathrm{Tr}\left\{\hat{\varrho}\,\hat{a}_{\lambda'\mathbf{q}'}^{+}\hat{a}_{\lambda\mathbf{q}}\right\}\,. \qquad (3.31)$$

After separation of $D_{0,\mathrm{sp}}^{\gtrless}$ in both Eqs. (3.27), the remaining terms appear as mutual complex conjugates and are identical for both the greater and the less function. The ground-state fluctuations are invariant, but the remainder depends on the expectation value in the specific base, or, in other words, the state of the system. It has thus to be attributed to the external *stimulation* or preparation of the system. By definition of the

componentless prefactor

$$C_{n,\lambda\mathbf{q}\lambda'\mathbf{q}'} = \langle \hat{a}^+_{\lambda'\mathbf{q}'} \hat{a}_{\lambda\mathbf{q}} \rangle - \langle \hat{a}_{\lambda\mathbf{q}} \rangle \langle \hat{a}^+_{\lambda'\mathbf{q}'} \rangle \tag{3.32}$$

it can be written in a more compact form as

$$D_{0,\mathrm{stim},ij}(1,2) = \frac{c}{2\mathrm{i}V} \sum_{\lambda\mathbf{q}} \sum_{\lambda'\mathbf{q}'} \frac{1}{\sqrt{qq'}} \Big\{ C_{n,\lambda\mathbf{q}\lambda'\mathbf{q}'}\, F_{\lambda\mathbf{q},i}(1) F^*_{\lambda'\mathbf{q}',j}(2) + C_{a,\lambda\mathbf{q}\lambda'\mathbf{q}'}\, F_{\lambda\mathbf{q},i}(1) F_{\lambda'\mathbf{q}',j}(2) + \ldots \text{ c.c. } \ldots \Big\} \,. \tag{3.33}$$

Hence, we find for the free fluctuations $D_0^{\gtrless}$ the general structure

$$D_0^{\gtrless}(1,2) = D_{0,\mathrm{sp}}^{\gtrless}(1-2) + D_{0,\mathrm{stim}}(1,2) \,. \tag{3.34}$$

This enables to distinguish not only between medium- and vacuum-induced contributions to the PGF, but also between those by the ground-state fluctuations and by external stimulation (*P-5*).

The decomposition into spontaneous and stimulated contributions is valid for systems in an arbitrary quantum state. It has been shown in *P-5* from a different perspective, based on the known and invariant form of the spectral function of the vacuum,

$$\hat{D}_0 = D_0^{\mathrm{ret}} - D_0^{\mathrm{adv}} = D_0^{>} - D_0^{<} \,, \tag{3.35}$$

together with Eq. (3.19). Explicit results for the prefactors C or $D_0^{\gtrless}$ in general are presented in *P-5* and *P-7* for a number of different quantum states, including squeezed states. The case of a *Fock (photon number) state* is especially instructive, since the mode population number $n^F_{\lambda\mathbf{q}}$ of the photon bath excited in the free space comes into play:

$$D_{0,\mathrm{stim},ij}(1-2) = \sum_{\lambda\mathbf{q}} \frac{c}{\mathrm{i}Vq}\, n^F_{\lambda\mathbf{q}} \mathrm{Re}\, \Big[F_{\lambda\mathbf{q},i}(1) F^*_{\lambda\mathbf{q},j}(2) \Big] \,. \tag{3.36}$$

It is further shown that all squeezed light states can be described in this approach, and that always a squeezed vacuum contribution is generated in the squeezing operation, corresponding, e.g., to a squeezed Fock state with mode occupation $n^F_{\lambda\mathbf{q}} \to 0$, but equivalent for all kinds of squeezed states.

The approach allows to consider an arbitrary field situation in the free space, since arbitrary states are allowed for $D_0^{\gtrless}$ and the mode expansion allows to select specific propagation directions by means of the weight factors $C_{n,\lambda\mathbf{q},\lambda'\mathbf{q}'}, C_{a,\lambda\mathbf{q},\lambda'\mathbf{q}'}$.

Now, Eq. (3.22c) determines the form of both spontaneous and stimulated fluctuations $D_0^{\gtrless}$ when propagating in presence of a medium. They are simply renormalized according to

$$D_{\mathrm{vac}}^{\gtrless}(1,2) = D_0^{\gtrless}(1,2;\mathbf{F}\to\mathbf{A}) \,, \tag{3.37}$$

i.e., with $\mathbf{F}$ replaced by the effective fields

$$\mathbf{A}_{\lambda\mathbf{q}}(1) = \varepsilon_T^{-1,\mathrm{ret}}(1,2)\,\mathbf{F}_{\lambda\mathbf{q}}(2)\,, \tag{3.38}$$

$$\mathbf{A}^*_{\lambda\mathbf{q}}(1) = \varepsilon_T^{-1,\mathrm{ret}}(1,2)\,\mathbf{F}^*_{\lambda\mathbf{q}}(2)\,, \tag{3.39}$$

which describe propagation of a classical plane wave in the presence of a bounded medium. The fields $\mathbf{A}_{\lambda\mathbf{q}}$ are normal mode expansions of the effective vector potential and solutions of Eq. (3.25).

3.4.4 Energy flow

Furthermore, articles *P-5* and *P-7* consider the absorption and emission of quantized light by bounded media starting from the requirement of energy conservation. For this, Poynting's theorem, Eq. (2.15), is expressed in terms of the photon Green's function by evaluating symmetrized quantum-mechanical expectation values as shown in *P-2* for slab geometry. However, the given relations must be re-assessed to ensure validity in a general (inhomogeneous) case. In all of the following summary, $\langle\hat{\mathbf{A}}\rangle = 0$, i.e., incoherent light, is assumed, while *P-7* describes the case for light with an arbitrary degree of incoherence.

The PGF formulation for Poynting's energy flux vector $\mathbf{S}$ is

$$S_i(1) = \frac{\mathrm{i}\hbar}{2}\frac{\partial}{\partial t_1}\sum_j \Big[\nabla_j(2)\left(D^{>}_{ji}(1,2) + D^{<}_{ji}(1,2)\right) - \nabla_i(2)\left(D^{>}_{jj}(1,2) + D^{<}_{jj}(1,2)\right)\Big]_{2\to 1}\,. \tag{3.40}$$

The splitting of the photon GF [Eq. (3.22a)] translates directly to $\mathbf{S}$:

$$\mathbf{S} = \mathbf{S}_{\mathrm{med}} + \mathbf{S}_{\mathrm{vac}}\,, \tag{3.41a}$$

$$\mathbf{S}_{\mathrm{vac}} = \mathbf{S}_{\mathrm{sp}} + \mathbf{S}_{\mathrm{stim}}\,. \tag{3.41b}$$

This enables us to identify the energy flux contributions caused by ground-state fluctuations and incident light and discuss them separately, no matter what energy flux is caused by processes in the medium.

Explicit relations for the energy flux $S(x)$ of incident light transmitted or reflected by a medium slab are derived in *P-5* and *P-7* with the help of the splitting property. For

example, the energy flux arising from $D_{0,\mathrm{stim}}$ in propagation direction is

$$S_{x,\mathrm{stim}}(1) = -\frac{\hbar c^2}{V}\sum_{\mathbf{q},\mathbf{q}'}\sqrt{\frac{q}{q'}}\mathrm{Im}\,\Big(C_n A_{\mathbf{q}}(x)\frac{\partial}{\partial x}A^*_{\mathbf{q}'}(x)\exp\left[\mathrm{i}(q_\parallel - q'_\parallel)\mathbf{r}_\parallel - \mathrm{i}c(q-q')t\right] \\ + C_a A_{\mathbf{q}}(x)\frac{\partial}{\partial x}A_{\mathbf{q}'}(x)\exp\left[\mathrm{i}(q_\parallel + q'_\parallel)\mathbf{r}_\parallel - \mathrm{i}c(q+q')t\right]\Big)\ . \quad (3.42)$$

It is shown that the scattering is always as follows: The amplitude is attenuated by the absolute square of the classical reflection or transmission coefficients r, t; in an instationary energy flow, also a phase delay of $q_\perp L + 2\arg r$ or $q_\perp L + 2\arg t$ is accumulated. For example, one obtains for the transmitted part of $S_{x,\mathrm{stim}}$ (in the not too restrictive but simplifying case of $C_n, C_a \propto \delta_{\mathbf{q},\mathbf{q}'}$)

$$S^t_{\mathrm{stim}} = \frac{\hbar c^2}{V}\sum_{\mathbf{q}} q_\perp |t_{\mathbf{q}}|^2\left(C_n - |C_a|\cos\left[2q_\perp x - 2cqt + \arg C_a + 2\arg t_{\mathbf{q}}\right]\right)\ . \quad (3.43)$$

3.4.5 Dissipation

The dissipation $W = \mathbf{jE}$ can be conveniently expressed with contour-ordered GFs and the Langreth theorem, yielding:

$$W(1) = \\ \frac{\mathrm{i}\hbar}{2}\frac{\partial}{\partial t_2}\left[P^{\mathrm{ret}}_{ij}(1,3)\left(D^{>}_{ji}(3,2) + D^{<}_{ji}(3,2)\right) + \left(P^{>}_{ij}(1,3) + P^{<}_{ij}(1,3)\right)D^{\mathrm{adv}}_{ji}(3,2)\right]\Big|_{2\to 1}\ . \quad (3.44)$$

After replacing $P^{\mathrm{ret}}, D^{\mathrm{adv}}$ using appropriate Keldysh GF identities [Eq. (2.43)], the time derivative acts on a unit step function introduced this way. The result is a δ term with an equal time commutation of $\hat{\mathbf{A}}$, which thus vanishes. The remaining unit step functions may be factored out respecting $2 \to 1$. We have the fully universal result

$$W(1) = \mathrm{i}\hbar\frac{\partial}{\partial t_2}\int \mathrm{d}\mathbf{r}_3 \int_{-\infty}^{t_1}\mathrm{d}t_3 \sum_{i,j}\left[P^{>}_{ij}(1,3)D^{<}_{ji}(3,2) - P^{<}_{ij}(1,3)D^{>}_{ji}(3,2)\right]\Big|_{2\to 1}\ . \quad (3.45)$$

It decomposes just the same way into medium- and vacuum-induced contributions. We concentrate on the latter one,

$$P^{>}(1,3)D^{<}_{\mathrm{vac}}(3,2) - P^{<}(1,3)D^{>}_{\mathrm{vac}}(3,2) =: w_{\mathrm{vac}}(1,2), \quad (3.46)$$

keeping in mind that it contains an inner $\int \mathrm{d}\mathbf{r}_3 \int_{-\infty}^{t_1}$, and analyze the effect of ground-state fluctuations $D_{0,\mathrm{sp}}$ and of a stimulation in the free space, $D_{0,\mathrm{stim}}$. We find:

$$w_{\mathrm{vac}} = w_{\mathrm{vac,sp}} + w_{\mathrm{vac,stim}} \,, \tag{3.47a}$$

$$\begin{aligned} w_{\mathrm{vac,sp}} &= P^{>} D^{<}_{\mathrm{vac,sp}} - P^{<} D^{>}_{\mathrm{vac,sp}} \\ &= \hat{P} D^{<}_{\mathrm{vac,sp}} - P^{<} \hat{D}_{\mathrm{vac}} \,, \end{aligned} \tag{3.47b}$$

$$w_{\mathrm{vac,stim}} = \hat{P} D_{\mathrm{vac,stim}} \tag{3.47c}$$

Any stimulation will thus lead to an additive component in the absorption/emission which is independent of the medium kinetics but proportional to its spectral function $\hat{P}$. The latter, in turn, can be interpreted as the microscopic absorptivity, at least in a steady-state (*P-2*). Hence, incident stimulated light will never trigger emission by recombination, it is just scattered by the medium [Eq. (3.47c)].

The spontaneous ground-state fluctuations, however, do couple to the medium kinetics and enter into a balance of generation and recombination [Eq. (3.47b)]. On the r.h.s. of Eq. (3.47b), this balance appears as classical scattering of incoming fluctuations [cf. $w_{\mathrm{vac,stim}}$] plus recombinations in the medium, $P^{<}$, triggered by the invariant spectral function of the vacuum-induced contribution. With this last term, obviously a representation of the spontaneous emission is found.

The interplay of fluctuations and medium kinetics in the dissipation will be analyzed in more detail in Sec. 3.5. For this, we will have to leave the general inhomogeneous case and return to steady-state slab geometry. Before doing that, let use conclude this section with a comparison of the present approach to quantum optics theories.

3.4.6 Comparison to quantum-optical approaches

Despite of their many (and experimentally confirmed) successes, the common theories in quantum optics (MW95; VW06) have difficulties to correctly incorporate the effects of absorptive matter on the propagation of quantized radiation. The same can be said about ground-state fluctuations of the field and spontaneous emission. To avoid these problems, effective Maxwell theories are employed, which consider all these effects jointly as "quantum noise" and phenomenologically introduce *noise currents* as their sources (HK96b). Light propagation through bounded media is described, e.g., by *input-output relations* (GW96; VW06), which rely on bulk media approximations.

The present PGF theory, in contrast, is very much a microscopic first-principles theory. It is valid for arbitrary geometries, media and quantum states of light. Spatial inhomogeneity is exactly considered. The ground-state fluctuations appear naturally in the photon operator commutation [Eq. (3.31)]. Through the splitting property, different contributions to the energy flow can be clearly identified. Absorption effects are effortlessly considered in the polarization function. Spontaneous emission is contained

as well [Eq. (3.47b)]. There is, hence, no need for the introduction of noise currents, and an exact correspondence of noise currents to medium currents as Keldysh GFs can be shown (HK95; VVH$^+$08). The drawback of the PGF theory is that, while results are exact in the considered model, the quantized representation of the light is lost, since the PGFs consist exclusively of expectation values.

The results presented above for the energy flow [Eqs. (3.42),(3.43); *P-5*, *P-7*] confirm previously obtained ones for the ground-state fluctuations (HK96b) and squeezed light (VVH$^+$08; VVM$^+$08; AL97; AL99) in slab geometry and generalize them according to the mentioned advantages of the theoretical approach.

Propagation of quantized light through linearly responding matter is also of great interest in the analysis of quantum-optical experiments, since the question arises whether passive optical devices may influence the quantum statistics of the light under study. *P-7* addresses this question by demonstrating the description of light propagation through a beam splitter within the split PGF framework.

3.5 The nonequilibrium energy flow law

A further analytic evaluation of the general PGF equations for energy flux and dissipation [Eqs. (3.40), (3.45)] seems out of reach at first. In the steady-state slab geometry, however, fruitful manipulations are possible due to the symmetries of the setup.

In *P-2*, the energy conservation condition in slab geometry was explored this way, and a quantum-kinetically exact energy flow law for the nonequilibrium was found, which may be seen as a generalization of the Kirchhoff and Planck radiation laws to nonequilibrium. Its derivation and discussion will be summarized in the present section. Thanks to the findings from *P-5* and *P-7*, some of the lengthy and complicated argumentation involved can now be expressed in a much more concise and natural manner. Additionally, a subtle approximation will be used [cf. Eq. (3.59)], which will allow us to focus on the central physical aspects in the derivation. For the full proof, however, it is referred to *P-2*. The different approach taken in this presentation will also reveal some new (unpublished) aspects of the theory.

3.5.1 Derivation

In Poynting's theorem [Eq. (2.15)], the time derivative of the field energy density vanishes in the steady state. Due to the slab geometry, energy can only flow in the x direction, and the evaluation of the integral form at the medium boundaries is very simple, yielding

$$\Delta S = S_x(x = {}^L\!/_2) - S_x(x = -{}^L\!/_2) = -\int_{-L/2}^{L/2} \mathrm{d}x\, W(x)\,. \tag{3.48}$$

The energy flux balance ΔS is determined by the dissipation $W(x) = j(x)E(x)$ and describes the resulting energy flux between the medium and its surrounding. In the case of an emitting medium and vanishing incident light, the energy flux will be equal at both sides (with opposite signs), and ΔS will be positive.

In the following, we will regard S and W as spectrally and directionally resolved quantities $s(\mathbf{q}_\parallel, \omega)$ and $w(\mathbf{q}_\parallel, \omega)$ in the sense of the expanded vector potential $A(x, \mathbf{q}_\parallel, \omega)$ [cf. Sec. 3.3], defined by

$$S(L/2) = \int_0^\infty \frac{\mathrm{d}\omega}{2\pi} \hbar\omega \int \frac{\mathrm{d}^2\mathbf{q}_\parallel}{(2\pi)^2} s(\mathbf{q}_\parallel, \omega) \tag{3.49}$$

$$\int \mathrm{d}x\, W(x) = \int_0^\infty \frac{\mathrm{d}\omega}{2\pi}\, \hbar\omega \int \frac{\mathrm{d}^2\mathbf{q}_\parallel}{(2\pi)^2}\, w(\mathbf{q}_\parallel, \omega)\,, \tag{3.50}$$

and suppress the parameters $\mathbf{q}_\parallel, \omega$ on the r.h.s. of equations for brevity.

The medium- and vacuum-induced contributions to the resolved dissipation are

$$w_{\mathrm{med}}(\mathbf{q}_\parallel, \omega) = \int \mathrm{d}x \int \mathrm{d}x' \left(P^{>}(x, x') D^{<}_{\mathrm{med}}(x', x) - P^{<}(x, x') D^{>}_{\mathrm{med}}(x', x)\right) \tag{3.51}$$

$$w_{\mathrm{vac}}(\mathbf{q}_\parallel, \omega) = \int \mathrm{d}x \int \mathrm{d}x' \left(P^{>}(x, x') D^{<}_{\mathrm{vac}}(x', x) - P^{<}(x, x') D^{>}_{\mathrm{vac}}(x', x)\right)\,. \tag{3.52}$$

For their further evaluation, the spectral function of the vacuum-induced PGF shall be introduced at first. It is given by the GF identity (2.45) as

$$\hat{D}_{\mathrm{vac}} = D^{>}_{\mathrm{vac}} - D^{<}_{\mathrm{vac}} = D^{>}_{\mathrm{vac,sp}} - D^{<}_{\mathrm{vac,sp}}\,. \tag{3.53}$$

From Eq. (3.30) follows an explicit expression in terms of the vector potential (*P-5*),

$$\begin{aligned} \hat{D}_{\mathrm{vac},ij}(1,2) &= \varepsilon^{-1,\mathrm{ret}}_{T,ik}(1,3) \hat{D}_{0,kl}(3,4) \varepsilon^{-1,\mathrm{adv}}_{T,lj}(4,2) \\ &= \sum_{\lambda\mathbf{q}} \frac{c}{2\mathrm{i}Vq} \left[A_{\lambda\mathbf{q},i}(1) A_{\lambda\mathbf{q},j}(2)^* - A_{\lambda\mathbf{q},i}(1)^* A_{\lambda\mathbf{q},j}(2)\right]\,, \end{aligned} \tag{3.54}$$

or, in slab geometry (*P-2*),

$$\hat{D}_{\mathrm{vac}}(x, x', \mathbf{q}_\parallel, \omega) = \frac{1}{2\mathrm{i}q_\perp} [A(x)A^*(x') + A(-x)A^*(-x')]. \tag{3.55}$$

The spectral function of the vacuum, $\hat{D}_0$, is invariant, so $\hat{D}_{\mathrm{vac}}$ depends only on the dielectric tensor $\varepsilon^{\mathrm{ret}}_T$, which represents the properties of the matter. It is, hence, a characteristic function of the system. Second, the distribution function $n^{\gtrless}$ is introduced as

$$n^{\gtrless}(\mathbf{q}_\parallel, \omega) = \frac{D^{\gtrless}_{\mathrm{vac}}}{\hat{D}_{\mathrm{vac}}}\,. \tag{3.56}$$

It obeys $n^> = 1 + n^<$ due to the definition of the spectral function. With regard to the expression for $D_{0,\mathrm{stim}}$ in a Fock state, Eq. (3.36) (see also *P-5*), $n^<$ (or short n) may be immediately interpreted as the photon distribution in the stimulated incident light and, hence, characterizes the external stimulation in the system. A closer look[1] reveals that $n^\gtrless$ includes the ground-state fluctuations as

$$n^\gtrless_{\mathrm{sp}} = \pm\frac{1}{2}\,, \qquad\qquad n^\gtrless = n^\gtrless_{\mathrm{sp}} + n_{\mathrm{stim}}\,. \tag{3.57}$$

In a Fock state, n_{stim} is equivalent to n^F. Because any mixed quantum states can be expanded into a basis of Fock states, we see easily that the distribution $n^\gtrless$ may be regarded as independent of spatial coordinates x, x'.

The situation for the polarization function is similar. Its spectral function $\hat{P}$ in the steady state is a characteristic function of the medium due to Eqs. (2.54) and the symmetry $\chi(x,x') = \chi(x',x)$:

$$\hat{P} = P^> - P^< = P^{\mathrm{ret}} - P^{\mathrm{adv}} = 2\mathrm{i}\mathrm{Im}\,P^{\mathrm{ret}} = -2\mathrm{i}\frac{\omega^2}{c^2}\chi \tag{3.58}$$

In analogy to the above case of the photon distribution $n^\gtrless$ describing the "external" excitation in the system, a distribution for the "internal" excitation states may be introduced,

$$b^\gtrless(x,x',\mathbf{q}_\parallel,\omega) = \frac{P^\gtrless(x,x')}{\hat{P}(x,x')}\,, \tag{3.59}$$

which likewise obeys $b^> = 1 + b^<$. In the following, $b^\gtrless(x,x',\mathbf{q}_\parallel,\omega)$ will be replaced by an effective distribution $b^\gtrless(\mathbf{q}_\parallel,\omega)$ for simplicity.[2]

Then, w_{med} can be rewritten as

$$w_{\mathrm{med}}(\mathbf{q}_\parallel,\omega) = (b^>b^< - b^<b^>)\int \mathrm{d}x_1\mathrm{d}x_2\mathrm{d}x_3\mathrm{d}x_4\hat{P}(x_1,x_2)D^{\mathrm{ret}}(x_2,x_3)\hat{P}(x_3,x_4)D^{\mathrm{adv}}(x_4,x_1) \tag{3.60}$$

and w_{vac} as

$$w_{\mathrm{vac}}(\mathbf{q}_\parallel,\omega) = (b^>n^< - b^<n^>)\int \mathrm{d}x\int \mathrm{d}x'\hat{P}(x,x')\hat{D}_{\mathrm{vac}}(x',x)\,. \tag{3.61}$$

[1] This can be shown by evaluation of the definition for $n^\gtrless$ with Eqs. (26),(28) from *P-5* knowing that $\mathrm{Im}\,n = 0$.

[2] The spatial homogeneity of the internal excitation implied here will, of course, be violated as soon as a slab consisting of different layers is taken into account. *P-2* defines $b^\gtrless(\mathbf{q}_\parallel,\omega)$ as the ratio of (x,x')-integrated, *global* polarization functions $\mathfrak{P}^\gtrless/\hat{\mathfrak{P}}$ and fully considers any possible spatial dependency of the internal excitations in slab geometry this way. This effective distribution $b^\gtrless$ is equivalent to the one used above, and the treatment of w_{vac} does not change much. However, in order to prove the vanishing of w_{med}, a much more elaborate discussion is required (*P-2*, Appendix B).

Now, the prefactor in w_{med} is zero, so the entire medium-induced contribution vanishes, and we only need to consider the vacuum-induced contribution in the following. Its prefactor reduces to $(n-b)$, and the remaining integral can be identified as the classical absorptivity a from Eq. (3.11). We obtain for the resulting energy flux leaving the slab surfaces (ΔS) in spectrally and directionally resolved representation

$$s(\mathbf{q}_\parallel,\omega) = [b(\mathbf{q}_\parallel,\omega) - n(\mathbf{q}_\parallel,\omega)]\, a(\mathbf{q}_\parallel,\omega)\,, \tag{3.62}$$

which represents already the nonequilibrium energy flow law. The energy flux is composed of an emission contribution, $s_e = ba$, and an absorption contribution, $s_a = -na$.

3.5.2 Interplay of light, matter and ground-state fluctuations

If the given incident incoherent radiation field is strong, i.e., for $n \gg b$, measuring the energy flow $s \approx s_a$ would provide the same information as a classical (coherent) reflection-transmission experiment, namely the absorptivity $a = s_a/n$. In the opposite case, $b \gg n \to 0$, the pure emission s_e into the vacuum can be measured, and the nonequilibrium distribution b is accessible to direct observation in experiments (SKS$^+$08, *P-2*).

The absorption s_a describes an energy flux as the response of the medium to the given nonequilibrium distribution n of incident external photons. In contrast, s_e describes the emission of light induced by internal optical excitations.

In the case of absorption ($a > 0$) the contribution of s_a is negative and that of s_e positive. In the presence of gain ($a < 0$), however, s_a becomes the positive contribution of amplified vacuum-induced light, while b changes sign so that s_e stays positive (for details, see *P-2*).

Let us analyze this in more detail. At first, we see the dissipation in Eq. (3.61) as a permanent (steady-state) balance of

- an optical excitation of the medium $b^>$ stimulated by incident photons (thus proportional to $n^< = n$)
- and recombination of optical excitations $b^<$ giving rise to stimulated ($\propto n$) and spontaneous emission ($\propto 1$).

Expressing the prefactor to Eq. (3.61) with the help of Eq. (3.57), we find again the structure of Eq. (3.47a),

$$w(\mathbf{q}_\parallel,\omega) = \left(\frac{1}{2} - b + n_{\mathrm{stim}}\right) a\,. \tag{3.63}$$

If we further assume that an equivalent decomposition is possible for $b^{\gtrless}$, we arrive at

$$w(\mathbf{q}_\parallel, \omega) = \left(2b^{>}_{\mathrm{sp}} n_{\mathrm{stim}} - 2n^{>}_{\mathrm{sp}} b_{\mathrm{stim}}\right)\, a = (n_{\mathrm{stim}} - b_{\mathrm{stim}})\, a\,, \tag{3.64}$$

i.e., the spontaneous ground-state fluctuations in the vacuum and in the medium compensate and do not contribute directly to the net dissipation (confirming quantum-optical theories, cf. HK96b), but they cross-couple to the stimulations. We are left with a semi-classical picture of the energy flux as a superposition of externally and internally stimulated energy fluxes, amplified or damped by a.

However, the presence of the ground-state fluctuations is indispensable for the mere occurrence of emission and absorption: If $n^{\gtrless}_{\mathrm{sp}}, b^{\gtrless}_{\mathrm{sp}}$ were ignored in the prefactor, the entire dissipation would vanish. Furthermore, it is the interplay of internal and external excitation states that leads to a nonzero net dissipation and thus gives rise to a resulting energy flux between the medium and its surrounding, ΔS [Eq. (3.61)]. In contrast, re-emission and re-absorption of internal excitations alone always cancels out, $b^{>}b^{<} - b^{<}b^{>} = 0$. This is just the prefactor that weights the medium-induced contribution to the dissipation [Eq. (3.60)]. Likewise, for the external photons holds $n^{>}n^{<} - n^{<}n^{>} = 0$, and they cannot contribute alone. These latter equations appear as a consequence of the definitions of b and n or, respectively, of their prerequisite, the assumption of a steady-state medium.

Last, it is noteworthy that both emission and absorption are governed by the same classical absorptivity a, even in the case of emission, which can only be understood as an effect of quantum mechanics. Also, it is the same for incoherent and coherent light (as the classical limit).

3.5.3 The Planck and Kirchhoff laws

Kirchhoff's law (Kir60) assumes a medium in thermal equilibrium and also in thermal equilibrium with its surrounding, and states that its emission s_e is proportional to its absorptivity a. This situation corresponds, in terms of the theory presented here, to vanishing net energy flow, $\Delta S = s_e - s_a = 0$, and in consequence, $b = n$.

Kirchhoff also knew that the proportionality factor n, later sometimes called the "Kirchhoff function", is a universal function of the temperature T and the frequency ω of the radiation, but the concrete form of $n(\omega, T)$ was subject to intense scientific debate for several decades.

In 1901, Planck (Pla01) presented his famous formula for the spectral radiance in thermal equilibrium and the corresponding energy density,

$$u(\omega) = \frac{\hbar\omega}{\exp\left(\frac{\hbar\omega}{k_B T}\right) - 1}\,. \tag{3.65}$$

In *P-2*, we show in a brief derivation that the energy flux of photons with this density corresponds to the energy flux $s_e = ba$ with b being a Bose function and $a = 1$ the absorptivity of an ideal *hohlraum*.

Thus, the energy flow law (3.62) can be seen as a generalization of Kirchhoff's and Planck's laws to cases where

- medium and surrounding are in different states ($b \neq n$), and
- the medium and/or the surrounding are in a nonequilibrium steady state.

In contrast to the original law, emission and absorption can be treated independently.

3.5.4 Quasi-equilibrium emission mechanisms and degeneration

In Planck's law, the distribution function of the internal optical excitations b is a Bose function. Indeed, b must always become a Bose function

$$b(\omega, \mu, T) = \frac{1}{\exp\left[\frac{1}{k_B T}(\hbar\omega - \mu)\right] - 1} \tag{3.66}$$

if the matter subsystem is in a thermodynamic quasi-equilibrium state (*P-2*). Then, the chemical potential μ describes the degree of excitation in the system, and for $\mu \to 0$, full thermal equilibrium and the Planck law are met as the limiting case. This behavior follows from the *Kubo–Martin–Schwinger (KMS) condition* (MS59; KB62; KSK05) applied to the polarization function. Thus, internal optical excitations behave always bosonic. This may be surprizing in view of the matter subsystem being fermionic, but it is ensured by the KMS condition regardless of the details of the matter.

This opens the door for a systematic study of the emission $s_e = ba$ and the underlying mechanisms in semiconductors excited to quasi-equilibrium, as presented in *P-2* and *P-3*. For this case, b can be set to a Bose function with the chemical potential μ and temperature T chosen according to the excitation of the medium, and the classical absorptivity a can be calculated as the l.h.s. of Eq. (3.11) from the solution of the boundary condition problem for classical wave propagation (see Sec. 3.3 and Fig. 3.3).

Chemical potential and temperature are reflected in the absorptivity, too, and the latter is connected via the susceptibility function to the Fermi distributions $f(\mu, T)$ of the carriers [cf. Sec. (3.2.3)]. Any semiconductor exhibits in principle an amplifying behavior (*gain*, $a < 0$) for low frequencies and absorbing behavior ($a > 0$) for higher frequencies, and the *crossover* $a = 0$ is found at $\hbar\omega = \mu$. Since the Bose function also switches its sign there, the emission stays positive for all ω. The strength of the gain increases with the excitation. In ZnSe, the gain region reaches the excitonic spectral range only at considerably high carrier densities of around $n_e = 2 \times 10^{17}\ \mathrm{cm}^{-3}$ (*P-2*; *P-6*; Fig. 3.1).

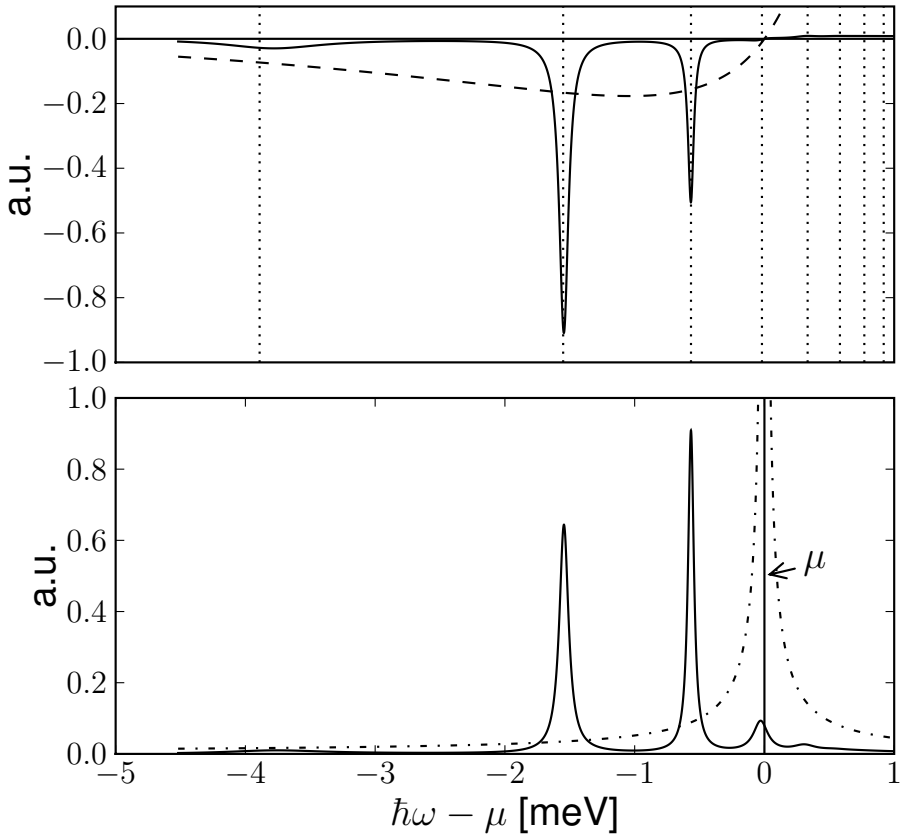

Figure 3.5: Absorptivity and emission spectra in a highly excited ZnSe slab ($L = 1.5\ \mu\mathrm{m}$, $T = 77\ \mathrm{K}$). The carrier density is $n_e = 2 \times 10^{17}\ \mathrm{cm}^{-3}$ and the crossover is at $\mu \approx 2807\ \mathrm{meV}$. The susceptibility was calculated from the SBE [Sec. 3.2.3] and corresponds to the example $\chi^{(4)}$ from *P-2* and *P-3*. Energy scale relative to the crossover energy. Vertical dotted lines mark Fabry–Perot resonance conditions. Upper panel: The dashed line shows $\mathrm{Im}\,\chi(\omega)$, i.e., the "gain". The absorptivity (solid) exhibits pronounced negative peaks located at the resonances, which surpass the absorptivity in the absorbing range by orders of magnitude. They give rise to strong emission peaks $s_e = ba$ (lower panel, solid). The Bose function, whose absolute value is shown in a dash-dotted line, shifts the weights between the emission peaks with respect to the absorptivity.

Figure 3.5 shows compactly the situation in a lasing ZnSe slab. The absorptivity exhibits pronounced negative peaks located at the Fabry–Perot resonances in the slab, which surpass the absorptivity in the absorbing range by orders of magnitude. They give rise to strong emission peaks. The Bose function shifts the weights between the peaks to those closer to the crossover.

Other interesting cases are discussed in *P-2* and *P-3*, e.g., a weakly excited but long slab with $b \ll 1$ in the excitonic spectral range. Its weak but nonzero excitation still produces a considerable emission. Second, a short but strongly excited slab is regarded. The unusual position of the Fabry–Perot resonances in this specific case force the emission to take place predominantly in the absorbing range close above the

crossover, where b is close to its singularity, $b \gg 1$, and gives rise to strong emission exceeding the former example by three orders of magnitude. This effect can be attributed to the degeneracy of the medium excitations ($b \gg 1$) (see articles for respective plots).

3.5.5 Low temperature behavior: Signatures of condensates in the photon Green's function

For $T \to 0$, the Bose function degenerates to a step function. Then, the emission

$$s_e(\omega, \mathbf{q}_\parallel) \to -\Theta(\mu - \hbar\omega) a(\omega, \mathbf{q}_\parallel) \tag{3.67}$$

vanishes completely in the absorption region $\hbar\omega > \mu$ and reflects exactly the gain $-a$ in the gain region $\hbar\omega < \mu$.

At low temperatures, quantum condensation, a topic which will be addressed in Chapter 4 in more detail, can occur in the medium. It should show up in some specific properties of the polarization function, and, in consequence, of the energy flow. This is the theoretical entry point for a possible self-consistent treatment of radiation and condensated matter and for the derivation of optical signatures which allow for experimental verification of quantum condensation and could serve as the "smoking gun" for the Bose–Einstein condensation of excitons whose existence is yet to be proven.

The rigorous particle GF analysis in KSH08, which will be discussed in Sec. 4.1, predicts that an anomalous contribution will appear in addition to the normal generation $P^>$ and recombination $P^<$ (*P-2*)

$$P^{\gtrless}(x, x') \quad \to \quad P^{\gtrless}(x, x') + P_{\mathrm{cond}}(x)\delta_{q_\parallel,0}\delta(x - x')\delta(\hbar\omega - \mu). \tag{3.68}$$

The strength P_{cond} is determined by the fraction of quasiparticles in the condensate. Since it appears identically in both the generation and the recombination, it cancels out in $\hat{P}$ and, consequently, in the classical absorptivity a according to Eqs. (3.11) and (3.58).

Hence, these effects will not appear directly in classical absorption experiments, where at best they show up as smooth changes in the spectral shape of the absorptivity a. However, an additional sharp peak at $\hbar\omega = \mu$ will enter the emission s_e via $b = P^</\hat{P}$ [Eq. (3.59)]. Its strength is $\propto P_{\mathrm{cond}}(x)|A(x)|^2$, and it would give evidence for a condensate, since the normal part of the emission just at this frequency tends towards zero for $T \to 0$ (*P-2*).

3.5.6 Generalization of the results to arbitrary geometries

The symmetry properties of the slab geometry have proven to be an invaluable benefit for the theoretical analysis of wave propagation and energy flow. However, it is a

severe approximation, since an infinite extension of the matter in two dimensions is required. Let us speculate briefly to what extent the exact results presented here can be generalized to more realistic geometries. The derivation of the energy flow law is based on three pillars, which all have to be generalized:

The first one is already accomplished with the derivation of a universal expression for $\hat{D}_{\mathrm{vac}}$, Eq. (3.54), in *P-5*. In *P-2*, the knowledge of the retarded photon GF, D^{ret}, was required to derive it. An expression for D^{ret} in slab geometry, however, could only be shown for restricted coordinate domains, which fortunately were sufficient to derive $\hat{D}_{\mathrm{vac}}$. While this derivation was already very subtle, a more general expression for D^{ret} seems far out of reach.

The second pillar, the proof of the vanishing of D_{med} in the dissipation, seems feasible, too. The path taken in this work does not rely on geometrical properties, nor does the more elaborate derivation in *P-2*, so the proof should be straightforward.

The third is the relation of the microscopic susceptibility and the effective classical absorptivity, Eq. (3.11). Its generalization is, as of yet, completely open. In its current form, this equation was proven by the evaluation of the Poynting vector at the medium boundaries (*P-2*). However, together with the formulation of Maxwell's boundary conditions, this will become a very complex task if curved surfaces are considered.

Chapter 4

The electron-hole plasma at low temperatures

After the detailed study of radiation in bounded media systems in the preceding chapter, we will now turn our attention towards the specific properties of the excited semiconductor and its electron-hole plasma (EHP). The bosonic internal optical excitation states responsible for the emission in this case are the polaritons, i.e., the quasiparticles of the polarization [Sec. 3.3.2] as a coupled state of photon field and matter. Their matter part are electron-hole pairs including, but not restricted to, excitons, which possess integer spin and thus may be described as bosons as well.

Due to the well-known properties of the Bose statistics (Bos24) (and given a reasonable lifetime of the pair states as realized in a quasi-equilibrium state), bosonic systems may develop spontaneous coherence, i.e., a macroscopic number of particles enters a single quantum state (Ein25), corresponding to a *condensation* in the phase space and known as *Bose–Einstein condensation (BEC)*. The properties of such a condensate are exotic and open fascinating experimental possibilities (Ket02; SBR03), however, extreme conditions (high density, low temperature) are necessary for it to be realized. Immediately the question is risen whether quantum condensation can be realized in an EHP. Besides opening new experimental possibilities yet to be explored, this would be a triumph of quantum field theory since the EHP is a rather abstract system and strongly coupled to its surrounding.

Indeed, it was quite early that an excitonic electron-hole plasma was proposed (BBB62) as a promising system for the experimental realization of BEC due to the favorable fact that the masses of its constituents are far lower than those in atomic systems, so that the conditions for condensation — estimated from those of the ideal Bose gas — are reached at relatively high temperatures. However, atomic systems can be isolated and manipulated far more easily than the EHP, and eventually evidence of BEC was found in gases of sodium and rubidium atoms first (AEM$^+$95; DMA$^+$95)[1]. A generally accepted confirmation of excitonic BEC in three-dimensional semiconduc-

[1] It is also to be mentioned that the condensation effects that give rise to the well-known suprafluidity of helium (He^4) are closely connected with the BEC, and that BEC has also been realized in other systems, such as in spin-polarized hydrogen, in the meantime.

tors, however, has not yet been presented despite continuing efforts (Sno02), and the most promising work today focuses on two-dimensional structures, such as coupled quantum wells (EM04; KRK$^+$06), or on exciton traps (BLI$^+$02).

While polaritons as optical excitation states clearly obey Bose statistics in quasi-equilibrium due to the KMS condition [Sec. 3.5.4], in electron-hole pairs the Fermi statistics of the underlying electrons and holes will become important at high densities, and the pair correlation changes drastically or may even be destroyed. In the high-density phase of the EHP, the *electron-hole liquid (EHL)*, cooperative electron-hole pairs may survive at deep enough temperatures, and their Bose condensation to a *Bardeen–Cooper–Schrieffer (BCS)* state, as known from the theory of supraconductivity (BCS57), may be expected. A theory for weakly interacting bosons in general was given by Bogolyubov, stronger interactions and the transition from a BEC to the BCS regime were considered by Keldysh and Kopaev, with notable additions by Nozières. In the following, the details of the condensation itself or the condensed phase will not be considered, and it is referred to MS00 for a joint presentation of these theories and their application to excitonic systems.

Rather, in view of the missing evidence for excitonic BEC, it is interesting to study the conditions for its appearance. In the next section, the paper KSH08, to which the author contributed numerical calculations, will be summarized. It presents an analysis of quantum condensation in EHP on the fermionic particle Green's function level, thus being able to cover both extreme cases of condensation as well as the transition between them, the *BEC-BCS crossover*, regardless of the widely different nature of the two phenomena. This transition is driven by the weakening of the coupling due to the many-particle effects (Coulomb and exchange interactions), whose strengths grow with increasing particle density and decreasing temperature, and leads finally to a breakup of the excitons, which is referred to as the *Mott effect*. For this, papers *P-4* and *P-6*, which are summarized in Sec. 4.2, focus on the quantitative evaluation of the many-particle effects in the excitonic EHP and finally give predictions for the occurrence of the Mott effect, and, hence, for the regions of existence of excitons and of the BEC of ideal (non-interacting) bosons in specific semiconductor materials.

From the experimental point of view, the challenge remains to drive the EHP into the necessary conditions. With resonant optical excitation by lasers, a high initial EHP density can be reached, but diffusion processes may cause a strong decrease. Also, the EHP temperature after excitation may be expected to be much higher than that of the semiconductor lattice, since both are only weakly coupled through phonon interactions. Furthermore, the independent measurement of EHP temperature and density is far from trivial. This is why data from experiments have to be taken with a grain of salt and it is difficult to compare them with theoretical results.

Experimental evidence of the BEC will rely on its specific optical signatures (Sno03). The Green's function approach summarized in Sec. 4.1 helps identifying signatures in the polarization function to be used in the PGF framework for the radiation in bounded media systems (semiconductor samples) [cf. Sec. 3.5.5], and the results presented in

Sec. 4.2 will provide a guideline for the choice of parameters (excitation density, temperature).

4.1 Quantum condensation in electron-hole plasmas

4.1.1 The gap function

Paper KSH08 considers the electron-hole pair correlations by the nonequilibrium two-particle Green's function defined as

$$G_{ab}(\underline{1}\underline{2},\underline{1}'\underline{2}') = \frac{1}{(\mathrm{i}\hbar)^2}\left\langle T_{\mathcal{C}}\,\hat{\Psi}_a(\underline{1})\hat{\Psi}_b(\underline{2})\hat{\Psi}_b^+(\underline{2}')\hat{\Psi}_a^+(\underline{1}')\right\rangle , \tag{4.1}$$

and makes use of a specific asymptotic behavior known for the correlation function in the condensate, namely the appearance of correlations that remain over a asymptotically large time span, or more precisely,

$$G_{ab}(\underline{1}\underline{2},\underline{1}'\underline{2}') = \tilde{G}_{ab}(\underline{1}\underline{2},\underline{1}'\underline{2}') + G_{ab}^{\mathrm{LRO}}(\underline{1}\underline{2},\underline{1}'\underline{2}')\,, \tag{4.2}$$

$$\lim_{\{t_1,t_2\}-\{t_1',t_2'\}\to\infty} \tilde{G}_{ab}(\underline{1}\underline{2},\underline{1}'\underline{2}') = 0\,, \tag{4.3}$$

$$\lim_{\{t_1,t_2\}-\{t_1',t_2'\}\to\infty} G_{ab}^{\mathrm{LRO}}(\underline{1}\underline{2},\underline{1}'\underline{2}') \neq 0\,. \tag{4.4}$$

This behavior is referred to as *time long-range order (TLRO)*. The appearance of a condensate is equivalent to that of a nonvanishing G_{ab}^{LRO}. $\tilde{G}_{ab}$ denotes the normal (non-condensed) phase.

On this basis, it was possible to show for thermodynamic quasi-equilibrium conditions that (underline denoting contour times suppressed in the following)

- G_{ab}^{LRO} is composed of solutions of the homogeneous Bethe–Salpeter equation (KSH08),

$$G_{ab}^{\mathrm{LRO}}(12,1'2') = F_{ab}(12)F_{ab}^*(1'2')\,, \tag{4.5}$$

- the TLRO terms appear equally in the one-particle self-energy,

$$\Sigma_a(1,1') = \tilde{\Sigma}_a(1,1') + \Sigma_a^{\mathrm{LRO}}(1,1')\,, \tag{4.6}$$

  with Σ_a^{LRO} being determined by the *gap function* Δ

$$\Sigma_a^{\mathrm{LRO}}(1,1') = \int_{\mathcal{C}} \mathrm{d}2\mathrm{d}2'\Delta_{ab}(1,2)\Delta_{ab}^*(1',2')G_b(2',2)\,, \tag{4.7}$$

$$\Delta_{ab}(1,2) = \mathrm{i}\hbar v_{ab}^s(1,2)F_{ab}(1,2)\,, \tag{4.8}$$

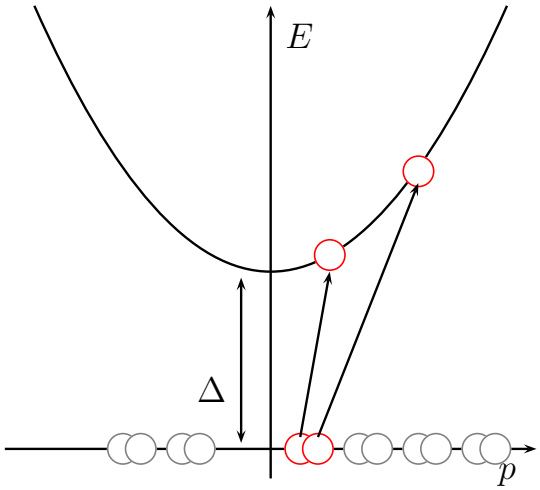

Figure 4.1: The gap function Δ determines the lowest possible one-particle energy and separates excited states on the dispersion parabola from the ground state. The drawing describes the situation in the BCS case.

which is here given with the effective interaction in the Bethe–Salpeter equation approximated by the screened potential v^s (dynamically screened ladder, Sec. 2.3.5),

- and a modified Dyson equation can be established,

$$\left(\mathrm{i}\hbar\frac{\partial}{\partial t_1}+\frac{\hbar^2\nabla_1^2}{2m_a}\right)G_a(1,1')-\int_{\mathcal{C}}\mathrm{d}\bar{1}\left[\tilde{\Sigma}_a(1,\bar{1})+\Sigma_a^{\mathrm{LRO}}(1,\bar{1})\right]G_a(\bar{1},1')=\delta(1-1')\,, \tag{4.9}$$

which describes the coupled dynamics of the condensed and the normal phase, and together with the Bethe–Salpeter equation represents a generalization of the Gorkov equations, known from the theory of superconductivity (AGD63), to nonequilibrium.

4.1.2 The phase boundary

Vanishing of the gap obviously also means vanishing of the condensed phase. The condition $\Delta_{ab} = 0$ thus marks the phase boundary, making the gap become a key quantity of the analysis.

An implicit expression for the gap function for electron-hole systems in quasi-equilibrium can be derived if the normal phase self-energy is taken in a static ap-

proximation (i.e., $\tilde{\Sigma}(\omega)$ does not depend on ω),

$$\Delta_{ab}(\mathbf{p}) = \int \frac{\mathrm{d}\bar{\mathbf{p}}}{(2\pi\hbar)^3} v^s_{ab}(\mathbf{p}-\bar{\mathbf{p}}) \frac{\Delta_{ab}(\bar{\mathbf{p}})}{\sqrt{[e_a(\mathbf{p})+e_b(\mathbf{p})]^2 + 4|\Delta_{ab}(\bar{\mathbf{p}})|^2}} \left[f(E^+(\bar{\mathbf{p}})) - f(E^-(\bar{\mathbf{p}})) \right] , \tag{4.10}$$

where f is the Fermi distribution and

$$E^{\pm}(p) = \frac{1}{2}(e_a - e_b) \pm \sqrt{\frac{1}{4}(e_a+e_b)^2 + |\Delta(p)|^2} \tag{4.11}$$

are renormalized dispersions depending on the quasiparticle energies $e_{a,b}$ (see KSH08 for details). The derivation employs further the *extended quasiparticle approximation (extended QPA)* [cf. *P-6*] for the spectral function of the one-particle GF, $\hat{G}$. The gap function has to be solved consistently with the particle density

$$n_e(\mu, T) = \int \frac{\mathrm{d}\mathbf{p}}{(2\pi\hbar)^3} \frac{\mathrm{d}\omega}{2\pi} \hat{G}_e(\mathbf{p},\omega)\, f(\omega) \,. \tag{4.12}$$

Equation (4.11) suggests the following physical interpretation of the gap: It determines the lowest possible one-particle energy and separates excited states from the ground state. Only if $\Delta > 0$, the ground state is stable and a macroscopic number of particles may condense into it (Fig. 4.1).

Then, the phase boundary has been evaluated in a linearized gap function equation implying $\Delta \to 0$,

$$\Delta_{ab}(\mathbf{p}) = -\frac{e^2}{\varepsilon_0 \varepsilon_r} \int \frac{\mathrm{d}\bar{\mathbf{p}}}{(2\pi\hbar)^3} \frac{\hbar^2}{(\mathbf{p}-\bar{\mathbf{p}})^2 + \hbar^2\kappa^2} \frac{2\Delta_{ab}(\bar{\mathbf{p}})}{e_a(\bar{\mathbf{p}}) + e_b(\bar{\mathbf{p}})} \left\{ 1 - f(e_a(\bar{\mathbf{p}})) - f(e_b(\bar{\mathbf{p}})) \right\} , \tag{4.13}$$

where the *inverse screening length* κ

$$\kappa^2 = \frac{e^2}{\varepsilon_0 \varepsilon_r k_B T} \left(\frac{\partial n_e^{\mathrm{id}}}{\mu_e} + \frac{\partial n_h^{\mathrm{id}}}{\mu_h} \right) , \tag{4.14}$$

defined in terms of ideal ($\Sigma = 0$) densities n^{id}, arises from statical approximation of the screened potential v^s (KKER86; KSK05), and the *Debye approximation* has been used for the one-particle self-energies contained in $e_{a,b}$,

$$\Sigma^D = \Sigma^{\mathrm{HF}} - \frac{\kappa e^2}{2} \,. \tag{4.15}$$

Parameters in KSH08 were taken for a model semiconductor with equal effective electron and hole masses ($m_e = m_h = m_0$, leading to equal chemical potentials) and exciton binding energy $E_b \approx -100\ \mathrm{meV}$ [according to the cuprous oxide ($\mathrm{Cu_2O}$) yel-

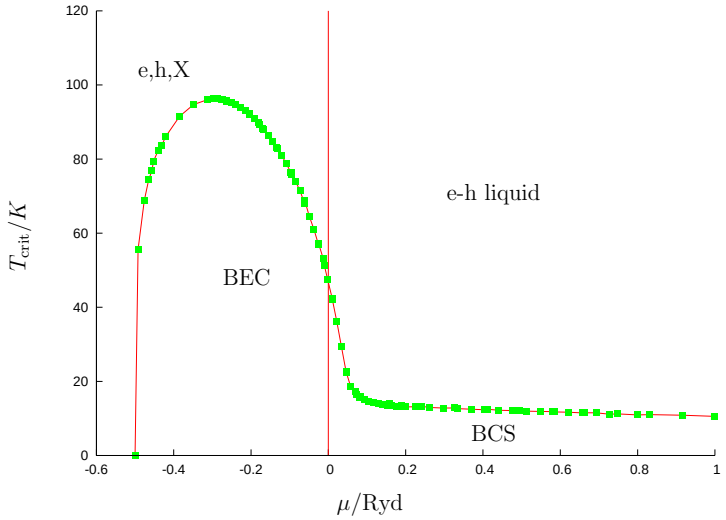

Figure 4.2: Phase boundary of quantum condensation as a function of the chemical potential in a model semiconductor with $m_e = m_h = m_0$. The crossover from BEC of excitons to the BCS condensate of cooperative electron-hole pairs appears as a smooth function.

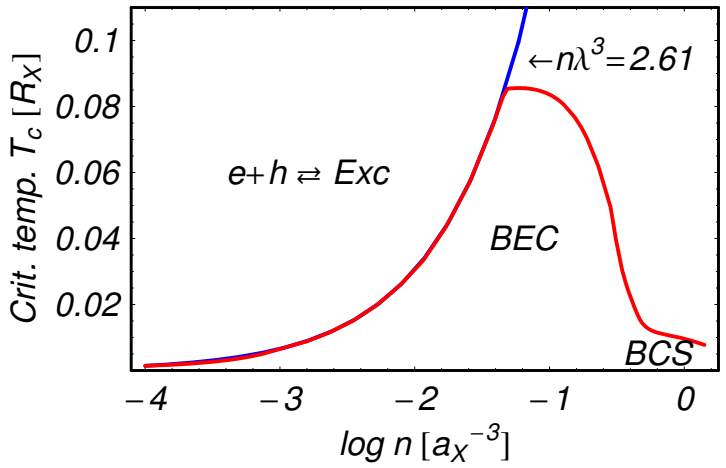

Figure 4.3: Phase boundary of quantum condensation. Mapping of $T_{\rm crit}(\mu)$ to densities given in units of the inverse excitonic Bohr radius $a_{\rm X}$. The phase boundary follows the Bose condensation condition of ideal excitons up to a certain density, then strongly deviates due to the breakup of the excitons, and smoothly crosses over to the BCS regime. From KSH08.

low series $1s$ state but disregarding the extraordinary central-cell correction (Mar92; KCB97)].

The outcome is a function $T_{\rm crit}(\mu)$ describing the onset of quantum condensation. The crossover from BEC of excitons to the BCS condensate of electron-hole pairs appears as a smooth function, in agreement with former work (NS85; BF06). The low-density onset of condensation is at $\mu_e = \mu_h = -0.5$ Ryd. Here, the chemical potential

sum $\mu_e + \mu_h$ reaches the exciton binding energy $E_b = -1\,\mathrm{Ryd}$. Section 4.2 will show that this means that the chemical potential of excitons μ_X will tend towards zero, where their bosonic distribution degenerates [cf. Eq. (4.25)]. Mapping of $T_\mathrm{crit}(\mu)$ to extended QPA densities n yields that the phase boundary indeed follows at first the ideal Bose condensation condition (Fig. 4.3) given by the *critical density*

$$n_\mathrm{crit}(T) = \left(\frac{2\pi m k_B T}{\hbar^2}\right)^{3/2} \zeta(3/2) \qquad\qquad \zeta(3/2) \approx 2.61\,. \tag{4.16}$$

For $\mu > 0$, bound states cannot exist, since the Bose distribution becomes meaningless. Thus, the corresponding vertical line in Fig. 4.2 marks an upper boundary of the existence of excitons. Accordingly, the density mapping shows a strong deviation from the ideal BEC behavior, which must be attributed to the breakup of the bound states (Mott effect). The detailed quantitative analysis of the latter is the objective of *P-6* and is summarized in the next section.

A few additional simple self-energy approximations have been checked numerically. However, in the light of the results from *P-6* (see following section), the choice of Σ in the quasiparticle energies as well as in the $\mu \to n$ mapping should be reconsidered.

4.2 Ionization equilibrium in the excitonic regime

In *P-4*, *P-6* the composition of the electron-hole plasma is regarded in the low excitation regime by an analysis of the particle density $n(\mu, T)$ [Eqs. (2.61), (4.12)], benefitting from prior knowledge about the behavior of the EHP, which is, in principle, well understood (KKER86; Zim88). The interplay of many-particle effects in the EHP is complicated, and its composition, hence, has to date mostly been regarded using simple limiting cases (non-degeneracy, Debye approximation) or rules of thumb (SC95; Kli95). The aim of the mentioned articles is a thorough derivation of the equations governing the plasma composition, an analysis of the influence of the many-particle effects, and to provide quantitatively reliable data for the Mott density as a guideline for BEC experiments.

4.2.1 Particle density in quasiparticle approximation

Just as in Sec. 4.1, papers *P-4*, *P-6* start from the particle density expressed in the GF form, Eq. (4.12). Assuming that the single-particle damping

$$\Gamma_a = 2\,\mathrm{Im}\,\Sigma_a^\mathrm{ret} \tag{4.17}$$

is small ($\Gamma \ll \mathrm{Re}\,\Sigma^\mathrm{ret}$), the spectral function $\hat{G}$ in the particle density is expanded with respect to Γ (extended QPA). Then, the damping is expressed using the screened

ladder approximation. This step introduces binary bound and scattering states via the T-matrix, and finally, a decomposition of the particle density n in the following form is obtained ($n_e = n_h$ due to electroneutrality):

$$n_a = n_{QP} + n_{\mathrm{bound}} + n_{\mathrm{scatt}} \,. \tag{4.18}$$

The first contribution is that of free particles with energies renormalized by the many-particle effects (quasiparticles), for which the RPA is employed,

$$\epsilon_a(\mathbf{k}) = \frac{\hbar^2 k^2}{2m_a} + \Sigma_a^{\mathrm{HF}}(\mathbf{k}) + \mathrm{Re}\,\Sigma_a^{\mathrm{RPA}}(\mathbf{k},\omega)\Big|_{\hbar\omega=\epsilon_a(\mathbf{k})} \,, \tag{4.19}$$

$$n_{QP}(\mu_a, T) = g_a \int \frac{\mathrm{d}\mathbf{k}}{(2\pi)^3} f_a(\epsilon_a(\mathbf{k}), \mu_a, T) \,, \tag{4.20}$$

where g_a is the degeneracy factor and f_a the Fermi distribution. The second contribution is that of bound states,

$$n_{\mathrm{bound}}(\mu_e, \mu_h, T) = g_e g_h \sum_{n,l} (2l+1) \int \frac{\mathrm{d}\mathbf{k}}{(2\pi)^3} \frac{1}{\exp\left[\frac{1}{k_b T}\left(\frac{\hbar^2 k^2}{2(m_e+m_h)} + E_{nl} - \mu_e - \mu_h\right)\right] - 1}, \tag{4.21}$$

where E_{nl} is the bound state energy of the level given by the quantum numbers n, l.

For the scattering contribution n_{scatt}, useful relations can hardly be obtained. Numerical evaluation of the Planck–Larkin terms (KKL84; KSK05) separable from n_{scatt} did not reveal a significant contribution. Since n_{scatt} is expected to become negligible in the low excitation, low temperature regime of interest here anyway, it is neglected in the following.

The total carrier density n_e [Eq. (4.18)] as a function of the chemical potentials μ_e, μ_h and temperature T provides complete thermodynamics of the partially ionized EHP.

At this point it is to be noted that the prerequisites for the extended QPA (i.e., small damping) as well as the neglection of scattering states conflict with the properties of the EHP in the crossover region, since one expects a transition from bound to scattering states driven by increasingly strong many-particle effects. The spectral function, while exhibiting clearly distinguishable peaks and a pair continuum at low damping, will broaden with increasing damping, such that a subdivision into bound and scattering states becomes problematic. However, the present approach can be justified if the Mott transition is an abrupt process.

4.2.2 Chemical picture and mass-action law

P-4 shows that Eq. (4.21) can easily be rewritten as

$$n_{\mathrm{X}}(\mu_{\mathrm{X}},T) = g_{\mathrm{X}} \sum_{n,l} (2l+1) \int \frac{\mathrm{d}\mathbf{k}}{(2\pi)^3} \frac{1}{\exp\left[\frac{1}{k_b T}\left(\frac{\hbar^2 k^2}{2m_{\mathrm{X}}} - \mu_{\mathrm{X}}\right)\right] - 1}\,, \tag{4.22}$$

effectively introducing the exciton [Sec. 2.1.2] as a new particle species in the plasma and fixing its properties as

$$g_{\mathrm{X}} = g_e g_h \tag{4.23}$$

$$m_{\mathrm{X}} = m_e + m_h \tag{4.24}$$

$$\mu_{\mathrm{X}} = \mu_e + \mu_h - E_{n,l}\,. \tag{4.25}$$

The exciton, as introduced here, obviously behaves statistically as an ideal (non-interacting) boson, and the possible singularity of the Bose function gives rise to the BEC phenomenon. The partial density of the excitons is connected with that of free electrons and holes via Eq. (4.25), which plays the role of a *mass-action law (MAL)* for the formation of a chemical (ionization) equilibrium

$$\mathrm{e} + \mathrm{h} \rightleftarrows \mathrm{X} \tag{4.26}$$

between charged and neutral chemical particles in an partially ionized plasma ("chemical picture"). For the characterization of the plasma composition, the *degree of ionization* α is introduced as the share of free and scattering particles in the plasma density,

$$\alpha = \frac{n_e^*}{n_e}\,, \qquad\qquad n_e^* = n_{QP} + n_{\mathrm{scatt}}\,. \tag{4.27}$$

For its calculation, the implicit equation

$$\mu_{\mathrm{X}}[(1-\alpha)n_e, T] = \mu_e[\alpha n_e, T] + \mu_h[\alpha n_e, T] - E_{n,l}[n_e, T] \tag{4.28}$$

is established in *P-4*.

Thus, two important quantities account for the many-particle effects and govern the ionization equilibrium: the chemical potential and the exciton binding energy. Their influence as well as their numerical calculation is addressed in Sec. 4.2.3.

The MAL and the exciton density relation appear obvious and intuitively clear. In the approach of *P-4*, *P-6*, they result from a rigorous quantum statistical derivation in the grand canonical ensemble. Indeed, the MAL has been evaluated before for the case of nondegenerate plasmas of various kinds, where it takes the well-known form of the *Saha equation* (EKK79; KSK05). Notable in this context is the work of Snoke and Crawford (SC95), who analyzed the nondegenerate EHP applying the Debye self-energy [Eq. (4.15)], also with regard to the BEC of excitons. This approach, however,

is far away from the capabilities of modern many-particle theory. In this sense, Eq. (4.28) can be seen as a generalization of the Saha equation to degenerate plasmas.

4.2.3 Effective ionization energy

Chemical potential

The chemical potentials $\mu_{e,h}(n,T)$ that appear in the MAL (4.28) can be obtained from numerical inversion of Eq. (4.20) with a given self-energy approximation. *P-6* compares

1. the Hartree-Fock approximation using $\Sigma(\mathbf{k}) = \Sigma^{\mathrm{HF}}(\mathbf{k})$, with the resulting chemical potential denoted by μ^{HF},
2. the Debye approximation μ^{D} according to Eq. (4.15), which is equivalent to a static limit of the RPA self-energy (*P-6*),
3. an approximation constructed in RZR84 from limiting cases and a few numerical results neglecting damping, denoted by μ^{RZR} (a slightly improved variant of μ^{Z} used in *P-4*),
4. the self-consistent solution of the RPA quasiparticle energy (4.19) with a first iteration of the density (4.20), denoted by μ^{iter} (see *P-6* for details). It is the most advanced approximation and serves as the benchmark in the comparison.

The difference of these chemical potentials to that of an equal ideal Fermi density, μ^{id}, is called the energy *shift* $\Delta\mu$ caused by the many-particle effects, $\mu(n,T) = \mu^{\mathrm{id}}(n,T) + \Delta\mu(n,T)$.[2] The shifts induce a van-der-Waals loop into the non-ideal $\mu(n)$ curves (*P-4*), which may be sign of a phase transition (KSK05).

It is found that the iterative procedure for μ^{iter} reduces both the real and imaginary part of the self-energy. Consequently, the Debye approximation gives a strongly exaggerated shift, while μ^{RZR} comes closer to μ^{iter} but is no satisfying replacement. At a closer look, the Hartree-Fock approximation appears a reasonable limiting case for high degeneracy conditions. This can be understood as the effects of phase-space filling exceeding Coulomb correlation effects.

Binding energy

The exciton binding energy changes only weakly with excitation. This is known from optical experiments with weak probe pulses, in which it can easily be determined

[2] In contrast to the energy shift regarded here, the *rigid shift* is usually defined as a wave-vector-independent approximation for the self-energy, $\Sigma \approx \Sigma(\mathbf{k})$ (Zim88; KSK05). The subtle differences shall not be commented on here.

from the spectra. Also, certain compensation effects in the many-particle interactions leading to a widely unchanged E_b have been pointed out both by analytic arguments and numerical studies (EKK79; MPH$^+$98). Thus, a constant binding energy $E_b = E_{1s} = -1\ \mathrm{Ryd}$, as chosen in *P-4*, is appropriate for low excitation. (We concentrate on the $1s$ state in the following.)

However, the interplay of chemical potential and binding energy in the MAL (4.28) is a very delicate one, and in the studies leading to *P-6* it was found that neglection of the seemingly unimportant contribution of shifts in the exciton energy leads to physically doubtful results (incomplete Mott transition).

The exciton binding energy can be calculated as the eigenvalue of its effective wave equation. In Bloch systems, the semiconductor Bloch equations [Sec. 3.2.3] can be solved equivalently, since both approaches agree for zero center-of-mass momentum (*P-6*). In Fig. 3.1, the binding energy appears as the absolute position of the lowest resonance, while the relative position of the onset of the continuum (*band edge*) is connected with the shift in the chemical potential, $\Delta\mu$.[3]

In *P-6*, we compare band edge shifts and binding energies according to different approximations applied for the collision term in the self-consistent solution of the SBE. The results agree with those for the chemical potential: The Hartree-Fock approximation is suitable for high degeneracy conditions, and the Debye approximation may become appropriate at very high temperatures but at low to room temperatures deviates strongly from the full calculation.

Ionization energy and Mott effect

The energy shifts result in a reduced *effective ionization energy* for the exciton, which is given by the difference between band edge and binding energy (EKK79; KSK05). Vanishing of this energy difference obviously means that bound states cannot exist and excitons must break up (Mott effect). The bound state vanishes and merges into the continuum of scattering states. Thus, the intersection point of band edge and binding energy curves marks the Mott density (Fig. 4.4).

Since we regard the excitons as ideal non-interacting particles [cf. Sec. 4.2.6], it is only the free carrier density n_e^* which enters the shifts. Thus, the Mott density given by the intersection is to be understood as the lower limit of the corresponding density in a partially ionized EHP, for the determination of which the ionization equilibrium (MAL) has to be evaluated.

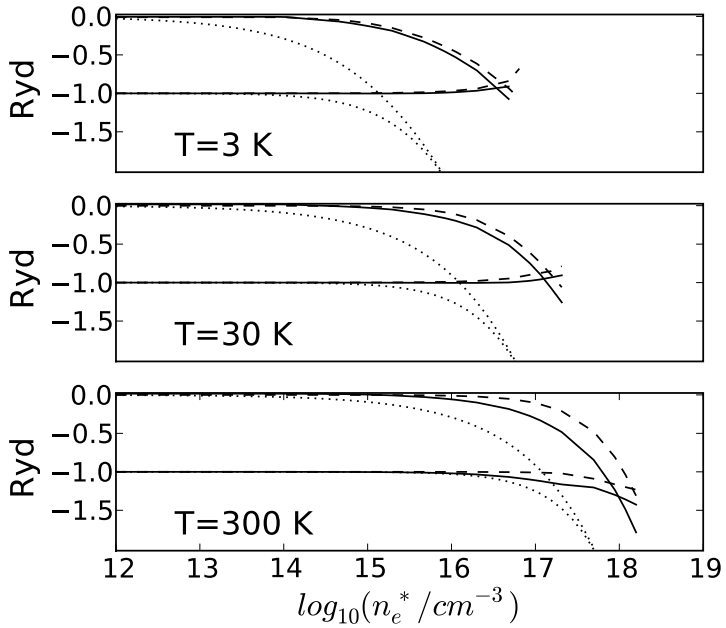

Figure 4.4: Density dependence of the band edge (upper curves) and exciton binding energy (lower curves) for three temperatures in ZnSe. Comparison of the full SBE calculation (solid), Hartree-Fock (dashed) and Debye approximations (dotted).

4.2.4 Ionization equilibrium

The numerical evaluation of the MAL (4.28) in the density-temperature plane (*P-4*, *P-6*) gives a good qualitative overview of the state of the EHP. Figure 4.5 shows calculations for a choice of approximations discussed above. In all of them, the Mott transition from the excitonic phase ($\alpha \approx 0$) to the fully ionized EHL ($\alpha \approx 1$) appears as a process which takes place abruptly with increasing density. Above the Mott density, the foundations of the present theory are, as already mentioned, no longer given. However, the theory may be used to determine this boundary, and above it the system is indeed fully ionized as shown.

With increasing temperature, even at low densities a smooth ionization is observed. This process is due to the increasing kinetic energy of the particles and known as *thermal ionization*. Furthermore, extending the calculation to lower densities, one would equally find a smooth ionization, which is known as *entropy ionization* and can be understood from the nondegenerate Saha equation form of the MAL (EKK79; KSK05).

In Fig. 4.5c, the triangle bordered by the red line denotes the area where conditions for the BEC of ideal excitons are met. The low density side of the triangle is determined by the critical density n_{crit}, which in the double logarithmic scale appears as a straight line. On the high density side, the Mott effect competes with the BEC. However, from

[3]The concrete form of this connection is subject to debate, but both shifts are a representation of the same physical effects and thus may be used synonymously in a qualitative discussion.

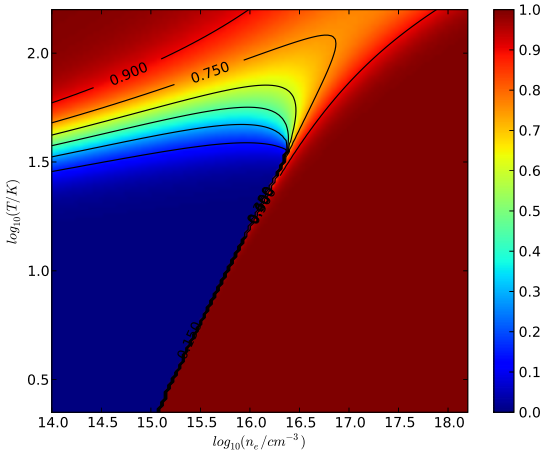

(a) Nondegenerate statistics, chemical potential in Debye approximation μ^D, and constant binding energy $E_b = -1\,\mathrm{Ryd}$. Theoretical level equivalent to the Saha equation calculations of SC95.

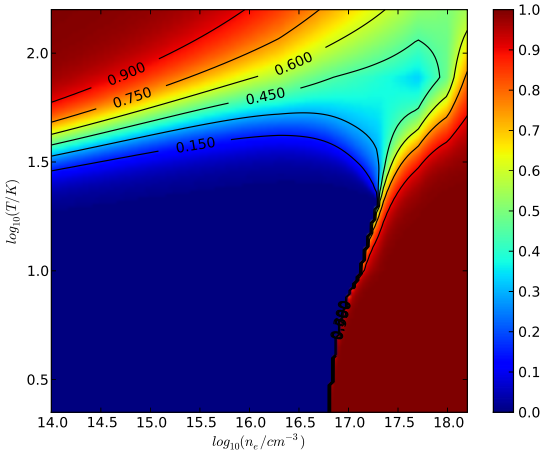

(b) Chemical potential μ^{RZR} according to RZR84, similar to the cuprous oxide calculations in *P-4*, but with improved binding energy $E_b(n_e)$ obtained from the SBE spectrum.

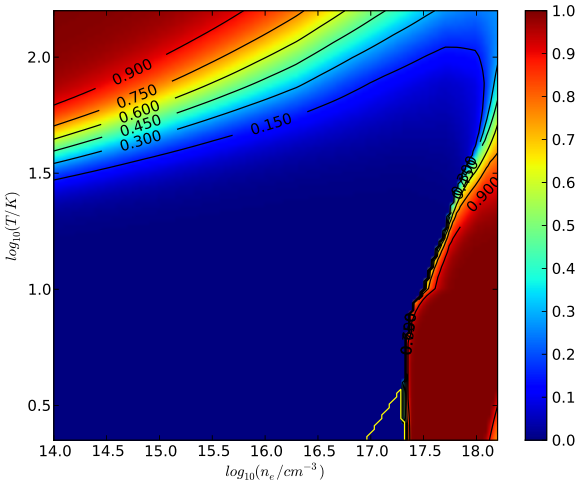

(c) Full calculation as in *P-6*. Chemical potential μ^{iter} and improved binding energy $E_b(n_e)$ from the SBE spectrum.

Figure 4.5: Degree of ionization α in ZnSe in the density-temperature plane, obtained from numerical evaluation of the mass-action law. Comparison of several approximations, showing a vast improvement. In (c), an area where BEC conditions are met appears in the parameter range (red triangle). Only the upper branch of the ionization hysteresis is shown.

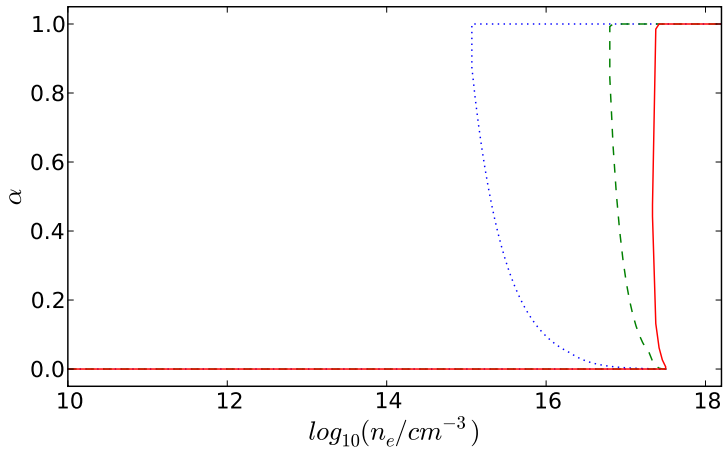

Figure 4.6: Hysteresis in the degree of ionization in ZnSe at $T = 2$ K with chemical potentials μ^{D} (dotted), μ^{RZR} (dashed) and μ^{iter} (solid).

the results presented in Sec. 4.1 it is clear that the breakup of excitons does not mean a vanishing of the condensed phase, and rather a smooth crossover to a BCS state is to be expected.

The comparison shows the vast improvement obtained with the approaches presented in *P-4* and *P-6*.

If a variation of the free carrier density is performed in the MAL at fixed (n_e, T), even the condensate can be considered correctly. Its partial density is determined as the *excess density*, i.e., the difference of n_e and the limited density of the $k > 0$ fraction, which is just the well-known critical density of the ideal Bose gas, Eq. (4.16).

It is to be noted that a BEC area will always show up at low enough temperatures (compare Fig. 4.5b, where the chosen temperature range is too narrow). However, the question is whether BEC may appear at EHP temperatures which are in reach experimentally. The answer depends strongly on the quality of the approximations involved.

4.2.5 Hysteresis

The graphical evaluation of Eq. (4.28) in *P-6* reveals clearly the possibility of multiple equilibrium solutions α for a given density and temperature. For low total densities n_e, there is only one solution, but for high densities, three are possible. In the latter case, one solution is always found at strong ionization $\alpha \to 1$, so that there is a hysteresis in the ionization behavior near the Mott density.

This hysteresis may give rise to phase transitions and entailing physical effects (EKK79). It has also been proposed to be exploited for producing the excitonic BEC at higher temperatures (SC95). However, it may just be a theoretical artefact. Our

comparison in *P-6* shows that application of better approximations for the chemical potentials and binding energy significantly reduces the extension of the hysteresis on the density axis (Fig. 4.6). Furthermore, similar considerations for other plasma types (SK82) suggest that it might vanish completely if exciton-exciton interaction is taken into account.

4.2.6 Non-interacting bosons?

Not only for the debate around the existence of an ionization hysteresis it would be advantageous to consider the interaction between excitons. One may expect corrections to the ionization behavior in general below the Mott density, where the exciton density is high, and it appears an undue simplification to neglect interactions in such dense regimes.

The inclusion of exciton-exciton interaction, however, is a complicated task, since in principle the four-particle collision problem has to be regarded. Previous results for this topic are sparse. The excitonic contribution to the polarization (and, hence, to band edge and binding energy shifts) is known to be small (RD78). Zimmermann and Schindler (ZS07) mapped the four-particle problem to an effective two-particle problem by considering electrons and holes separated spatially in coupled quantum wells, and found the interaction to be much weaker than in a plain Hartree-Fock calculation.

A promising idea to include exciton-exciton interaction into the MAL is to extend the kinetic energy term in Eq. (4.21) by a k-independent self-energy shift determined by a hard-body or four-particle potential (OO01), whose strength is chosen according to these theoretical results and experimental experience (SRK09).

Chapter 5

Summary

The problem of light propagation through bounded media has been treated with special attention to spatial inhomogeneity and signatures of condensation effects in electron-hole systems.

Spatial inhomogeneity is a consequence of the breach of translational invariance due to the presence of medium boundaries. It is connected with optical effects, e.g., due to the confinement of excitations and their decay in the vicinity of the surfaces, and, hence, is important for the study of confined systems such as semiconductor slabs, heterostructures, quantum wells, etc. It is however, often disregarded, and a bulk approximation is used instead.

Quantum condensation is an interesting phenomenon from the experimental as well as from the theoretical point of view. Since the electron-hole plasma is an integral part of the semiconductor, optical signatures become the key for the proof of existence of condensates as well as for their further analysis. The form of these signatures is subject to debate, and they will always be imprinted to a significant background signal from the internal interactions and external perturbations the plasma is inevitably exposed to. In optical probing, both plasma and radiation are coupled and thus need to be treated in a theory that is aware of this coupling, i.e., stems from a joint theory of light and matter.

The present work reports progress in several related aspects. It gives an introduction to the theoretical framework used, and reviews and summarizes the author's published articles and manuscripts cohesively. Newer results help to present others more compactly and in more detail as in the original work. A special case is Sec. 4.1, which presents the results of an article to which the author contributed numerical calculations only, but which fits neatly into the account on quantum condensation given here.

For the joint description of light and matter, the present work relies on the *nonequilibrium Green's function* concept. It is introduced in Chapter 2 with foundation on the axiomatic basis of light-matter interaction, the *Maxwell* and *Newton–Lorentz equations*, followed by the formulation and description of the according Hamiltonian. The strict coupling of the photon and particle Green's functions via their respective self-energies

has to be abandoned soon but remains as a fundamental feature of the theory which may be explored further for systematic studies of the mutual interactions in more detail.

Careful and correct formulation of the fundamental energy conservation condition (*Poynting's theorem*, Sec. 2.2.2) for bounded media systems as well as of their electromagnetic properties (susceptibility, Sec. 3.1) lead to advances even in the well-known classical description of wave propagation. Problems with the historical, widely followed form of Poynting's theorem are pointed out. The proposed new formulation, Eq. (2.13), has the advantage of strictly separating electromagnetic from mechanical (kinetic) energies and providing a consistent universal definition of the energy densities. Of course, this fundamental issue is of major importance for all subsequent considerations concerning bounded media systems, where significant energy transformation must occur in the vicinity of the medium surfaces.

A choice of relevant susceptibility function approximations in the excitonic spectral range is presented in Sec. 3.2, and different approximation schemes for a classical treatment of light propagation in bounded media systems, i.e., reflection, transmission and absorption, are discussed together with their problems and implications (Sec. 3.3).

Then, the transition is made to the nonclassical description of light propagation with the help of the *photon Green's function*, whose "greater" and "less" components describe correlations and fluctuations of the electromagnetic vector potential (Sec. 3.4). The exact consideration of spatial inhomogeneity and arbitrary medium properties succeeds in linear approximation by exploiting the fundamental and universal *splitting property* of the PGF, Eq. (3.22a), which is derived and discussed in Sec. 3.4.2: It gives a satisfying explanation for the "theoretical artifact" of infinitesimal "vacuum polarization" and allows regarding light incident from the free space and light induced by electronic processes in a medium separately. Incident field fluctuations are found to propagate in a way that can be traced back to classical wave propagation, and their GF representation, Eq. (3.22c), opens the possibility to consider incident light in arbitrary quantum states [Eq. (3.27)].

Consequently, the role of ground-state fluctuations in the optical field and transmission (scattering) of nonclassical light in linear approximation are discussed in a new quality. Prior results obtained from effective theories are confirmed and generalized to spatially inhomogeneous systems with arbitrarily dispersive and absorptive media. A first application example is a passive optical device (like mirror or beam splitter) in experimental setups for quantum optics and the question of their influence on the properties of nonclassical light (e.g., squeezed light, Sec. 3.4.4).

Restricting the theory to steady-state media in slab geometry, a nonequilibrium energy flow law, Eq. (3.62), can be obtained from the PGF formulation of Poynting's theorem. Thanks to the splitting property, the derivation can be given in a compact and instructive form (Sec. 3.5). The net energy flow leaving the slab surfaces appears as the balance of emission and absorption, and, interestingly, both are governed by the classical absorptivity of the medium. Their strengths depend further on the distribu-

tion of excitations in the medium and in the surrounding photon bath, respectively. In this sense, the energy flow law is a generalization of the Kirchhoff and Planck radiation laws to the nonequilibrium steady state (Sec. 3.5.3).

A closer look at the interplay of light and matter in the PGF dissipation terms in Sec. 3.5.2 provides insight into the mechanisms of (spontaneous and stimulated) light emission and absorption. The role of the ground-state fluctuations is highlighted: They do not contribute to the net energy flow, but cross-couple to the excitations (or *stimulations*) in the medium or photon bath, respectively, and are thus indispensable for emission and absorption to occur.

Here, the Green's function formalism shows its strengths: In a system governed by a highly complicated Hamiltonian, it helps to keep a manageable set of quantities and equations, and to manipulate *structures* that abstract from inner details. Relations and identities become apparent, and it is easier – while not trivial – to keep track of the physical meaning of these structures during the manipulations.

The nonequilibrium energy flow law is then demonstrated in the study of emission from semiconductor slabs at different degrees of excitation (Sec. 3.5.4). For quasi-equilibrium, the distribution of optical medium excitations can be shown to develop into a Bose distribution, which is linked to the excitation density via the chemical potential. If the latter approaches the crossover from absorbing to amplifying behavior in the absorptivity function, degeneracy effects become apparent in the emission. From this point of view, optical medium excitation states are always bosonic, regardless of the underlying fermionic particle system, and lasing appears just as a quasithermal emission phenomenon.

At low temperatures, the emission is predicted to completely vanish in the absorptive spectral range, and this will also be true if quantum condensation occurs. Chapter 4 gives an introduction to quantum condensation phenomena in general and to excitonic BEC as a special case. Section 4.1 reviews an approach to quantum condensation in electron-hole plasma on the particle GF level, from which several properties of the polarization function for the PGF can be deduced, that is especially a cancellation of the condensate contribution to the absorption. A BEC signature will thus have to be searched for in the emission, e.g., in the photoluminescence signal, where it should appear as a delta-shaped peak at the frequency corresponding to the chemical potential [Eq. (3.68)].

The particle GF approach to quantum condensation evaluates the vanishing of the gap function, Eq. (4.13), as the condensate phase boundary. The qualitative overview shows a smooth crossover from the excitonic condensate (BEC) to the BCS-like condensate of electron-hole pairs in the high-density electron-hole liquid. In Fig. 4.3, a strong deviation of the phase boundary from ideal bosonic behavior at higher densities indicates the breakup of the excitons due to the increasing strength of the many-particle effects. The neutral excitons are ionized to electron-hole pairs. This *Mott transition* effectively represents a boundary for excitonic BEC. Hence, Sec. 4.2 is concerned

with a quantitative analysis of the ionization equilibrium in the excitonic regime in order to provide a reliable estimate of the Mott density.

For this, a description of the plasma composition by its degree of ionization is developed starting from the GF expression for the bulk carrier density. The intuitive mass-action law for the ionization equilibrium, Eq. (4.28), as well as bosonic statistics for the excitons, Eq. (4.22), follow. For the numerical evaluation, the density and temperature dependence of the chemical potentials of the carriers as well as of the exciton binding energies are needed. Several approximations are compared and briefly discussed. Self-consistent calculations considering damping effects show a vast improvement over former approaches, as can be seen from the resulting maps of the degree of ionization, Fig. 4.5. The lowering of the effective ionization energy, a consequence of the many-particle effects that leads to the breakup, is illustrated.

The degree of ionization is known to exhibit a hysteresis below the Mott density, which was argued to be a theoretical artifact but was also proposed to be exploited for obtaining excitonic BEC. The improved numerical calculations show a strongly reduced hysteresis, supporting the former case. Last, the sparse proposals concerning the inclusion of exciton-exciton interactions in spite of purely non-interacting excitons are briefly discussed.

Published articles

Article P-1

Poynting's theorem and energy conservation in bounded media

Bibliographical reference

RICHTER, F. ; FLORIAN, M. ; HENNEBERGER, K.:
Poynting's theorem and energy conservation in the propagation of light in bounded media.
In: *Europhys. Lett.* 81 (2008), S. 67005

Article P-2

Generalized radiation law for excited media in a nonequilibrium steady state

Bibliographical reference

RICHTER, F. ; FLORIAN, M. ; HENNEBERGER, K.:
Generalized radiation law for excited media in a nonequilibrium steady state.
In: *Phys. Rev. B* 78 (2008), S. 205114

Article P-3

Quasi-equilibrium emission of excited semiconductors

Bibliographical reference

RICHTER, F. ; MANZKE, G. ; HENNEBERGER, K.:
Quasi-equilibrium emission of excited semiconductors.
In: *Phys. status solidi C* 6 (2009), S. 528.

Article P-4

Ionization equilibrium and Mott transition in an excited semiconductor, phase diagram

Bibliographical reference

RICHTER, F. ; SEMKAT, D. ; KREMP, D. ; HENNEBERGER, K.:
Ionization equilibrium and Mott transition in an excited semiconductor, phase diagram.
In: *Phys. status solidi C* 6 (2009), S. 532.

Article P-5

Exact property of the nonequilibrium photon Green function for bounded media

Bibliographical reference

HENNEBERGER, K. and RICHTER, F.:
Exact property of the nonequilibrium photon Green function for bounded media.
In: *Phys. Rev. A* 80 (2009), S. 013807.

Submitted articles and manuscripts

Article P-6

Ionization equilibrium in an excited semiconductor: Mott transition vs. Bose-Einstein condensation

Bibliographical reference

SEMKAT, D. ; RICHTER, F. ; KREMP, D. ; MANZKE, G. ; KRAEFT, W.-D. ; HENNEBERGER, K.:
Ionization equilibrium in an excited semiconductor: Mott transition vs. Bose-Einstein condensation.
submitted — later published as: *Phys. Rev. B* 80 (2009), S. 155201.

Article P-7

Green function approach to scattering of nonclassical light by bounded media

Bibliographical reference

RICHTER, F. ; VASYLYEV, D. Y. ; HENNEBERGER, K.:
Green function approach to scattering of nonclassical light by bounded media.
arXiv:0903.5238 – (2009).

Bibliography

AEM+95 ANDERSON, M. H. ; ENSHER, J. R. ; MATTHEWS, M. R. ; WIEMAN, C. E. ; CORNELL, E. A.: Observation of Bose-Einstein Condensation in a Dilute Atomic Vapor. In: *Science* 269 (1995), S. 198

AG84 AGRANOVICH, V.M. ; GINZBURG, V.L.: *Crystal Optics with Spatial Dispersion and Excitons*. Springer, Berlin, 1984

AGD63 ABRIKOSOV, A. A. ; GORKOV, L. P. ; DZYALOZHINSKI, I. E.: *Methods of Quantum Field Theory in Statistical Physics*. Prentice-Hall, 1963

AL97 ARTONI, M. ; LOUDON, R.: Quantum theory of optical pulse propagation through an absorbing and dispersive slab. In: *Phys. Rev. A* 55 (1997), S. 1347

AL99 ARTONI, M. ; LOUDON, R.: Propagation of nonclassical light through an absorbing and dispersive slab. In: *Phys. Rev. A* 59 (1999), S. 2279

BBB62 BLATT, J. M. ; BÖER, K. W. ; BRANDT, W.: Bose-Einstein Condensation of Excitons. In: *Phys. Rev.* 126 (1962), S. 1691

BCS57 BARDEEN, J. ; COOPER, L. N. ; SCHRIEFFER, J. R.: Theory of Superconductivity. In: *Phys. Rev.* 108 (1957), S. 1175

BF06 BRONOLD, F. X. ; FEHSKE, H.: Possibility of an excitonic insulator at the semiconductor-semimetal transition. In: *Phys. Rev. B* 74 (2006), S. 165107

BLI+02 BUTOV, L. V. ; LAI, C. W. ; IVANOV, A. L. ; GOSSARD, A. C. ; CHEMLA, D. S.: Towards Bose-Einstein condensation of excitons in potential traps. In: *Nature* 417 (2002), S. 47

BM76 BISHOP, M. F. ; MARADUDIN, A. A.: Energy flow in a semi-infinite spatially dispersive absorbing dielectric. In: *Phys. Rev. B* 14 (1976), S. 3384

Bos24 BOSE, S. N.: Plancks Gesetz und Lichtquantenhypothese. In: *Zeitschrift für Physik* 26 (1924), S. 178

CDG89 COHEN-TANNOUDJI, Claude ; DUPONT-ROC, Jaques ; GRYNBERG, Gilbert: *Photons and atoms*. Wiley, New York, 1989

CDL77 COHEN-TANNOUDJI, Claude ; DIU, Bernard ; LALOË, Franck: *Quantum mechanics*. Wiley, New York, 1977

Dan84 DANIELEWICZ, P.: Quantum theory of nonequilibrium processes, I. In: *Annals of Physics* 152 (1984), S. 239

Des03 DESJARLAIS, M. P.: Density-functional calculations of the liquid deuterium Hugoniot, reshock, and reverberation timing. In: *Phys. Rev. B* 68 (2003), S. 064204

DMA+95 DAVIS, K. B. ; MEWES, M. O. ; ANDREWS, M. R. ; DRUTEN, N. J. ; DURFEE, D. S. ; KURN, D. M. ; KETTERLE, W.: Bose-Einstein Condensation in a Gas of Sodium Atoms. In: *Phys. Rev. Lett.* 75 (1995), S. 3969

DuB67 DUBOIS, D. F.: Plasmas and Radiation. In: BRITTIN, W. E. (Hrsg.): *Lectures in Theoretical Physics* Bd. IX C, Gordon and Breach, New York, 1967, S. 469–620

Dys49 DYSON, F. J.: The S Matrix in Quantum Electrodynamics. In: *Phys. Rev.* 75 (1949), S. 1736

Ein25 EINSTEIN, Albert: Quantentheorie des einatomigen idealen Gases. In: *Sitzungsberichte der preußischen Akademie der Wissenschaften* 3 (1925)

EKK79 EBELING, W. ; KRAEFT, W.-D. ; KREMP, D.: *Theory of Bound States and Ionization Equilibrium in Plasmas and Solids*. Mir, Moskau, 1979

Ell57 ELLIOTT, R. J.: Intensity of Optical Absorption by Excitons. In: *Phys. Rev.* 108 (1957), S. 1384

EM04 EISENSTEIN, J. P. ; MACDONALD, A. H.: Bose–Einstein condensation of excitons in bilayer electron systems. In: *Nature* 432 (2004), S. 691

FBM04 FENNEL, T. ; BERTSCH, G.F. ; MEIWES-BROER, K.-H.: Ionization dynamics of simple metal clusters in intense fields by the Thomas-Fermi-Vlasov method. In: *The European Physical Journal D* 29 (2004), S. 367

FKU+91 FRÖHLICH, D. ; KULIK, A. ; UEBBING, B. ; MYSYROWICZ, A. ; LANGER, V. ; STOLZ, H. ; OSTEN, W. von d.: Coherent propagation and quantum beats of quadrupole polaritons in Cu_2O. In: *Phys. Rev. Lett.* 67 (1991), S. 2343

Flo08 FLORIAN, M.: *Polariton-Effekte in Halbleiter-Nanostrukturen*, Univ. Rostock, Diplomarbeit, 2008

For09 FORTMANN, C.: Single-particle spectral function for the classical one-component plasma. In: *Phys. Rev. E* 79 (2009), S. 016404

Fra03 FRANZ, R.: *Polariton effects in the reflection of pumped ZnSe layers*, Univ. Rostock, Diplomarbeit, 2003

FSSR09 FRENCH, M. ; SCHWARTZ, R. ; STOLZ, H. ; REDMER, R.: Electronic band structure of Cu2O by spin density functional theory. In: *Journal of Physics: Condensed Matter* 21 (2009), S. 015502

GW96 GRUNER, T. ; WELSCH, D.-G.: Quantum-optical input-output relations for dispersive and lossy multilayer dielectric plates. In: *Phys. Rev. A* 54 (1996), S. 1661

Hal92 HALEVI, P.: *Spatial Dispersion in Solids and Plasmas*. North-Holland, Amsterdam, 1992

Hau01 HAUG, H.: Dressing up bare particles. In: *Nature* 414 (2001), S. 261

Hed65 HEDIN, Lars: New Method for Calculating the One-Particle Green's Function with Application to the Electron-Gas Problem. In: *Phys. Rev.* 139 (1965), S. A796

Hen98 HENNEBERGER, K.: Additional Boundary Conditions: An Historical Mistake. In: *Phys. Rev. Lett.* 80 (1998), S. 2889

Hen08a HENNEBERGER, K.: An exact property of the nonequilibrium photon Green function for bounded media. (2008). – arXiv:0810.5058v1

Hen08b HENNEBERGER, K.: Generalizing Planck's Law: Nonequilibrium Emission of Excited Media. In: *Phys. Status Solidi B* 246 (2008), S. 283

HJ96 HAUG, H. ; JAUHO, A.-P.: *Quantum Kinetics in Transport and Optics of Semiconductors*. Springer, Berlin, 1996 (Springer Series in Solid-State Sciences 123)

HK90 HAUG, H. ; KOCH, S. W.: *Quantum Theory of the Optical and Electronic Properties of Semiconductors*. 4th edition, 2004. World Scientific, Singapore, 1990

HK95 HENNEBERGER, K. ; KOCH, S. W.: Quantum Kinetic Theory of the Semiconductor Laser. In: KOCH, S. W. (Hrsg.): *Microscopic theory of semiconductors: Quantum Kinetics, Confinement and Lasers*, World Scientific, Singapore, 1995, S. 131–166

HK96a HENNEBERGER, K. ; KOCH, S. W.: Quantum Kinetics of Semiconductor Light Emission and Lasing. In: *Phys. Rev. Lett.* 76 (1996), S. 1820

HK96b HENRY, Charles H. ; KAZARINOV, Rudolf F.: Quantum noise in photonics. In: *Rev. Mod. Phys.* 68 (1996), S. 801

Hop58 HOPFIELD, J. J.: Theory of the Contribution of Excitons to the Complex Dielectric Constant of Crystals. In: *Phys. Rev.* 112 (1958), S. 1555

Hv98 HOLM, B. ; VON BARTH, U.: Fully self-consistent GW self-energy of the electron gas. In: *Phys. Rev. B* 57 (1998), S. 2108

Jac99 JACKSON, J. D.: *Classical Electrodynamics*. Wiley, New York, 1999

Jah96 JAHNKE, F.: *A many-body theory for laser emission and excitonic effects in semiconductor microcavities*, Phillips-Universität Marburg, Habilitationsschrift, 1996

JL98 JAN, J. F. ; LEE, Y. C.: Bose–Einstein condensation of excitons in two dimensions. In: *Phys. Rev. B* 58 (1998), S. R1714

KB62 KADANOFF, L. P. ; BAYM, G.: *Quantum Statistical Mechanics*. Benjamin, New York, 1962

KCB97 KAVOULAKIS, G. M. ; CHANG, Yia-Chung ; BAYM, Gordon: Fine structure of excitons in $\mathrm{Cu_2O}$. In: *Phys. Rev. B* 55 (1997), Nr. 12, S. 7593

Kel64 KELDYSH, L. V.: In: *Zh. Eksp. Teor. Fiz.* 47 (1964), 1515 S. – [Soviet Phys. JETP **20**, 1018 (1965)]

Kel03 KELDYSH, L. V.: Real-time nonequilibrium Green's functions. In: BONITZ, M. (Hrsg.) ; SEMKAT, D. (Hrsg.): *Progress in Nonequilibrium Green's Functions II*, World Scientific, Singapore, 2003, S. 4–17

Ket02 KETTERLE, Wolfgang: Nobel lecture: When atoms behave as waves: Bose-Einstein condensation and the atom laser. In: *Rev. Mod. Phys.* 74 (2002), S. 1131

KHR+07 KIETZMANN, A. ; HOLST, B. ; REDMER, R. ; DESJARLAIS, M. P. ; MATTSSON, T. R.: Quantum Molecular Dynamics Simulations for the Nonmetal-to-Metal Transition in Fluid Helium. In: *Phys. Rev. Lett.* 98 (2007), S. 190602

Kir60 KIRCHHOFF, G.: Ueber das Verhältniss zwischen dem Emissionsvermögen und dem Absorptionsvermögen der Körper für Wärme und Licht. In: *Annalen der Physik* 185 (1860), S. 275

KK06 KIRA, M. ; KOCH, S. W.: Many-body correlations and excitonic effects in semiconductor spectroscopy. In: *Progress in Quantum Electronics* 30 (2006), S. 155

KKER86 KRAEFT, W.-D. ; KREMP, D. ; EBELING, W. ; RÖPKE, G.: *Quantum Statistics of Charged Particle Systems*. Plenum Press, New York and London, 1986

KKL84 KREMP, D. ; KRAEFT, W. D. ; LAMBERT, A. J. D.: Equation of state and ionization equilibrium for nonideal plasmas. In: *Physica A* 127 (1984), S. 72

Kli95 KLINGSHIRN, C. F.: *Semiconductor Optics*. 3rd. ed. (2007). Springer, Berlin, 1995

KRK+06 KASPRZAK, J. ; RICHARD, M. ; KUNDERMANN, S. ; BAAS, A. ; JEAMBRUN, P. ; KEELING, J. M. J. ; MARCHETTI, F. M. ; SZYMAŃSKA, M. H. ; ANDRÉ, R. ; STAEHLI, J. L. ; SAVONA, V. ; LITTLEWOOD, P. B. ; DEVEAUD, B. ; DANG, L. S.: Bose-Einstein condensation of exciton polaritons. In: *Nature* 443 (2006), S. 409

KSH08 KREMP, D. ; SEMKAT, D. ; HENNEBERGER, K.: Quantum condensation in electron-hole plasmas. In: *Phys. Rev. B* 78 (2008), S. 125315

KSK05 KREMP, D. ; SCHLANGES, M. ; KRAEFT, W.-D.: *Atomic, Optical, and Plasma Physics*. Bd. 25: *Quantum Statistics of Nonideal Plasmas*. Springer, Berlin, 2005

Lan76 LANGRETH, D. C.: Linear and Nonlinear Response Theory with Applications. In: DEVREESE, J. T. (Hrsg.) ; VAN DOREN, E. (Hrsg.): *Linear and Nonlinear*

Electron Transport in Solids, Plenum, New York, 1976

LL60 LANDAU, L. D. ; LIFSHITZ, E. M.: *Electrodynamics of Continuous Media*. 2., deutsche Ausgabe (Akademie Verlag, Berlin 1971). Pergamon, Oxford, 1960

Mah90 MAHAN, G. D.: *Many-Particle Physics*. 2nd edition, 1993. Plenum Press, New York and London, 1990

Mar92 MARTIENSSEN, W. (Hrsg.): *Landolt-Börnstein. Numerical data and functional relationships in science and technology: new series*. Bd. III-17. Springer, Berlin, 1992

MH02 MANZKE, G. ; HENNEBERGER, K.: Quantum-Kinetic Effects in the Linear Optical Response of GaAs Quantum Wells. In: *Phys. status solidi B* 234 (2002), S. 233

MM73 MARADUDIN, A. A. ; MILLS, D. L.: Effect of Spatial Dispersion on the Properties of a Semi-Infinite Dielectric. In: *Phys. Rev. B* 7 (1973), S. 2787

MPH+98 MANZKE, G. ; PENG, Q. Y. ; HENNEBERGER, K. ; NEUKIRCH, U. ; HAUKE, K. ; WUNDKE, K. ; GUTOWSKI, J. ; HOMMEL, D.: Density Dependence of the Exciton Energy in Semiconductors. In: *Phys. Rev. Lett.* 80 (1998), S. 4943

MS59 MARTIN, Paul C. ; SCHWINGER, Julian: Theory of Many-Particle Systems. I. In: *Phys. Rev.* 115 (1959), S. 1342

MS00 MOSKALENKO, S. A. ; SNOKE, D. W.: *Bose–Einstein Condensation of Excitons and Biexcitons*. Cambridge University Press, 2000

MW95 MANDEL, L. ; WOLF, E.: *Optical coherence and quantum optics*. Cambridge University Press, 1995

MW05 MARTIENSSEN, W. (Hrsg.) ; WARLIMONT, H. (Hrsg.): *Springer Handbook of Condensed Matter and Materials Data*. Springer, Berlin, 2005

MZ02 MULJAROV, E. A. ; ZIMMERMANN, R.: Exciton polariton including continuum states: Microscopic versus additional boundary conditions. In: *Phys. Rev. B* 66 (2002), S. 235319

Nel95 NELSON, D. F.: Deriving the transmission and reflection coefficients of an optically active medium without using boundary conditions. In: *Phys. Rev.*

E 51 (1995), S. 6142

NS85 NOZIÈRES, P. ; SCHMITT-RINK, S.: Bose condensation in an attractive fermion gas: From weak to strong coupling superconductivity. In: *Journal of Low Temperature Physics* 59 (1985), S. 195

NSB+01 NÄGERL, J. S. ; STABENAU, B. ; BÖHNE, G. ; DREHER, S. ; ULBRICH, R. G. ; MANZKE, G. ; HENNEBERGER, K.: Polariton pulse propagation through GaAs: Excitation-dependent phase shifts. In: *Phys. Rev. B* 63 (2001), S. 235202

OO01 OKUMURA, S. ; OGAWA, T.: Boson representation of two-exciton correlations: An exact treatment of composite-particle effects. In: *Phys. Rev. B* 65 (2001), S. 035105

ORR02 ONIDA, Giovanni ; REINING, Lucia ; RUBIO, Angel: Electronic excitations: density-functional versus many-body Green's-function approaches. In: *Rev. Mod. Phys.* 74 (2002), S. 601

Pek57 PEKAR, S.I.: In: *Zh. Eksp. Teor. Fiz.* 33 (1957), 1022 S. – [Sov. Phys. JETP **6**, 785 (1958)]

Pla01 PLANCK, Max: Ueber das Gesetz der Energieverteilung im Normalspectrum. In: *Annalen der Physik* 309 (1901), S. 553

Poy84 POYNTING, J. H.: On the Transfer of Energy in the Electromagnetic Field. In: *Philosophical Transactions of the Royal Society* 175 (1884), S. 277

PP05 PAIS, A. ; PENROSE, R.: *Subtle Is the Lord: The Science and the Life of Albert Einstein*. Oxford University Press, 2005

RD78 RÖPKE, G. ; DER, R.: The influence of two-particle states (excitons) on the dielectric function of the electron - hole plasma. In: *Phys. status solidi B* 92 (1978), S. 501

RZR84 RÖSLER, M. ; ZIMMERMANN, R. ; RICHERT, W.: The Electron-Hole Plasma at Finite Temperatures. In: *Phys. status solidi B* 121 (1984), S. 609

SBR03 SENGSTOCK, Klaus ; BONGS, Kai ; REICHEL, Jakob: Das ideale Quantenlabor: Bose-Einstein-Kondensation. In: *Physik in unserer Zeit* 34 (2003), Nr. 4, S. 168

SC95 SNOKE, D. W. ; CRAWFORD, J. D.: Hysteresis in the Mott transition between plasma and insulating gas. In: *Phys. Rev. E* 52 (1995), S. 5796

Sch01 SCHMIELAU, T.: *Optische und Ein-Teilchen-Eigenschaften von Halbleitern*, Univ. Rostock, Diss., 2001

SCJ02 SCHUMACHER, S. ; CZYCHOLL, G. ; JAHNKE, F.: Microscopic Description of Exciton-Polaritons in Thin Semiconductor Layers. In: *Phys. status solidi B* 234 (2002), S. 172

SCJ+04 SCHUMACHER, S. ; CZYCHOLL, G. ; JAHNKE, F. ; KUDYK, I. ; RÜCKMANN, H. I. ; GUTOWSKI, J. ; GUST, A. ; ALEXE, G. ; HOMMEL, D.: Polariton propagation in shallow-confinement heterostructures: Microscopic theory and experiment showing the breakdown of the dead-layer concept. In: *Phys. Rev. B* 70 (2004), S. 235340

SJK+01 SCHNEIDER, H. C. ; JAHNKE, F. ; KOCH, S. W. ; TIGNON, J. ; HASCHE, T. ; CHEMLA, D. S.: Polariton propagation in high quality semiconductors: Microscopic theory and experiment versus additional boundary conditions. In: *Phys. Rev. B* 63 (2001), S. 045202

SK82 SCHLANGES, M. ; KREMP, D.: The equation of state for the hydrogen plasma on account of atom-atom interaction. In: *Annalen der Physik* 39 (1982), S. 69

SKS+05 SEEMANN, M. ; KIESELING, F. ; STOLZ, H. ; FRANZ, R. ; MANZKE, G. ; HENNEBERGER, K. ; PASSOW, T. ; HOMMEL, D.: Carrier-induced changes of the phase of reflected light at a pumped ZnSe layer. In: *Phys. Rev. B* 72 (2005), S. 075204

SKS+06 SEEMANN, M. ; KIESELING, F. ; STOLZ, H. ; MANZKE, G. ; HENNEBERGER, K. ; PASSOW, T. ; HOMMEL, D.: Phase resolved polariton interferences in a ZnSe-ZnSSe heterostructure. In: *Phys. status solidi C* 3 (2006), S. 2453

SKS+08 SEEMANN, M. ; KIESELING, F. ; STOLZ, H. ; FLORIAN, M. ; MANZKE, G. ; HENNEBERGER, K. ; HOMMEL, D.: Absorption and emission of polariton modes in a ZnSe-ZnSSe heterostructure. In: *Phys. status solidi B* 245 (2008), S. 1093

Sno02 SNOKE, D.: Spontaneous Bose coherence of Excitons and Polaritons. In: *Science* 298 (2002), S. 1368

Sno03 SNOKE, D. W.: When should we say we have observed Bose condensation of excitons? In: *Phys. Status Solidi B* 238 (2003), S. 389

SRK09 SEMKAT, D. ; RICHTER, F. ; KREMP, D.: Exciton-exciton interaction in the ionization equilibrium in excited semiconductors. (2009). – to be published

SW02 SCHÄFER, W. ; WEGENER, M.: *Semiconductor optics and transport phenomena*. Springer, Berlin, 2002

Tan95 TANGUY, Christian: Optical Dispersion by Wannier Excitons. In: *Phys. Rev. Lett.* 75 (1995), S. 4090

Tan99 TANGUY, Christian: Analytical expression of the complex dielectric function for the Hulthén potential. In: *Phys. Rev. B* 60 (1999), S. 10660

THC+00 TIGNON, J. ; HASCHE, T. ; CHEMLA, D. S. ; SCHNEIDER, H. C. ; JAHNKE, F. ; KOCH, S. W.: Unified Picture of Polariton Propagation in Bulk GaAs Semiconductors. In: *Phys. Rev. Lett.* 84 (2000), S. 3382

Tol56 TOLL, John S.: Causality and the Dispersion Relation: Logical Foundations. In: *Phys. Rev.* 104 (1956), S. 1760

VP04 VENGER, E. F. ; PISKOVOI, V. N.: Consistency of boundary conditions in crystal optics with spatial dispersion. In: *Phys. Rev. B* 70 (2004), S. 115107

VVH+08 VASYLYEV, D.Yu. ; VOGEL, W. ; HENNEBERGER, K. ; SCHMIELAU, T. ; WELSCH, D.-G.: Propagation of nonclassical optical radiation through a semiconductor slab. In: *Phys. Rev. A* 78 (2008), S. 033837

VVM+08 VASYLYEV, D. ; VOGEL, W. ; MANZKE, G. ; HENNEBERGER, K. ; WELSCH, D.-G.: Nonclassicality of radiation fields propagating in complex material systems. In: *Phys. Status Solidi B* 246 (2008), S. 293

VW06 VOGEL, W. ; WELSCH, D.-G.: *Quantum Optics*. 3rd ed. Wiley-VCH, Weinheim, 2006

Wan37 WANNIER, Gregory H.: The Structure of Electronic Excitation Levels in Insulating Crystals. In: *Phys. Rev.* 52 (1937), S. 191

YC05 YU, P. Y. ; CARDONA, M.: *Fundamentals of Semiconductors*. Springer, Berlin, 2005. – 3rd. ed.

Zim88 ZIMMERMANN, R.: *Many-particle Theory of Highly Excited Semiconductors*. Teubner, Leipzig, 1988

ZS07 ZIMMERMANN, R. ; SCHINDLER, Ch.: Exciton-exciton interaction in coupled quantum wells. In: *Solid State Commun.* 144 (2007), S. 395

List of publications

Author's peer-reviewed journal publications

1. RICHTER, F. ; FLORIAN, M. ; HENNEBERGER, K.:
   Poynting's theorem and energy conservation in the propagation of light in bounded media.
   In: *Europhys. Lett.* 81 (2008), S. 67005.

2. RICHTER, F. ; FLORIAN, M. ; HENNEBERGER, K.:
   Generalized radiation law for excited media in a nonequilibrium steady state.
   In: *Phys. Rev. B* 78 (2008), S. 205114.

3. RICHTER, F. ; MANZKE, G. ; HENNEBERGER, K.:
   Quasi-equilibrium emission of excited semiconductors.
   In: *Phys. status solidi C* 6 (2009), S. 528.

4. RICHTER, F. ; SEMKAT, D. ; KREMP, D. ; HENNEBERGER, K.:
   Ionization equilibrium and Mott transition in an excited semiconductor, phase diagram.
   In: *Phys. status solidi C* 6 (2009), S. 532.

5. HENNEBERGER, K. ; RICHTER, F.:
   Exact property of the nonequilibrium photon Green function for bounded media.
   In: *Phys. Rev. A* 80 (2009), S. 013807.

Manuscripts submitted to peer-review journals

1. SEMKAT, D. ; RICHTER, F. ; KREMP, D. ; MANZKE, G. ; KRAEFT, W.-D. ; HENNEBERGER, K.:
   Ionization equilibrium in an excited semiconductor: Mott transition vs. Bose-Einstein condensation.

submitted — later published as *Phys. Rev. B* 80 (2009), S. 155201.

Contributions to the arXiv.org e-print archive

1. RICHTER, F. ; VASYLYEV, D. Y. ; HENNEBERGER, K.:
   Green function approach to scattering of nonclassical light by bounded media.
   (2009). – arXiv:0903.5238

Contributions to national and international conferences

- F. Richter and K. Henneberger:
  Quantum-optical radiation laws for excited semiconductors.
  Poster at *International Conference on Optics of Excitons in Confined Systems (OECS)*,
  Madrid, Spanien, 7.–11. September 2009

- G. Manzke, D. Semkat, F. Richter, D. Kremp, and K. Henneberger:
  Mott transition versus Bose–Einstein condensation of excitons.
  Poster at *International Conference on Optics of Excitons in Confined Systems (OECS)*,
  Madrid, Spanien, 7.–11. September 2009

- F. Richter, D. Semkat, and K. Henneberger:
  Photon Green's function for bounded media: Splitting property and nonequilibrium radiation laws.
  Contributed talk at *Progress in Nonequilibrium Green's Functions IV*,
  Glasgow, UK, 17.–21. August 2009

- D. Semkat, F. Richter, D. Kremp, G. Manzke, W.-D. Kraeft, and K. Henneberger:
  Ionization equilibrium in electron-hole plasmas: Mott effect vs. Bose–Einstein condensation.
  Poster at *Progress in Nonequilibrium Green's Functions IV*,
  Glasgow, UK, 17.–21. August 2009

- F. Richter, D. Semkat, D. Kremp, and K. Henneberger:
  Phase diagram of the excited semiconductor: Ionization equilibrium, Mott transition and BEC.
  Poster at *International Conference on Correlation Effects in Radiation Fields (CERF)*,
  Rostock, 8.–10. September 2008

- F. Richter, G. Manzke, and K. Henneberger:
  Emission of excited semiconductors in quasi-equilibrium: Spatial dispersion, degeneracy, lasing.
  Poster at *International Conference on Correlation Effects in Radiation Fields (CERF)*,
  Rostock, 8.–10. September 2008

- F. Richter, G. Manzke, and K. Henneberger:
  Non-equilibrium energy flow in bounded media.
  Poster at *International Workshop on Nonlinear Optics and Excitation Kinetics in Semiconductors (NOEKS)*,
  Klink (Müritz), 26.–29. Mai 2008

- F. Richter, D. Semkat, D. Kremp, and K. Henneberger:
  Ionization equilibrium and Mott transition in an excited semiconductor, phase diagram.
  Poster at *International Workshop on Nonlinear Optics and Excitation Kinetics in Semiconductors (NOEKS)*,
  Klink (Müritz), 26.–29. Mai 2008

- F. Richter, R. Schwartz, T. Schmielau, K. Henneberger, and H. Stolz:
  Mott transition and region of existence of excitonic BEC.
  Poster at *Frühjahrstagung der Deutschen Physikalischen Gesellschaft*,
  Regensburg, 26.–30. März 2007